ACUTE AND CHRONIC EFFECTS OF AMPK ACTIVATION ON SKELETAL MUSCLE FATTY ACID AND CARBOHYDRATE METABOLISM

A Thesis

Presented to

The Faculty of Graduate Studies

of

The University of Guelph

by

ANGELA C. SMITH

In partial fulfilment of requirements

for the degree of

Doctor of Philosophy

August, 2006

ABSTRACT

ACUTE AND CHRONIC EFFECTS OF AMPK ACTIVATION ON SKELETAL MUSCLE FATTY ACID AND CARBOHYDRATE METABOLISM

Angela C. Smith
University of Guelph

Advisor:
Dr. D.J. Dyck

AMP-activated protein kinase (AMPK) has been proposed to be an important energy-sensing enzyme, responding to increases in the AMP:ATP and Cr:PCr ratio. However, AMPK regulation of fatty acid (FA) metabolism and glucose oxidation is not completely understood. There is controversy regarding the effects of AMPK activation on fat-carbohydrate substrate selection and the role that AMPK plays in regulating the use of endogenous triacylglycerol (TAG) stores. It was hypothesized that an AICAR-induced decrease in glucose oxidation would be secondary to stimulation of FA oxidation occurring with adequate FA availability, and therefore inhibit TAG hydrolysis. In order to gain further insight into the role of AMPK in the regulation of substrate use during contraction, the second set of acute studies examined the regulatory role that AICAR activation of AMPK may be playing with tetanic contraction, specifically whether AICAR would increase AMPK activation above the threshold set by high intensity tetanic contraction and therefore see further increased rates of substrate oxidation.

Acute AICAR treatment in isolated skeletal muscle activated AMPKα2 and simultaneously increased FA and glucose oxidation, while having no effects on

intramuscular TAG metabolism, regardless of FA availability. Pyruvate dehydrogenase was also activated by AICAR, supporting the effects on glucose oxidation. AMPKα2 was activated by contraction and was further activated by the combination of AICAR and contraction. This led to further stimulation of FA oxidation, but inhibited TAG hydrolysis, suggesting that FA metabolism is very sensitive to AMPK activation. The already maximal rates of glucose oxidation were not further increased by AICAR.

Based on the above results, we hypothesized that 8 weeks of metformin and/or exercise (AMPK activators) would have insulin-sensitizing effects and prevent the progression of diabetes in the high-fat fed female Zucker diabetic fatty (ZDF) rat, an inducible model of diabetes. Metformin and exercise prevented the progression of diabetes, primarily by reducing plasma membrane-associated fatty acid translocase expression (FAT/CD36) and reducing the content of reactive lipid intermediates (DAG, ceramide) postulated to interfere with the insulin-signaling pathway in skeletal muscle. FA oxidation was unaffected by these treatments. Therefore, increasing FA oxidation in skeletal muscle may not be necessary and reducing FA transporters and reactive lipid species may be an important contributor in preventing diabetes.

ACKNOWLEDGEMENTS

I would first and foremost like to thank my thesis Advisor, Dr. David Dyck. Even from my Undergraduate years, you had confidence in me and allowed me to contribute to the laboratory, both in my own research and the research of others. Your knowledge, guidance, patience and perseverance have made this degree challenging and very rewarding and I am so grateful. You have been an inspiration and have set high standards for the type of scientist I aspire to be.

I would also like to thank my Committee members Dr. Arend Bonen, Dr. Sandra Peters and Dr. Lawrence Spriet. Your approachability and time involved in the development and completion of each of my studies has been invaluable and it has been so rewarding to learn from each of you.

There are many colleagues that I wish to thank in the laboratories of Dr. David Dyck, Dr. Lawrence Spriet and Dr. Arend Bonen. The ZDF study would not have been possible without the support of Kerry Mullen, Kathryn Junkin, Kristin Pandke and Patricia Kirby, who gave an incredible amount of time, care and knowledge to animal care, feeding, treadmill training and data collection. Dr. Clinton Bruce, Dr. Trent Stellingwerff, Brianne Thrush and Patricia Parsons were also instrumental with technical support and knowledge involved in both acute studies and the ZDF studies. In the Bonen lab, the technical knowledge and support of Dr. Carley Benton, Jennifer Nickerson and

Laelie Snook were invaluable in the completion of ZDF study and I am so grateful to each of you for always having time for me.

I would like to thank my parents, Marlene and Gary and my brother, Michael. I would also like to thank my "extended" family, Debbie and John Smale. You have been a source of continuous support and extreme patience throughout my academic pursuits and I love you all. I also give much thanks to David and Kelly D'Cruz, who have really been a big part of my life and have supported my academic goals, especially during the last year of my studies.

Last, but certainly not least, I would like to thank Geoff Smale. You have been by my side throughout this entire journey and your love, strength and guidance have helped me strive for and achieve all of my goals.

TABLE OF CONTENTS

List of Tables

Appendix 2: Metformin and Exercise Pilot Data

Appendix 3: Research Diets C13004 High Fat Diet Information

Appendix 4: Quality Control for Plasma Glucose Determination

Appendix 5: Western Blot Protocols For Proteins Examined in Chapter 5

List of Figures

Chapter 5: Reduced Fatty Acid Uptake and Lipid Accumulation as Potential Mechanisms for Metformin and Exercise in the Prevention of Diabetes in High-Fat Fed Female Zucker Diabetic Rats

ABBREVIATIONS

ACC	acetyl-CoA carboxylase
AICAR	5-aminoimidazole-4-carboxamide ribonucleoside
Akt/PKB	Akt/protein kinase B
AMP	adenosine monophosphate
AMPK	AMP-activated protein kinase
AMPKK	AMP-activated protein kinase kinase
araA	adenosine 9-β-D-arabunofuranoside
ATP	adenosine triphosphate
C	Control diet (Low-fat Purina Formulab® 5008)
Ca^{2+}	calcium
CaMKK	Ca^{2+}/calmodulin protein kinase kinase
CHO	carbohydrate
CoA	coenzyme A
CPT-I	carnitine palmitoyl transferase I
Cr	creatine
DAG	diacylglycerol
FA	fatty acid
FABPpm	fatty acid binding protein (plasma membrane isoform)
FAT/CD36	fatty acid translocase/CD36
G-6-P	glucose-6-phosphate
GLUT4	glucose transporter-4

GPAT	*sn*-glycerol-3-phosphate acyltransferase
GTP	guanidine triphosphate
HFA	high fatty acid, 1.0 mM
HF	high-fat diet (Research Diets C13004)
HF-E+M	high-fat diet, with combination exercise and metformin
HF-Ex	high-fat diet, with exercise
HF-Met	high-fat diet, with metformin
HKII	hexokinase II
HMG-CoA reductase	3-hydroxy-3-methylglutaryl-CoA reductase
HSL	hormone sensitive lipase
IRS-1	insulin receptor substrate 1
LFA	low fatty acid, 0.2 mM
MCD	malonyl-CoA decarboxylase
P_i	inorganic phosphate
pACC	phosphorylated acetyl-CoA carboxylase
pAMPK	phosphorylated AMP-activated protein kinase
PCr	phosphocreatine
PDH	pyruvate dehydrogenase
PFK	phosphofructokinase
PGC-1α	peroxisome proliferator activated receptor-gamma coactivator 1-α
PKC	protein kinase C
PPARγ	peroxisome proliferator-activated receptor-γ

RG	red gastrocnemius
SCD	stearoyl-CoA desaturase
Ser	serine
T2DM	Type 2 diabetes mellitus
TAG	triacylglycerol
tAMPK	total AMPK alpha
Thr	threonine
TZD	thiazolidinedinones
UCP-3	uncoupling protein-3
ZMP	5-aminoimidazole-4-carboxamide ribonucleoside monophosphate, AMP analogue

CHAPTER 1: REVIEW OF LITERATURE

AMP-Activated Protein Kinase

Introduction

Protein kinases are the largest known eukaryotic protein superfamily, with at least 500 genes encoding different members of this class of proteins (71). These proteins are enzymes that alter the function of other proteins by covalently attaching the gamma phosphate of ATP to a protein alcohol (on Ser or Thr) and/or protein phenolic (on Tyr) target. This forms the major cellular system that responds to extracellular signals (hormones, neurotransmitters, growth and differentiation factors, nutritional and environmental stress) and changes cellular function and metabolism in eukaryotic cells (71, 72). Protein kinases can also rapidly switch the activities of cellular proteins through a G protein-mediated cycle, involving GTP as the phosphate donor, as well as allosteric (non-covalent) regulation, whereby a ligand binds to modify the activity of downstream proteins (72).

AMP-activated protein kinase (AMPK) has emerged as an important metabolic enzyme, and it has been suggested that this enzyme cascade plays a role in the regulation of a variety of metabolic processes in skeletal muscle, by phosphorylating and modulating the activity of key, rate-limiting enzymes. Early studies identified AMPK as an important regulator of cholesterol synthesis and *de novo* lipogenesis in liver (10, 31). Later studies demonstrated AMPK-mediated effects on fatty acid (FA) metabolism (increased FA oxidation, decreased triacylglycerol (TAG) synthesis) (125, 130) and stimulation of glucose uptake (13, 125) in skeletal muscle.

Abnormalities in FA metabolism in skeletal muscle in obese, insulin resistant states include reductions in FA oxidation (89, 102, 105) and accumulation of intramuscular lipids (1, 11, 25, 136, 160, 178, 179, 190). Skeletal muscle oxidative capacity has been shown to be a better predictor of insulin sensitivity than TAG accumulation (23), suggesting that AMPK may be involved in the regulation of FA partitioning and quite possibly, the prevention of insulin resistance and Type 2 diabetes mellitus (T2DM). However, the role that AMPK plays in the regulation of FA metabolism and glucose utilization is unclear and the potential of AMPK activation in the prevention of T2DM in the obese state is largely unknown.

Therefore, the primary objectives of this thesis were to examine 1) the acute metabolic effects of activating AMPK; and 2) whether interventions known to activate AMPK in skeletal muscle (the anti-diabetic drug metformin and exercise) could prevent the progression of T2DM in an obese, high-fat fed rodent model, the Zucker diabetic fatty (ZDF) rat.

The following literature review will begin by outlining the discovery of AMPK and the AMPK signaling cascade. The regulation of fat and carbohydrate (CHO) fuel selection in resting and contracting skeletal muscle and the role that AMPK plays in acute and chronic regulation of fat and CHO metabolism will be discussed. This review will then discuss the pathogenesis and abnormalities of FA metabolism in skeletal muscle insulin resistance. Lastly, this review will outline interventions known to activate AMPK (exercise, adipokines, anti-diabetic agents) and potentially alter FA metabolism in obese insulin resistant states.

Discovery of AMP-activated Protein Kinase

An unknown protein was initially described in 1973 as an "activity" that phosphorylated and inactivated 3-hydroxy-3-methylglutaryl-CoA reductase (HMG-CoA reductase), altering cholesterol synthesis in liver (10). This protein was later named AMP-activated protein kinase (AMPK), as this single protein was activated by AMP to elicit an ATP-dependent inactivation of both HMG-CoA reductase (phosphorylation of Ser781) and acetyl-CoA carboxylase (ACC; phosphorylation of Ser79) in rat liver (31). Initially it was unclear whether AMPK had a significant role in other tissues, as the assay was dependent on the use of these two hepatic enzymes to quantify activity. The development of a synthetic peptide based on the amino acid sequence around Ser79 of ACC (SAMS peptide, sequence: HMRS**A**MSGLHLVKRR) which replaced the cAMP-dependent protein kinase phosphorylation site at Ser 77 with an Arg residue, allowed for the specific study of AMPK activity in multiple tissues (42). Initially, high basal AMPK activity suggested that this enzyme may play a more important role in tissues with very high rates of lipid metabolism (liver, mammary gland) and less AMPK activity in other tissues such as kidney and skeletal muscle suggested that AMPK may not be important in all tissues (42). However, further studies indicated that AMPK may in fact play an important functional role in skeletal muscle. Skeletal muscle possesses abundant AMPK mRNA (42) and AMPK protein is present predominantly in a dephosphorylated (less active) isoform (191), suggesting that it has a significant capacity for stimulation.

Further study of the structure of AMPK in subsequent years allowed for the identification of the enzyme as a heterotrimeric complex, consisting of an initially identified catalytic alpha (α) subunit (p63) (30), and two regulatory subunits, beta (β) and gamma (γ) (171). Further investigation demonstrated that the AMPK heterotrimeric complex is composed of different isoforms (α_1, α_2, β_1, β_2, γ_1, γ_2, γ_3), each being expressed by seven different genes. The predominant complex found in most cells is the $\alpha_1\beta_1\gamma_1$ enzyme, with skeletal muscle possessing the unique property of expressing all three γ isoforms (73). AMPK exists in the cytoplasm but also as a localized nuclear fraction (2), with the α2 subunit showing sublocalization in both the cytosol and the nuclei of muscle, and is involved in metabolic gene transcription (157).

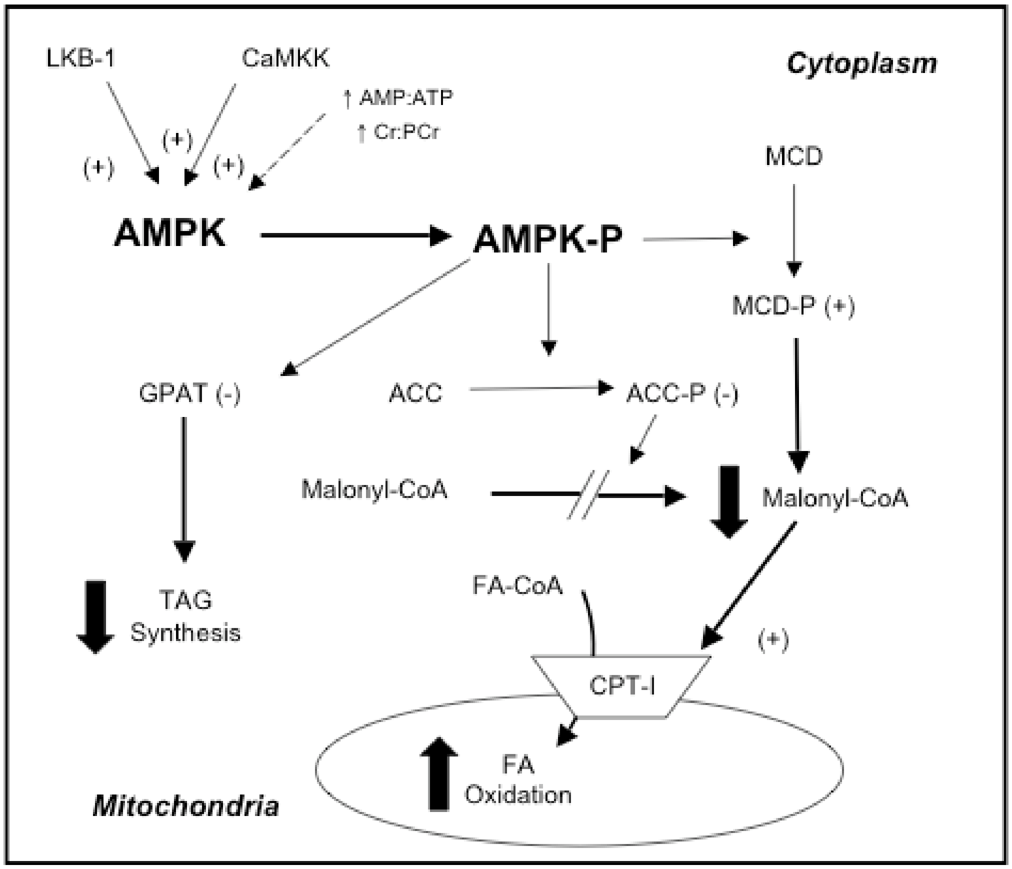

Figure 1: AMPK Signaling Cascade

AMPK is activated by phosphorylation via at least two upstream AMPK kinases, LKB-1 and Ca^{2+}-calmodulin protein kinase kinase (CaMKK), as well as allosterically by increases in the AMP:ATP and Cr:PCr ratio. Activated AMPK then phosphorylates and regulates the activity of key rate-limiting enzymes in FA oxidation (via acetyl-CoA carboxylase (ACC) and malonyl-CoA decarboxylase (MCD)) and triacylglycerol (TAG) synthesis (*sn*-glycerol-3-phosphate acyltransferase (GPAT).

AMPK Signaling Pathway

AMPK is activated by a number of putative upstream kinases, as well as allosterically by an increase in the AMP:ATP and Cr:PCr ratios, signaling a decrease in energy provision within the cell, with a subsequent cascade leading to the inhibition of energy consuming processes and an activation of ATP producing pathways (*Figure 1 and Figure 2*). Indeed, AMPK has been demonstrated to be involved in the stimulation of FA oxidation (125, 130), inhibition of TAG synthesis (3, 130), increased GLUT4 expression (97), activation of GLUT4 translocation (152) and stimulation of glucose uptake (125), leading to increased ATP synthesis and a restoration of cellular homeostasis. The enzyme cascade involves a number of important enzymes and regulators, both upstream and downstream of AMPK itself (*Figure 1*).

i) Upstream Cascade Intermediates

Recent evidence suggests that at least two upstream AMPK kinase (AMPKK) enzymes may be involved in the regulation of AMPK phosphorylation and activity. Early evidence in rat liver extracts identified a distinct endogenous "kinase kinase" which activated both highly purified native AMPK and the 63 kDa catalytic subunit in the presence of Mg[γ^{32}P]ATP (194). Activation of AMPK by AMPKK required AMP, was antagonized by high ATP concentrations and AMPKK was not inactivated by protein phosphatases. With the use of Mg[γ^{32}P]ATP and subsequent chromatography techniques, the major site of phosphorylation and activation of AMPK by AMPKK was discovered to be threonine-172 (Thr172) on the catalytic α-subunit (75). Enhanced techniques allowed for a more rigorous >1000-fold purification process of AMPKK from rat liver, although this AMPKK was not isolated to purity (75). Due to the persistent technical difficulties in purifying the AMPKK enzyme(s) using conventional protein purification processes (chromatography) and no subsequent cDNA cloning analyses available, candidate "kinase kinase" enzymes were not identified.

Later evidence in yeast (*Saccharomyces cerevisiae*) identified three protein kinases, Elm1p, Pak1p and Tos3p that phosphorylate and activate Snf1 (sugar non-fermenting 1), the yeast homolog of AMPK (85, 183). Additionally, Tos3 phosphorylated and activated mammalian AMPK *in vitro* (85) demonstrating functional conservation of this kinase cascade between yeast and mammals. The closest homologues in the mammalian genome are the tumour suppressor LKB1 and Ca^{2+}/calmodulin-dependent protein kinase kinase (CaMKK), making these two proteins candidates for putative AMPKK enzymes.

LKB1 was subsequently shown to be capable of phosphorylating and activating bacterially expressed AMPK *in vitro* (85). LKB1 also co-purified with AMPKK during chromatography purification of cell extracts from rat liver, was able to phosphorylate and activate the catalytic α isoforms of AMPK, and subsequent immunoprecipitation with anti-LKB1 resulted in an immunocomplex that was able to activate AMPK, accounting for the majority of the kinase kinase activity compared to the remaining supernatant (209). However, mechanisms regulating LKB1 activity in skeletal muscle are poorly understood. LKB1 is present in muscle in high amounts (155) and may be constitutively active and not respond to changes in AMP *in vitro* (209) or in rat skeletal muscle (155). LKB1 is not activated by *in situ* contraction, 5-aminoimidazole-4-carboxamide ribonucleoside (AICAR) and phenformin (a metformin analogue), all of which activate AMPK via either AMP-dependent (contraction, AICAR) and AMP-independent (phenformin) mechanisms (*Figure 2*) (155). This leads to the possibility that LKB1 may be involved in an AMP-dependent mechanism which may allow for AMP to bind specifically to AMPK, inducing an allosteric change in the conformation of the enzyme and making AMPK a better substrate for LKB1, with LKB1 itself not requiring AMP.

The presence of other upstream AMPKKs was suggested when significant basal AMPK activity was still exhibited in mouse embryo fibroblasts (MEF) (77) and HeLa cells (91) which lack LKB1 and rat liver cells expressing a dominant negative LKB1 isoform (209). Activation of AMPK in MEF and HeLa cells occurs with a Ca^{2+} ionophore, A23187, which is subsequently antagonized by the CaMKK inhibitor STO-609, suggesting a (CaMKK) Ca^{2+}-dependent mechanism (77, 91). Two isoforms of CaMKK (α and β) exist in mammalian cells, with overexpression and siRNA cell models suggesting that CaMKKβ may be the important isoform for both basal and activated (hydrogen peroxide, osmotic stress and ionomycin) AMPK activity (77, 91, 208).

These recent studies raise the possibility that multiple 'kinase kinase' cascades may converge on AMPK. However, the presence of additional upstream activators that absolutely require AMP is suggested by early studies showing that purified rat liver AMPK absolutely required AMP for phosphorylation and activation by an upstream

AMPKK (75). Also limiting the study of these enzymes in skeletal muscle is the fact that the generation of LKB -/- mice is embryonically lethal (203) and the lack of specificity of the CaMKK inhibitor STO-609, which also inhibits AMPK and LKB1 (77).

ii) Downstream Cascade Intermediates

Much work has investigated the roles that malonyl-CoA, ACC and malonyl-CoA decarboxylase (MCD) play in the regulation of fat metabolism in multiple tissues. Malonyl-CoA is the first committed intermediate in *de novo* synthesis of FA in liver and is formed through the rate-limiting carboxylation of acetyl-CoA through ACC (*Reaction 1*) and is removed by MCD (*Reaction 2*).

$$\text{Acetyl-CoA} + HCO_3^- + \text{ATP} \rightarrow \text{Malonyl-CoA} + \text{ADP} + P_i \qquad [\textit{Reaction 1}]$$

$$\text{Malonyl-CoA} \rightarrow \text{Acetyl-CoA} + CO_2 \qquad [\textit{Reaction 2}]$$

Malonyl-CoA was first shown to inhibit CPT-I by McGarry *et al.* in 1977 (120). CPT-I spans the outer mitochondrial membrane and is the rate-limiting enzyme in FA entry and subsequent oxidation and ketogenesis in liver. Malonyl-CoA inhibition of CPT-I is a key regulatory step in tissues such as liver and adipose tissue to ensure that when glucose is abundant, it is directed to fat synthesis, while a coordinate inhibition in FA oxidation occurs. Malonyl-CoA and CPT-I were later found to be present in a variety of non-hepatic rodent tissues, including heart and skeletal muscle, with isolated skeletal muscle mitochondrial CPT-I being ~200-times more sensitive to malonyl-CoA inhibition than the liver isoforms, requiring a much lower (~34 nM) malonyl-CoA I_{50} concentration than in liver (I_{50}=2700 nM) (121).

Since skeletal muscle has very little or no capacity for *de novo* lipogenesis, there was speculation that malonyl-CoA may be playing a role in other FA-related processes. Indeed, malonyl-CoA content decreases substantially during fasting and starvation in liver, heart and skeletal muscle (121), when these tissues rely on FA oxidation as the key source of energy. This led to the hypothesis that malonyl-CoA may be an important regulator of CPT-I and subsequent FA oxidation in multiple tissues and that there may be situations where inhibition of CPT-I is relieved by decreased concentrations of malonyl-CoA, allowing for increased FA oxidation in skeletal muscle.

Similar situations to fasting/starvation include prolonged submaximal exercise bouts, in which FA oxidation is a major energy source for working muscle. Winder *et al.* found that malonyl-CoA content decreased in rat gastrocnemius muscle after an acute 30 min treadmill exercise protocol (21m/min, 15% grade) (198). Further studies showed that malonyl-CoA decreases in both a fiber-type and time-dependent manner, with the most rapid decreases seen in oxidative red quadriceps (Type IIA; 5 min, 52% of resting malonyl-CoA) > gastrocnemius (mixed fiber type; 10 min, 30-40% of resting malonyl-CoA) > soleus (Type I; 20 min, 61% of resting malonyl-CoA) > white quadriceps (Type IIB; initial 5 min 55% increase; 120 min, 25% of resting malonyl-CoA) (199). With the exception of white quadriceps, changes in malonyl-CoA content occurred before any significant increase in plasma FA, suggesting that malonyl-CoA and CPT-I are mechanisms that regulate substrate selection for oxidation within rat skeletal muscle itself (199). However, it is important to note that although the AMPK-malonyl-CoA-CPT-I axis was the prevailing hypothesis for the regulation of FA oxidation during fasting and exercise, functional FA oxidation measurements were never measured until *in vitro* activation of AMPK was possible (**See Regulation of Fat and Carbohydrate Fuel Selection in Skeletal Muscle**).

Subsequently, much work was done to investigate the regulatory role of ACC in various rat tissues. Data emerged from a number of laboratories suggesting that ACC was present in multiple extra-hepatic tissues, including liver (17, 189), heart (17, 189) and skeletal muscle (17, 188, 189, 200). Early evidence suggested that purification of ACC from cytosolic fractions of rat liver yielded two biotin-containing, high molecular weight proteins, a predominant 265 kDa species (~85-90% of total mass) and a 280 kDa species (~10-15% of total mass) (17). Further analyses of tissue distribution of these two species demonstrated that both isoforms were present in liver, brown adipose tissue and mammary gland, while the 280 kDa species was only present in heart and diaphragm muscle (17). Additional characterization of rat gastrocnemius and quadriceps skeletal muscle has suggested that a biotin-containing cytosolic ACC is present in skeletal muscle, with malonyl-CoA formation being dependent on the presence of ACC, citrate (allosteric activator and precursor of cytoplasmic acetyl-CoA via ATP citrate lyase), bicarbonate and ATP (188). Isoform-specific examination suggested that both 265 kDa and 280 kDa ACC protein contents in liver decreased with fasting, leading to decreased malonyl-CoA content (121) and were induced with refeeding of a high-carbohydrate diet.

However, the protein content of the 280 kDa isoform in skeletal muscle was unaltered by nutritional manipulations (17), suggesting different functions of these two ACC isoforms in different tissues.

The first direct evidence of an interaction between ACC and AMPK emerged in 1996 when Winder and Hardie (200) demonstrated *in vitro* that ACC purified from rat gastrocnemius and quadriceps was phosphorylated by purified rat liver AMPK in the presence of ATP and the extent of phosphorylation was enhanced by AMP. Coordinate regulation of AMPK and ACC was also demonstrated *in vivo* in rodent red quadriceps muscle after a short-term (up to 30 min) treadmill exercise bout where AMPK activity was increased by 5 min and sustained over 30 min, which was accompanied by sustained decreases in ACC activity and malonyl-CoA content, all occurring by 5 min (200). However, it was not known whether changes in ACC activity were contraction-mediated (ie. due to changes in Ca^{2+} and/or increased AMP) or attributed to hormonal changes (increased epinephrine) that occur during exercise. Further investigation using *in situ* electrical stimulation of the hindlimb of rats allowed for the isolation of contraction-mediated effects with no associated changes in epinephrine and allowed for the contralateral leg to act as a control. Indeed, *in situ* electrical stimulation showed a rapid (5 min) decrease in ACC activity, leading to decreased malonyl-CoA content (10 min) in the gastrocnemius-plantaris muscle group. However these changes were not concurrent with increased upstream AMPK activity, which was not significantly increased until 20 min of electrical stimulation (92). The reasons for this disparity may not have been due to a lack of regulation of ACC by AMPK. Small, undetectable increases in AMPK phosphorylation and activity may lead to rapid and amplified ACC activity. Possibly more important was the estimated free AMP concentration that increased early in the protocol (10 min), suggesting that allosteric activation of AMPK by the increased AMP:ATP ratio is also an important regulator of AMPK. Allosteric regulation of AMPK is not quantifiable after tissue lysis and protein extraction. The AMPK-SAMS activity assay is an important and valid technique for examining AMPK regulation of ACC/malonyl-CoA and FA oxidation, however, the assay only measures activity attributed to the increased phosphorylation state of AMPK.

Changes in malonyl-CoA content are also regulated by malonyl-CoA decarboxylase (MCD), which is seldom measured in skeletal muscle. Therefore, most studies have typically only examined the synthesis rates of malonyl-CoA (ie. ACC) and negated the degradation rates via MCD. The few studies that have examined MCD in rat skeletal muscle have shown that MCD degrades malonyl-CoA and is regulated by AMPK activation with *in situ* contraction (154), treadmill exercise (137) and AICAR (154). Activity of MCD is similar to ACC activity in soleus muscle (3), and AMPK coordinately deactivates ACC and activates MCD (137), allowing for dual control of malonyl-CoA content.

Although malonyl-CoA content decreases during exercise in rat skeletal muscle, there is much speculation as to the extent to which malonyl-CoA plays a role in the regulation of FA oxidation in both rat and human skeletal muscle during exercise. Resting values of malonyl-CoA in human muscle are ~1/10 of that in rat muscle (~0.2

nmol/g in human muscle vs. ~1.5-2 nmol/g in rat muscle) (9, 43, 134). Furthermore, the IC_{50} concentration of malonyl-CoA for CPT-I is ~34 nM (121), suggesting that CPT-I is maximally inhibited even at rest and reductions in malonyl-CoA would not further impact FA oxidation rates. In human muscle, malonyl-CoA content decreases only modestly at the onset of low intensity exercise (1 min; 35% VO_{2max}) but returns to rest values after 10 min (135) and remains unchanged during moderate intensity exercise in humans (134, 135), where fat utilization is predominant. At higher intensity exercise outputs, an expected increase in malonyl-CoA to inhibit FA oxidation does not occur (135) and even modest decreases (-12-17%) in malonyl-CoA content has been observed (43), suggesting that malonyl-CoA does not diminish FA oxidation at high power outputs. Compartmentalization of malonyl-CoA is possible, as malonyl-CoA content is typically measured in whole muscle homogenate and raises the possibility that there may be a shift in sensitivity of local mitochondrial concentrations of malonyl-CoA that would interact with CPT-I.

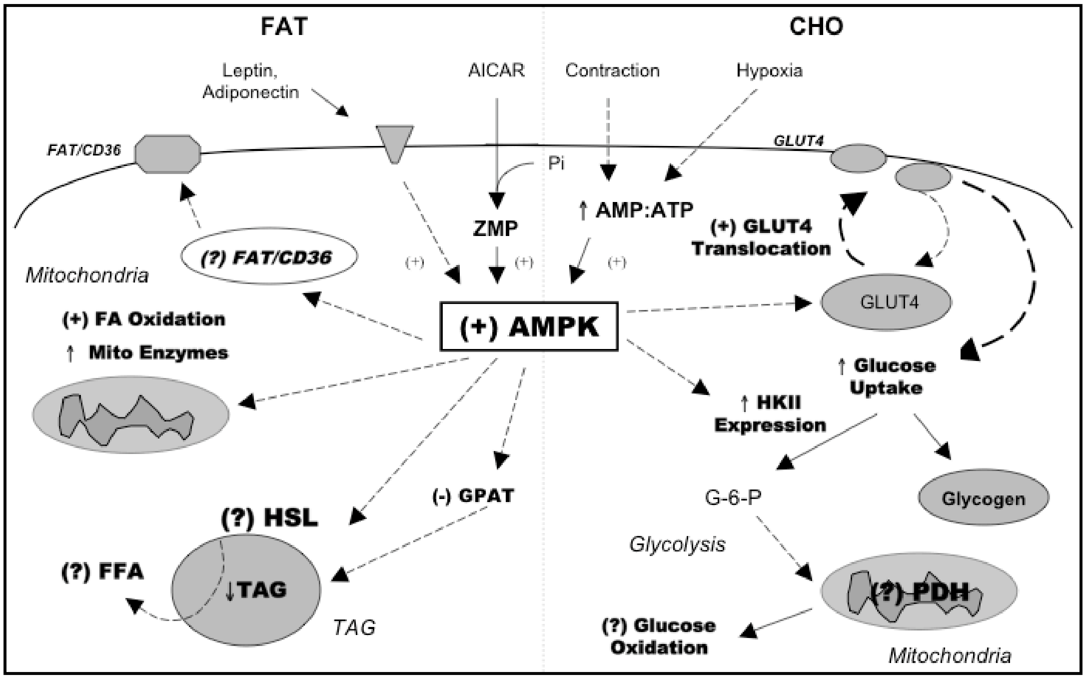

Figure 2: AMPK Regulation of Fat and Carbohydrate (CHO) Metabolism
AMPK activation leads to increased GLUT4 translocation and increased glucose uptake, and the stimulation of energy producing pathways, including FA oxidation, while inhibiting energy consuming pathways, such as TAG synthesis. Less known are the effects of AMPK on important rate-limiting enzymes, such as pyruvate dehydrogenase (PDH) activity and subsequent glucose oxidation. AMPK regulation of hormone sensitive lipase (HSL) is poorly understood, as it appears that AICAR activation of AMPK inhibits HSL.

Regulation of Fat and Carbohydrate Fuel Selection in Skeletal Muscle

Skeletal muscle is a major contributor to whole-body energy metabolism, accounting for >80% of total insulin-stimulated glucose disposal, and predominantly utilizes FA during fasting and low- to moderate-intensity exercise (151). With evidence suggesting that AMPK is a component of an important energy-sensing system, this protein kinase cascade offered a more contemporary hypothesis for substrate selection in skeletal muscle. This differed from the traditional glucose fatty-acid cycle originally proposed by Randle *et al* (144) in 1963 to explain the substrate-driven reciprocal relationship between rates of glucose and FA oxidation. In certain states such as fasting, starvation and diabetes, FA released from adipose tissue stores increase and accumulation of plasma FA and ketone bodies from incomplete hepatic FA oxidation occurs. These FA and ketone bodies are available for uptake and preferential use by muscle. In studies mainly conducted in heart and diaphragm muscle, four main regulatory steps in CHO metabolism were identified as being inhibited by increased FA and ketone bodies through the accumulation of their respective allosteric inhibitors. These included membrane transport (inhibition of hexokinase (HK)), phosphorylation of glucose (hexokinase reaction, by an increase in glucose-6-phosphate, G-6-P), phosphofructokinase (PFK) activity (inhibition by increased cytosolic citrate), and pyruvate dehydrogenase (PDH) activity (mediated by increased [acetyl-CoA]/[CoA]).

Since the original glucose-fatty acid cycle hypothesis was proposed, there has been much debate as to the extent to which this reciprocal substrate-driven cycle may regulate glucose and FA oxidation in skeletal muscle. Cardiac and diaphragm muscle differ from skeletal muscle as they display high oxidative capacity, and a significant ability to oxidize exogenous FA and regulate substrate use based on constant contractile activity. Skeletal muscle is a dynamic tissue, which is not as oxidative and must respond to sudden changes in energy utilization (rest to contraction). There is evidence that this cycle may be occurring at rest, as a select number of *in vivo* studies in healthy humans have shown that elevated plasma FA levels inhibit whole-body glucose disposal during hyper- and euglycemic hyperinsulinemic clamps (104, 149). On the contrary, a number of studies in healthy (207), obese (14) and diabetic (15) humans have failed to demonstrate similar effects of elevated FA inhibiting whole-body glucose metabolism at rest. Furthermore, extrapolating these results to skeletal muscle, especially contracting skeletal muscle, is presumptuous. The classic study to support the existence of the glucose fatty-acid cycle in contracting perfused rat hindlimb muscle is that by Rennie & Holloszy in 1977 (147). However, many subsequent studies have failed to support the operation of this cycle in contracting muscle in both rodent (52, 53, 55) and human (54) models, where it is clear that elevations in citrate and acetyl-CoA content are not responsible for decreased CHO utilization. Pooled data from short-term intense exercise protocols in humans suggest that increased FA may spare glycogen by regulating the post-transformational modification of glycogen phosphorylase through changes in high-energy phosphates (AMP, ADP, P_i) (52, 54).

Therefore, a more contemporary hypothesis of the regulation of glucose and FA metabolism in contracting skeletal muscle may be mediated by changes in the energy charge (activation of AMPK through increased AMP:ATP ratio) and fine-tuning with substrate changes (ie. malonyl-CoA).

Acute AMPK Regulation and Substrate Use in Resting Skeletal Muscle

i) Regulation of Intramuscular Triacylglycerol

The study of acute AMPK regulation of metabolism has been made possible by the development of a cell-permeable AMPK activator, 5-aminoimidazole-4-carboxamide ribonucleoside (AICAR). AICAR enters the cell and is phosphorylated by adenylate kinase to form the AMP analogue, 5-aminoimidazole-4-carboxamide ribonucleoside monophosphate (termed ZMP). This phosphorylated ZMP compound is sustained at high levels within the cell (125) and mimics the increased AMP:ATP ratio observed during metabolic stress (hypoxia, contraction, exercise) (*Figure 2*) (153) and has been shown to activate purified AMPK *in vitro* (40). Early studies in rat hepatocytes (40) and adipocytes (40, 181) demonstrated that incubation with AICAR resulted in 3- to 8-fold increased AMPK activity, decreased lipid synthesis and inhibited lipolysis induced by the β-adrenergic agonist isoprenaline. At least some of AICAR's effects in these cells were shown to be due to increased phosphorylation and inactivation of known targets of activated AMPK, HMG-CoA reductase in hepatocytes (40) and ACC in hepatocytes and adipocytes (181). Adipocyte hormone sensitive lipase (HSL) contains two phosphorylation sites, the basal (Ser565) and cAMP-dependent protein kinase (protein kinase A) regulatory (Ser 563) sites and it was further postulated that AMPK may be phosphorylating the basal site, thereby modifying the activity of HSL during times of adrenergic stimulation and playing an anti-lipolytic role *in vivo* (181). However, regulation of skeletal muscle TAG hydrolysis is poorly understood. A muscle-specific isoform of HSL has been identified (110) and is activated by both epinephrine (109) and contraction (111), in at least a partially additive manner, suggesting regulation by distinct mechanisms. Skeletal muscle AICAR-stimulated AMPK activation would be expected to stimulate intramuscular TAG hydrolysis and subsequent FA oxidation for energy production. Paradoxically, AICAR treatment has been shown to inhibit epinephrine-stimulated HSL activation in L6 myotubes (193) and an anti-lipolytic effect of AICAR treatment has been demonstrated in rat soleus muscle (3) and in C_2C_{12} myotubes (130).

ii) Regulation of FA Oxidation

The first evidence of a direct link between a decrease in malonyl-CoA content, and an increase in FA oxidation in skeletal muscle was with the use of AICAR. AICAR decreases malonyl-CoA content in isolated soleus muscle (3), similar to the known effects of treadmill exercise (200) and *in situ* muscle contraction (92) in rats. Merrill *et al*. (126) showed that during a 45-minute rat hindlimb perfusion protocol, changes in gastrocnemius-plantaris AMPK regulatory cascade (increased AMPK activity, decreased ACC activity and decreased malonyl-CoA) were associated with increased hindlimb FA oxidation by 15 minutes of AICAR exposure. Furthermore, AICAR treatment in highly oxidative mouse soleus muscle *in vitro* increased FA oxidation while simultaneously inhibiting TAG synthesis (130). These effects were postulated to include both the AMPK-ACC-malonyl-CoA axis to partition FA to oxidation, and the inhibition of mitochondrial *sn*-glycerol-3-phosphate acyltransferase (GPAT) (*Figure 2*). GPAT is thought to be the first committed step in TAG synthesis, although this was only demonstrated in isolated rat hepatocytes and not in intact muscle due to very low levels of GPAT expression in the latter tissue (130). Further investigation of changes in malonyl-CoA content via stimulation with AICAR in isolated EDL led to a two-fold increase in MCD activity (154). This suggests that activation of AMPK not only phosphorylates and inactivates ACC but also phosphorylates and activates MCD, allowing for dual control of malonyl-CoA content and FA oxidation in muscle.

iii) Regulation of Glucose Uptake

Also important was the finding that AICAR simultaneously increased glucose uptake (*Figure 2*) into hindlimb muscles over the 45-minute protocol that demonstrated increased FA oxidation rates (126). There has been debate as to the extent that AICAR activates AMPK and stimulates glucose uptake in specific muscle fiber types. Acute AICAR treatment increases AMPK activity 60-90 min after AICAR injections or infusions in glycolytic and oxidative muscle fibers (2, 12, 13, 97, 201). Subsequent stimulation of glucose uptake with AICAR in glycolytic muscle has been consistently shown both *in vivo* and *in vitro* (2, 8, 12, 97), while increased glucose uptake only seems to occur with *in vivo* infusion of AICAR in oxidative soleus and red gastrocnemius (RG) (12, 13). This raises the possibility of the dissociation of AMPK activity from glucose uptake in oxidative skeletal muscle. Nonetheless, AMPK activation may be increasing the ability of muscle to meet energy needs by stimulating both fatty acid oxidation and glucose uptake.

Further study pertaining to AMPK regulation of glucose uptake has involved the use of the putative AMPK inhibitors, adenosine 9-β-D-arabunofuranoside (araA) and iodotubercidin. Preincubation with araA and iodotubercidin decreased AICAR-induced AMPKα2 activity (131) and decreased 3-O-methyl-glucose uptake (3-O-MG) in isolated rat epitrochlearis muscle (131) and isolated rat ventricular papillary muscle (152). Insulin-stimulated glucose uptake involves an insulin receptor-associated PI3-kinase mechanism, and both of these putative inhibitors had no effect on insulin-stimulated glucose uptake in ventricular papillary muscle (152), suggesting that AMPK activation during metabolic stress and subsequent increases in glucose uptake are independent of the PI3-kinase signaling pathway. This PI3-kinase independent pathway has also been shown with the combination of AICAR and wortmannin, a specific PI3-kinase inhibitor (78). However, the specificity of these putative AMPK inhibitors has been a matter of debate. Specifically, iodotubercidin also inhibits basal (no AICAR) AMPKα2 activity and contraction-stimulated 3-O-MG uptake is inhibited with araA but not iodotubercidin (131), suggesting that these substances may have non-specific effects on regulatory steps in basal and contraction-stimulated conditions.

iv) Regulation of Glucose Oxidation

Few studies have specifically examined the effect of AICAR on subsequent glucose oxidation. In isolated human endothelial cells, AICAR simultaneously increased both FA and glucose oxidation, leading to an increase in ATP provision (41). The only study to date using isolated skeletal muscle showed that 60 min of AICAR exposure in oxidative soleus muscle from fed rats decreased glucose oxidation secondary to an increase in FA oxidation (ie. glucose fatty-acid cycle) (100). However, teleologically, one would expect that in response to a decrease in cellular energy charge, AMPK activation would simultaneously increase ATP production from both FA and glucose oxidation in skeletal muscle.

v) Acute AMPK Regulation of Gene and Protein Expression

AMPK signaling has been shown to be involved in rapid, short-term mRNA and protein synthesis regulation that may be involved in altering metabolic function under conditions of fuel depletion, such as fasting and exercise. Specifically, AICAR treatment in isolated EDL muscle (217) or after a single subcutaneous AICAR injection (177) increases uncoupling protein-3 (UCP-3) (177, 217) and hexokinase (HK)-II (177) mRNA, and UCP-3 protein expression in as little as 30 minutes (217). Longer-term upregulation of GLUT4 mRNA 13 hours after a subcutaneous AICAR injection has also been demonstrated in white and red quadriceps, but not soleus muscle (215). These data suggests rapid AMPK-mediated upregulation of genes involved in increased uptake and metabolism of FA and glucose.

Chronic AMPK Regulation and Substrate Use in Resting Skeletal Muscle

AMPK is activated during exercise (200) and is associated with increased glucose uptake and FA metabolism in skeletal muscle. Therefore, it has been suggested that chronic effects of endurance exercise that increase insulin sensitivity may be reproduced by repeated injections of AICAR in rats. Chronic AICAR treatment (daily injections, ranging from 5 days (28, 84, 97) to 2 (184) or 4 (201) weeks) has multiple effects on rat skeletal muscle, including increased total muscle GLUT4 protein expression (84, 97, 201), increased insulin-stimulated plasma membrane GLUT4 protein content (28), increased insulin-stimulated glucose uptake (28, 97), increased HK protein content (84, 201) and increased glycogen content (84).

The potential for increased mitochondrial biogenesis and oxidative capacity with chronic AICAR treatment has also been observed with increased PPARgamma-coactivator-1α (PGC-1α) protein content (184), increased activity of mitochondrial enzymes (201), increased UCP-3 as well as changes in fiber type composition in EDL with decreased percentage of Type IIb (fast glycolytic) and concomitant increases in Type IIa (fast oxidative-glycolytic) fibers (184).

Additionally, chronic AICAR administration in models of insulin resistance and diabetes have demonstrated beneficial effects on insulin sensitivity. In insulin resistant obese Zucker rats, daily AICAR injections decreased fasting glucose and insulin, normalized oral glucose tolerance and increased insulin-stimulated glucose uptake and total muscle GLUT4 expression in mainly fast-twitch muscle fibers (27). Additionally, obese Zucker rats showed decreased plasma triglycerides and free fatty acids, increased plasma HDL and decreased systolic blood pressure (27), suggesting that AICAR may be activating AMPK in other tissues such as liver. As well, in *ob/ob* and *db/db* mice, AICAR (2x/day for 8 days) decreased blood glucose concentrations and increased total GLUT4 protein content in muscle, although this was accompanied by increased serum TG content (70). This raises potential safety concerns of AICAR as a pharmacological activator of AMPK, as large doses are required (at least 1mg/g body weight) and the potential for effects in multiple tissues, especially the liver, as AICAR induces liver hypertrophy (201). Nonetheless, chronic effects of exercise have been mimicked with AICAR injections and this has raised the possibility of the use of AMPK activators in treating individuals with T2DM.

AMPK Regulation of Metabolism During Muscle Contraction and Exercise

Acute AMPK Regulation and Substrate Use During Contraction & Exercise

i) Regulation of FA Oxidation

Early studies in rats showed that treadmill exercise decreased malonyl-CoA levels (198) was due to concomitant activation of AMPK, which subsequently phosphorylated and inactivated ACC (200) and provided strong evidence that AMPK activation could increase FA oxidation for ATP provision (125). However, AMPK may not be critical for the regulation of malonyl-CoA levels and subsequent FA oxidation during lower intensity muscle contraction (145) and exercise (131, 146, 198-200). In rats, malonyl-CoA levels decrease during moderate- to high-intensity treadmill exercise (21 m/min, 15% grade, at least 20 min) (198-200) and upon examination of different treadmill exercise intensities over 20 min (10, 20, 30, 40 m/min, 5% grade), it was suggested that although ACC activity and malonyl-CoA content decreased over all intensity levels in fast-twitch oxidative red quadriceps muscle, AMPK activity only increased at intensities above 20 m/min (146). This has also been confirmed in rats for a longer duration of one hour, demonstrating that AMPKα2 was only elevated after running at 32m/min, but not 18 m/min (131). In addition, low intensity electrical stimulation protocols in perfused rat hindquarters suggest that although malonyl-CoA is decreased (~50%) and FA oxidation is increased (~75%), AMPKα2 activity is not elevated (145).

Whether the AMPK-ACC-malonyl-CoA axis is important in determining substrate utilization in humans is a matter of debate. Indeed, activation of AMPKα2 across different exercise intensities does not support AMPK having a major role in FA oxidation in humans. AMPKα2 activation has been observed during moderate- (above 60% VO_{2max}) (35) to high-exercise intensity (80-85% VO_{2max}) (35, 206) exercise, whereas maximal rates of FA oxidation occur most prominently with lower intensity exercise (151). Furthermore, calculated FA oxidation rates increase in parallel with ACC phosphorylation at low- and moderate-intensity exercise (35), suggesting that ACC is very sensitive to exercise and undetectable changes in AMPK may possibly be having an effect on the downstream signaling cascade. In addition, resting levels of malonyl-CoA in humans are much lower than rats (43, 134) and malonyl-CoA levels do not decrease during 70 minutes of sub-maximal (~65% VO2max) cycling exercise (134).

ii) Regulation of Glucose Uptake

Merrill *et al*. demonstrated that AICAR stimulated glucose uptake in perfused rat hindlimb muscle (125), and provided the first evidence that the AMPK signaling pathway might be responsible for contraction-mediated increases in glucose uptake in skeletal muscle. In isolated rat epitrochlearis muscle, glucose transport rates were increased with electrical stimulation, AICAR and insulin, whereas AMPK was activated by electrical stimulation and AICAR, but not with insulin (13, 78). The combination of AICAR and insulin had additive effects on glucose uptake, and wortmannin (a specific PI3-kinase inhibitor) inhibited insulin-stimulated glucose uptake but had no effect on AICAR or contraction-stimulated glucose uptake. These data, along with the lack of additivity of glucose uptake when AICAR and contraction were combined (12, 78) suggests that

AICAR and contraction stimulate glucose transport by similar insulin-independent mechanisms and that AMPK was involved in contraction-stimulated glucose uptake.

However, there is much debate as to the extent to which AMPK is necessary for exercise-stimulated glucose transport in skeletal muscle. A more robust 3- to 5-fold activation of AMPK has been observed in glycolytic epitrochlearis muscle (2), while more modest 2- to 3-fold AMPK activation in oxidative soleus muscle (78) is seen in short-term (10 min), tetanic contraction protocols. In oxidative rat soleus muscle, AICAR did not increase 2-deoxyglucose transport or AMPK activity from fasted rats (2) whereas in soleus muscle from rats with high glycogen content, contraction increased glucose transport without any increases in AMPK activity (44). More definitive evidence came from detailed studies by Mu *et al*. (128), who constructed transgenic mice expressing an inactive "dominant negative" AMPKα2 subunit mutant, which completely replaces the endogenous AMPKα1 and AMPKα2 subunits in the heterotrimeric $\alpha\beta\gamma$ complex. Basal AMPK activity is almost undetectable in these mice and there is no increase in contraction-mediated AMPK activity; however, only AICAR- and hypoxia-stimulated glucose uptake were completely abolished, while there was only a partial reduction in contraction-stimulated glucose uptake (128), suggesting that although AMPK has been shown to be involved in contraction-stimulated glucose transport, it is not necessary and there are likely other mechanisms that regulate this process, such as a Ca^{2+}-mediated mechanism.

Chronic AMPK Regulation: Effects of Endurance Exercise

AMPK has been suggested to be involved in some of the chronic adaptations to endurance training, such as increased mitochondrial content and increased respiratory capacity. AMPK activity is decreased in rat (48) and human (133) muscle after prior exercise training, which is not due to differences in cellular energy charge (AMP, ATP), but rather might be due to increased glycogen stores observed in trained individuals. Acute elevation of glycogen by prior exercise and diet manipulation in rats is associated with reduced AMPK activation either with AICAR (204) or with exercise in humans (205). The regulatory β-subunit of AMPK contains a glycogen-binding domain, which may interact with muscle glycogen to decrease the activity of AMPK when glycogen is plentiful. This glycogen regulatory mechanism might allow for the interplay between the allosteric (AMP/ATP) regulation of glycogenolysis through glycogen phosphorylase and PFK, without allowing for AMPK activation, ensuring that when glycogen stores are plentiful, they are preferentially used for ATP synthesis. When glycogen stores deplete, however, AMPK is activated and blood-borne glucose and FA may be oxidized for energy (71).

Although little is known regarding the underlying mechanisms that induce chronic adaptations from endurance training, it is plausible that increases in mitochondria and GLUT4 may be AMPK-mediated. AMPK may be involved in activation of gene transcription, as AMPKα2-containing isoforms are known to localize to the nucleus (2). PGC-1α is an important gene transcription coactivator involved in mitochondrial biogenesis, and PGC-1α mRNA in rat epitrochlearis muscle increases after an acute 6-

hour swimming exercise bout, which was associated with a four-fold activation of AMPK (185) and is sustained during short-term exercise training up to seven days (68). These sustained changes in PGC-1α mRNA are associated with increased levels of mitochondrial enzyme and GLUT4 protein expression in as early as five days (7) and suggests that AMPK may be involved in the mechanisms that allow for greater substrate utilization after endurance training.

Mechanisms of Skeletal Muscle Insulin Resistance: Association with Obesity and Type 2 Diabetes

Prevalence and diagnosis of diabetes

Type 2 diabetes mellitus (T2DM) is the most common chronic metabolic disease in Western society (106), with a prevalence of 4.8% in Canada. Data from the National Diabetes Surveillance System, National Population Health Survey, and the Canadian Community Health Survey estimate 1,128,500 cases of diabetes diagnosed by health professionals in Canada; however, with an estimated one-third of cases that remained undiagnosed, up to 1.7 million Canadians are estimated to be living with diabetes (79). The diagnosis of diabetes is made in an individual displaying one of the following criteria; 1) symptoms of diabetes (including fatigue, excessive thirst, excessive urination, unexplained weight loss) plus a casual plasma glucose value ≥11.1 mmol/L; or 2) fasting plasma glucose values (+6 hr) ≥7.0 mmol/L; or 3) a 2-hour oral glucose tolerance test (OGTT) plasma glucose value ≥11.1 mmol/L (123). Independent risk factors for T2DM include being overweight, physical inactivity, smoking and high blood pressure. Among individuals with self-reported diabetes, 74.3% are overweight and 65.1% are inactive (79), suggesting that increasing rates of obesity may be linked to the development of diabetes. These modifiable risk factors may also play a role in preventing diabetes and decreasing the burden of diabetes-related complications of the kidneys, eyes and vasculature. Indeed, the economic burden of diabetes is estimated at $1.6 billion in direct and indirect health care costs (79), indicating that steps need to be taken to decrease the prevalence of T2DM.

Abnormalities in fat metabolism and the pathogenesis of insulin resistance in skeletal muscle

The mechanisms of the development of T2DM are not fully understood but may involve at least three stages including 1) *insulin resistance*, characterized by normal or elevated insulin levels (hyperinsulinemia) to overcome resistance and maintain normoglycemia; 2) *post-prandial hyperglycemia*, as the pancreas cannot produce enough insulin in response to a glucose load; and 3) *fasting hyperglycemia*, impairing or destroying beta cells, leading to reduced insulin production and full-blown diabetes (4). It is the insulin resistant stage that is the focus of much research into the underlying mechanisms that prevent insulin signaling to increase glucose uptake and utilization in muscle in overweight and obese states. It is becoming increasingly apparent that defects in skeletal muscle FA metabolism are involved. At the level of FA uptake, the putative transporter, fatty acid translocase/CD36 (FAT/CD36) protein content at the plasma membrane is higher in obese Zucker rats (117) and obese humans (21). Also of particular interest is the role that the accumulation of reactive lipid species and the reduced capacity for FA oxidation in skeletal muscle appear to play in the etiology of obesity-related insulin resistance.

i) Muscle Lipid Accumulation

The accumulation of intramuscular TAG was originally thought to be associated with insulin resistance in both high-fat (HF) fed rats (178) and humans (136). However, during *in vitro* muscle contractions of rat muscle, FA are both oxidized and esterified into TAG at high rates (49) and increased TAG synthesis rates are seen at rest in rat soleus muscle after 8 weeks of endurance training (50). Furthermore, the paradoxical findings that endurance-trained athletes actually have increased insulin sensitivity and oxidative capacity, despite elevated skeletal muscle TAG (65) suggest that it is likely that elevated TAG stores may only be a marker of dysfunctional muscle FA metabolism in sedentary and obese individuals. The accumulation of more reactive lipid intermediates, such as diacylglycerol (DAG) and ceramide may be the more likely mechanistic link for insulin resistance associated with obesity. Indeed, acute insulin resistance can be induced by elevating plasma FA with the infusion of Intralipid/heparin during hyperinsulinemic-euglycemic clamp conditions in as little as 3-6 hours (18, 69, 95, 149). As well, chronic insulin resistance can be induced in rodents on a HF diet in as little as 3-4 weeks (11, 187). Acute and chronic FA exposure is suggested to inhibit insulin-stimulated glucose transport and/or glucose phosphorylation (19, 149) and is thought to be related to the increase in DAG and ceramide content (*Figure 3*), which disrupt the insulin-signaling pathway.

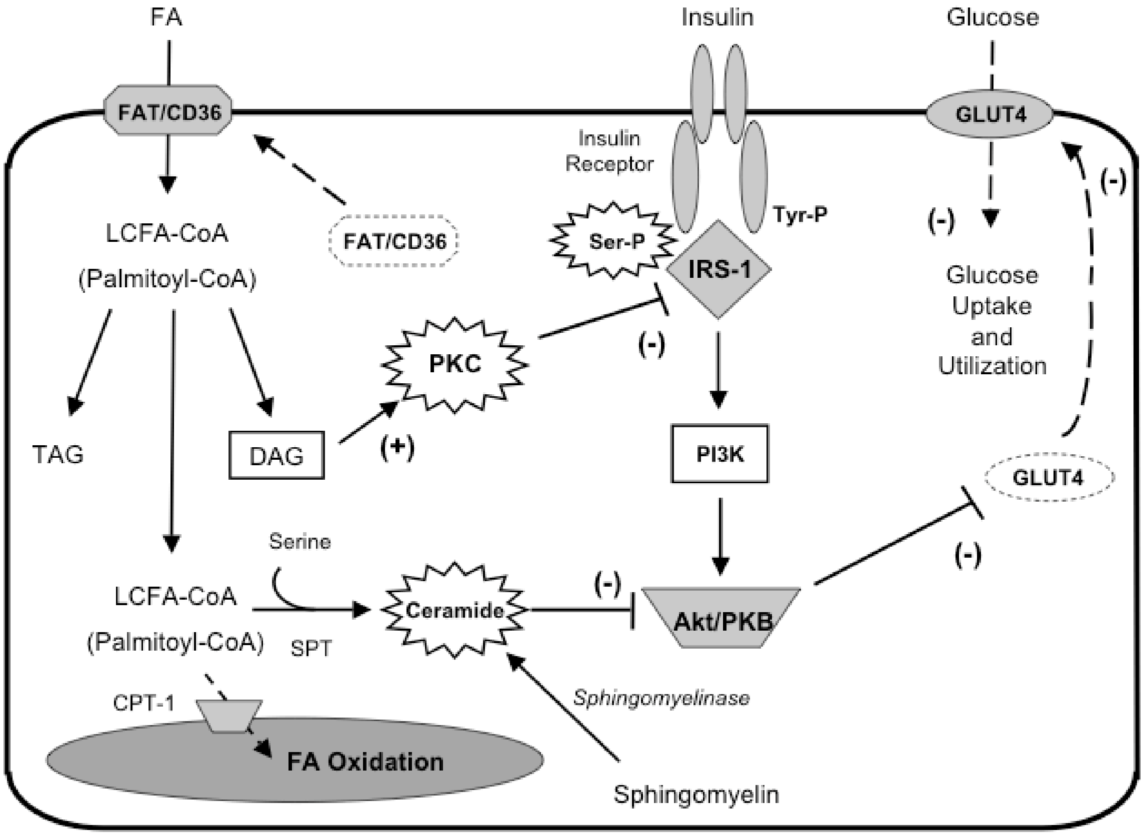

Figure 3: Proposed mechanism of inhibition of the insulin-signaling pathway by diacylglycerol (DAG)/protein kinase C (PKC) and ceramide

Insulin binds to the insulin receptor and induces autophosphorylation of tyrosine (Tyr-P) residues and activates IRS-1, thus stimulating a cascade of reactions that activate GLUT4 translocation and glucose uptake. An increase in DAG content is postulated to allosterically activate certain PKC isoforms in muscle. Activated PKC induces phosphorylation of serine (Ser-P) resides on the insulin receptor or IRS-1 and disrupts insulin signaling. Ceramide is formed via two major pathways 1) through serine palmitoyl transferase (SPT) and 2) through *de novo* synthesis from sphingomyelin. Ceramide is postulated to inhibit downstream components of the insulin-signaling pathway, namely Akt/protein kinase B (PKB). Both DAG and ceramide are increased in insulin resistant states and disruptions of the insulin-signaling pathway are thought to inhibit GLUT4 translocation and glucose uptake.

Specifically, DAG species are allosteric activators of protein kinase C (PKC) isoforms and increased DAG content have been observed acutely over 6 hours of lipid infusion (95) and in chronic insulin resistant states, such as HF- fed rats (11, 160), obese Zucker rats (190) and obese humans (25). Specific isoforms of PKC have been suggested to be translocated to the cell membrane and activated by DAG in skeletal muscle in insulin resistant states. Notably, PKCθ (11, 69) and PKCε (11, 160) in rats and PKCβ and PKCδ in humans (95) translocate to the plasma membrane and are activated during acute lipid infusion. Subsequent PKC phosphorylation of Ser/Thr residues of insulin receptor substrate-1 (IRS-1) occurs, thereby interrupting insulin-stimulated tyrosine phosphorylation of IRS-1 (95, 218).

Ceramide species are part of a specific plasma membrane sphingomyelin-signaling pathway and are thought to be specific second messengers in this system. Total skeletal muscle ceramide content is negatively associated with insulin sensitivity (179). Furthermore, with acute Intralipid/heparin infusion in humans, a decrease in insulin sensitivity is observed (-25%) which was accompanied by ~50% increase in ceramide content (179). Chronically, increased skeletal muscle ceramide content is observed in models of insulin resistance, including obese Zucker rats (190) and obese humans (1). Ceramides cause insulin resistance by inhibiting more distal components of the insulin-signaling pathway, specifically Akt/protein kinase B (PKB) (161, 182).

ii) Muscle Oxidative Capacity in Obese, Insulin Resistant States

Obesity-related, insulin resistant states are characterized by an impaired capacity to oxidize FA in skeletal muscle, which appears to exacerbate lipid accumulation in skeletal muscle. Insulin sensitivity is significantly correlated with muscle oxidative capacity (23) and shown to be a better predictor of insulin sensitivity than TAG stores in obesity, T2DM and with training (23, 66, 124, 148). Indices of oxidative capacity are reduced, including a decrease in Type I muscle fibers (83) mitochondrial content (86) and function (103), CPT-I activity (25, 101, 105, 162) and oxidative enzyme capacity (25, 162), as well as increased cytoplasmic fatty acid binding protein (FABPc) and plasma membrane fatty acid binging protein (FABPpm) (162). In support of this, initial studies by Kelley *et al*. suggested that fasting FA oxidation in obese subjects (BMI ~33-34 kg/m^2) was reduced despite similar FA uptake across the leg (101). However, subsequent studies directly examining skeletal muscle FA metabolism (intact muscle strips, homogenates) suggests that there may be a "threshold" of decreased FA oxidation seen in morbidly obese (BMI ~40-53 kg/m^2) (89, 105), but not modestly obese subjects (BMI ~30-34 kg/m^2) (89, 175). The increased adiposity may have even more severe, detrimental effects on muscle oxidative capacity.

iii) Exercise and Endurance Training Interventions as a Proposed Mechanism to Increase Insulin Sensitivity in Obese, Insulin Resistant States

Dietary-induced weight loss does not appear to be sufficient to correct insulin resistance in obese states (67), as accompanying endurance training interventions appear to be an important factor in increasing insulin sensitivity (66). It is suggested that exercise interventions that increase insulin sensitivity involve both reducing the accumulation of reactive lipid species and increasing FA oxidation (oxidative capacity) in muscle. Indeed, prolonged acute exercise (46) and exercise training (47) decreases the content and composition of ceramides in rat skeletal muscle. Furthermore, one-legged exercise training in healthy subjects (80) and cycling exercise in obese (25) subjects has shown no differences in TAG composition, but rather increases in polyunsaturated structural phospholipids (80) and reductions in total DAG and ceramide content (25) have been observed.

Furthermore, increased mitochondrial FA oxidation, CPT-I activity and insulin sensitivity have been observed in obese subjects after training (25). Interestingly, increased FA utilization after training in obese subjects may not only require CPT-I, but also FAT/CD36, which has been shown to increase localization with CPT-I after a diet and exercise weight loss regime (-12 ± 0.1 % body weight loss, -9.1 ± 2.0 % body fat loss), potentially leading to increased FA oxidation rates (159).

Whether AMPK signaling is related to decreased reactive lipid intermediates and increased oxidative capacity in skeletal muscle is a matter of debate. In healthy rats undergoing a moderate intensity treadmill exercise protocol, an increase in the regulatory AMPKγ3 isoform was seen only in oxidative red quadriceps muscle (48). On the other hand, in healthy humans who participated in 3 weeks of one-legged knee-extensor exercise training, increases in catalytic AMPKα1 and AMPKα2 activity, coinciding with increased AMPKα phosphorylation and increased ACC phosphorylation were observed (60). Obese, insulin resistant rodents have abnormalities in the LKB-1-AMPK-PGC-1α pathway in skeletal muscle, including decreased LKB-1 expression, decreased AMPKα and ACC phosphorylation and decreased PGC-1α protein expression (170). With training, LKB-1, AMPKα1 and PGC-1α protein content increases (170). In addition, a 12-week training program in healthy subjects decreased malonyl-CoA, increased the activity of MCD and increased PGC-1α protein expression without any observed changes in AMPK phosphorylation (108), suggesting that changes downstream of AMPK can persist and may be related to increased FA oxidation.

iv) Roles of Adipokines and Anti-diabetic Agents in Insulin Resistance, Obesity and Type 2 Diabetes

Adipokines. Our understanding of adipocyte biology has changed substantially over the past decade, as evidence has emerged to suggest that adipose tissue is not simply an inert organ that stores TAG. Rather, adipose tissue is also an endocrine organ that secretes a large number of hormones, adipokines and lipids, which exert regulatory effects on energy homeostasis/body weight, and glucose and fat metabolism in multiple tissues. A number of these factors, termed adipokines, have been discovered, including tumor necrosis factor-α (TNF-α) and resistin, thought to play a role in insulin resistance. On the other hand, leptin and adiponectin are suggested to regulate FA oxidation and accumulation in muscle, thereby increasing insulin sensitivity and potentially having effects on reactive lipid species.

Leptin (127, 129, 172, 174) and adiponectin (24, 186, 210) stimulate skeletal muscle FA oxidation and leptin also prevents lipid accumulation by decreasing TAG esterification (129, 172). These effects have been shown to be mediated, at least in part, through the activation of AMPK (24, 127, 210). The partitioning of FA to oxidation may be part of the insulin sensitizing effect that leptin (98, 163) and adiponectin (24) have in muscle, as it is likely that these adipokines may also have effects on reactive lipid intermediates, DAG and ceramide. Studies of rats fed a HF diet for 4 weeks (172) and studies in *rectus abdominus* muscle obtained from obese humans subjects suggest that leptin- (174) and adiponectin-stimulated (24) FA oxidation is impaired (ie. leptin and adiponectin resistance) and this may be a factor in the development of insulin resistance in skeletal muscle. Indeed, plasma levels of leptin are increased, suggesting resistance (87, 119, 122) while levels of adiponectin are decreased (5, 195) in obese humans. Additionally, although the treatment of recombinant leptin was originally proposed to induce weight loss in obese subjects, this was a variable effect only seen at high doses of leptin (~20-fold increases) (82). Lifestyle factors (diet, exercise) may play a role in at least partially reversing leptin resistance, as observed in HF-fed rats in which a small proportion of fat is replaced by omega-3 polyunsaturated FA (172) and in endurance trained HF-fed rats (176).

Anti-diabetic drugs. Interest in the AMPK pathway for the treatment of T2DM has emerged since the discovery that AMPK is indirectly activated by metformin (61, 216) and thiazolidinediones (TZDs), including rosiglitazone (61) and troglitazone (113).

Although metformin (dimethylbiguanide·hydrochloride) has been prescribed as an anti-diabetic drug for many years, its mechanism of action has remained elusive. Bioavailability of metformin is suggested to be ~40-60% (158) and liver concentrations > 180 μM can be achieved in rats after a 50 mg/kg dose, which is lower than doses typical required for efficacy in diabetic rats (> 100 mg/kg) (216). Many of metformin's effects are proposed to be mediated through enhanced insulin sensitivity of the liver, primarily due to decreased hepatic glucose output, but limited evidence of increased insulin-stimulated glucose uptake (22, 216) have also been reported. Recent evidence suggests that metformin's effects may be due, at least in part, to the activation of AMPK in liver (37, 76, 211, 216) as well as skeletal muscle (61, 132, 216). Acute activation (ie. 6-24 hours) of the AMPK cascade in muscle cell culture (61) and liver (76) is thought to be mediated through an adenine nucleotide-independent mechanism (61, 76). However, prevention of acute lipid-induced (5 hr lipid infusion) insulin resistance in rodents with one-week prior treatment of metformin (and the TZD, rosiglitazone, *below*) was associated with changes in liver, but not muscle and adipose tissue AMPK activity (37, 211). The length of time of chronic treatment of metformin might be of importance for AMPK activation, as metformin treatment in human subjects with T2DM (initially 500 mg/day, increased to 2g/day) increased AMPKα2 activity by 4 weeks (+52%) and up to 10 weeks (+80%) (132). This activation was associated with increased AMPKα phosphorylation (Thr172), and decreased ACC activity, likely due to a decrease in muscle energy charge (decreased ATP at 4 weeks; decreased PCr at 10 weeks) (132), indicating a possible adenine nucleotide-dependent mechanism in humans. The proposed mechanism that may explain both metformin (56) and TZD (26) activation of AMPK is through the inhibition of Complex I of the respiratory chain, potentially resulting in inhibition of ATP production (ie increased AMP:ATP ratio).

There is controversy regarding metformin's acute effects on FA metabolism. With the use of adenoviral-mediated expression of both constitutively active and kinase-dead AMPKα in human HepG2 hepatocytes, AMPK phosphorylation has been shown to be a necessary component of metformin's effects to decrease intracellular TAG levels (214). An increase in FA oxidation in hepatocytes has been shown in as little as 4 hours (216), while another study found no effect on FA oxidation or TAG esterification in hepatocytes (62). There is a paucity of data regarding metformin's direct effects on skeletal muscle FA metabolism. A recent study suggests that metformin activation of AMPKα2 in skeletal muscle may have direct muscle effects on FA metabolism (38). Metformin prevented the insulin-induced suppression of FA oxidation in oxidative SOL and also suppressed insulin-stimulated incorporation into TAG in glycolytic epitrochlearis muscle (38). These direct alterations in FA metabolism in muscle may be part of the mechanism by which metformin increases glucose uptake and insulin sensitivity in muscle.

A newer class of anti-diabetic drugs, the TZDs, are insulin-sensitizing agents used to treat T2DM. Their proposed mechanism of action in skeletal muscle was traditionally thought to be secondary to effects in adipose tissue, as TZDs are agonists of the nuclear transcription factor, peroxisome proliferator-activated receptor-γ, (PPARγ), which is almost exclusively expressed in adipose tissue. PPARγ increases insulin sensitivity through changes in gene transcription that increase adipocyte differentiation (166), thus decreasing FA release and increasing adiponectin plasma levels in lean, obese and diabetic subjects (212), and stimulating AMPK and FA oxidation in skeletal muscle (24, 210). Whether PPARγ is directly involved with insulin sensitivity in skeletal muscle is a matter of debate, as PPARγ is expressed in very low levels (166). Muscle-specific PPARγ deletion causes insulin resistance in mice, which was not reversed with 3 weeks of TZD treatment (81). However, rosiglitazone incubation in cell culture derived from human skeletal muscle (61) and troglitazone in isolated rat EDL (113) activate AMPK by an increase in the AMP:ATP ratio (61, 113) and increase glucose uptake in muscle (113). Furthermore, it is likely that TZDs have an effect on skeletal muscle FA metabolism, as 2 weeks of troglitazone treatment increased FA oxidation in isolated SOL muscle from male Zucker diabetic fatty (ZDF) rats (93). Interestingly, cultured muscle cells from subjects with T2DM demonstrate a decrease in FA uptake compared to cells cultured from healthy subjects, and exposure to chronic (4 days) TZDs, normalized FA uptake, increased FA oxidation, which was associated with increased FAT/CD36 protein expression (197), suggesting increased oxidative capacity.

CHAPTER 2: STATEMENT OF THE PROBLEM AND RATIONALE FOR THE STUDIES

The primary purpose of this thesis was to examine the acute and chronic effects of AMPK activation on skeletal muscle FA and glucose metabolism in rodent skeletal muscle.

The initial studies of this thesis investigated the acute effects of AMPK activation on FA and glucose oxidation, both at rest and during tetanic contraction in isolated rat soleus muscle. Previous studies have been limited and equivocal in determining whether AMPK activation with AICAR leads to simultaneous increases in FA and glucose oxidation. With AMPK proposed to be an important regulatory enzyme sensing changes in energy status through increases in the AMP:ATP and Cr:PCr ratio, it would seem teleological that AMPK would upregulate ATP provision from all available energy sources. Also, the regulation of endogenous TAG metabolism is poorly understood. Specifically, AICAR activation of AMPK has a paradoxical anti-lipolytic effect in hepatocytes and adipocytes (40, 181) and inhibits isoprenaline-induced HSL activation in L6 myocytes (193). Furthermore, the role of AMPK in contraction-mediated regulation of FA metabolism and glucose oxidation is a matter of debate, as data from low-intensity hindlimb muscle stimulation (145) and dominant inhibitory AMPK mutant mice strains (128) suggest that AMPK is only one factor in the regulation of substrate use in contracting skeletal muscle. Therefore, the acute (60 min) effects of AICAR treatment on FA metabolism and glucose oxidation, at rest and during contraction, were examined in isolated rat soleus muscle. Regulation of AMPK was assessed with the AMPK-SAMS activity assay. FA metabolism was measured using the pulse-chase technique, which allows for the simultaneous determination of rates of endogenous and exogenous FA oxidation as well as esterification and hydrolysis of endogenous TAG. To determine the mechanisms of substrate provision at rest, PDHa and its allosteric regulator, pyruvate were examined. ***It was hypothesized in the studies at rest, that an AICAR-induced decrease in glucose oxidation that is secondary to a stimulation of FA oxidation should occur with adequate FA availability, but not lower FA levels when rates of oxidation are low. The hypotheses in the contraction studies were that AICAR would increase AMPK activity above the threshold set by high intensity tetanic contraction; and furthermore, that the combination of AICAR and contraction would result in additional increases in FA and glucose oxidation. Additionally, it was hypothesized that AICAR would inhibit TAG hydrolysis both at rest and during contraction.***

AMPK has also been proposed to be a potential therapeutic target for the alleviation of insulin resistance in obese states. In skeletal muscle, AMPK is activated by exercise (200, 206), adipokines (127, 210), antidiabetics such as metformin (132, 216) and TZDs (61, 113), all of which increase insulin sensitivity. Based on results from acute studies in this thesis, it was postulated that activators of AMPK (metformin, exercise or their combination) would prevent derangements in glucose homeostasis in the female ZDF rat, a HF diet, inducible model of diabetes; and further, to determine whether improvements may be related to changes in skeletal muscle FA metabolism and AMPK regulation. Female ZDF rats were fed either a control diet or a diabetogenic, HF diet either alone or in combination with metformin supplemented in the food, treadmill exercise or the combination of exercise and metformin for 8 weeks. Insulin sensitivity was assessed by the examination of soleus muscle basal and insulin-stimulated glucose transport *in vitro*. Additionally, acute (60 min) FA oxidation and esterification to TAG was assessed with ^{14}C palmitate tracers *in vitro* and chronic changes in fat transporters and reactive lipid species were assessed in skeletal muscle. ***It was hypothesized that metformin and exercise, alone or in combination, would improve systemic glycemic control and skeletal muscle insulin-stimulated glucose transport. Furthermore, improvements would be related to decreased FA uptake and improved partitioning of FA to oxidation and away from accumulation in skeletal muscle.***

Chapter 3: AMP-kinase Activation with AICAR Simultaneously Increases Fatty Acid and Glucose Oxidation in Resting Rat Soleus Muscle

As published, with minor modifications:

Angela C. Smith, Clinton R. Bruce, and David J. Dyck. AMP-kinase activation with AICAR simultaneously increases fatty acid and glucose oxidation in resting rat soleus muscle. *J Physiol* 565(2): 537-546, 2005.

Introduction

AMP-activated protein kinase (AMPK) is an important energy sensor within skeletal muscle. AMPK is activated allosterically by an increase in the AMP:ATP and Cr:PCr ratio, as well as covalently by AMPKK (74). AMPK is activated by muscle contraction (2, 78, 94), and pharmacologically by AICAR. AICAR is a cell-permeable compound, which is phosphorylated to form ZMP, and mimics the effects of AMP on the AMPK signaling cascade. The metabolic effects of AICAR include an increase in glucose uptake (13, 78, 125, 131), and a repartitioning of FA toward oxidation (3, 100, 125, 130) and away from intramuscular TAG esterification (130). Thus, pharmacological activation of AMPK appears to result in an increase in ATP-producing pathways, as is also observed during contraction.

Regulation of TAG hydrolysis in skeletal muscle is poorly understood. AICAR-stimulated AMPK activation would be expected to stimulate TAG hydrolysis and subsequent oxidation for energy production. Paradoxically, AICAR treatment has been shown to have an anti-lipolytic effect in rat soleus muscle (3) and C_2C_{12} myotubes (130). In adipose tissue, AMPK phosphorylates HSL, having no effect on the activity of the enzyme in its basal state, but inhibits further phosphorylation by protein kinase A (64), preventing isoprenaline-induced lipid hydrolysis (40, 181).

Another area of controversy is the effect of AICAR on glucose oxidation in skeletal muscle. Previous studies have measured AICAR's ability to increase glucose uptake (13, 78, 125, 131) and increase glycogen synthesis (6). However, few studies have specifically examined the effect of AICAR on glucose oxidation. In isolated human endothelial cells, AICAR simultaneously increased FA oxidation and glucose oxidation, leading to an increase in ATP production (41). The only study using isolated skeletal muscle showed that 60 min of AICAR exposure in oxidative rat soleus muscle decreased glucose oxidation secondary to an increase in FA oxidation (ie. glucose-fatty acid cycle) (100). However, teleologically, one would expect that in response to a decrease in cellular energy charge, AMPK activation would simultaneously increase ATP production from both FA and glucose oxidation.

Therefore, in the present study we utilized palmitate and glucose tracers to examine AICAR's acute effects on FA and glucose metabolism, as well as pyruvate dehydrogenase activation (PDHa), a key regulatory site of glucose oxidation. We utilized high-fatty acid (HFA, 1 mM) and low-fatty acid (LFA, 0.2 mM) buffers to determine whether AICAR-induced changes in glucose oxidation were dependent on changes in FA oxidation. Thus, an AICAR-induced decrease in glucose oxidation that is secondary to a stimulation of FA oxidation should occur with adequate FA availability, but not lower FA levels, when rates of oxidation are low. Furthermore, we also wished to confirm that AICAR-induced AMPK stimulation results in a reduction in TAG hydrolysis. Specifically, we also examined whether any AICAR-induced reduction in hydrolysis was dependent on FA availability, as increased FA availability is known to reduce lipolysis (49), potentially due to AMPK activation.

Methods

Animals and Preparation of Muscle Strips

Female Sprague-Dawley rats (Charles River Laboratory, QC; wt: 215 ± 2 g) were used for all experiments. Animals were housed in a controlled environment on a 12:12-h reversed light-dark cycle and fed Purina rat chow and water *ad libitum*. All procedures were approved by the Animal Care Committee at the University of Guelph. Animals were anesthetized with an intraperitoneal injection of pentobarbital sodium (6mg/100g body mass) prior to all experimental procedures. Longitudinal soleus muscle strips were carefully dissected with tendons intact using a 27-gauge needle. Each strip was sutured, removed and suspended on brass hooks in a 7 mL incubation reservoir in order to maintain resting tension. Seven milliliters of warmed (30°C), pre-gassed (95% O_2-5% CO_2) modified Kreb's-Henseleit buffer (KHB) containing 4% FA-free bovine serum albumin (Boehringer, QC, Canada), 10 mM glucose, and 1 mM palmitate, was immediately added to the incubation reservoir. This was the base buffer for all experiments and was maintained at 30°C, and continuously gassed during all stages except the *Chase Phase* (*see below*). A layer of heavy mineral oil was placed on top of the incubation buffer at all stages of the procedure in order to maintain gassing pressures. At the termination of the dissection procedure, the rats were humanely euthanized with an intracardiac injection of pentobarbital sodium. Muscle viability was assessed by measuring phosphagen content (ATP, PCr, Cr) in a separate set of experiments.

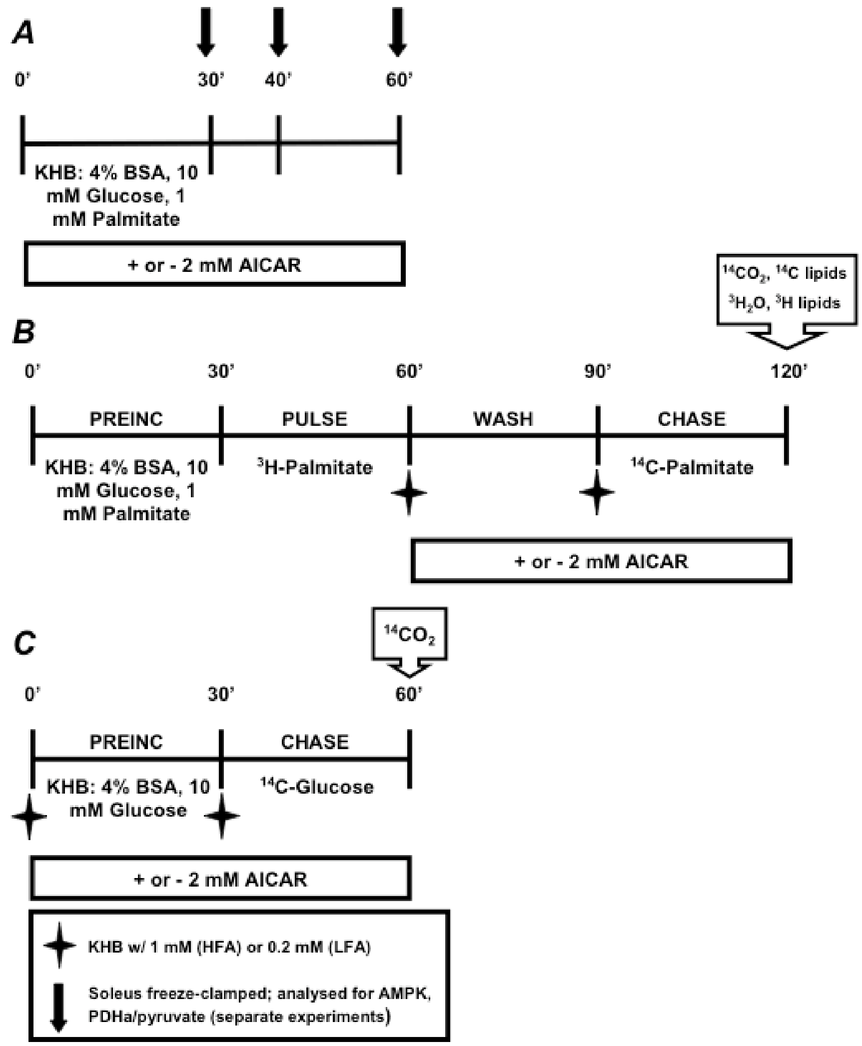

Figure 4: Incubation protocol for time-course experiments for AMPK, pyruvate dehydrogenase activation (A), FA metabolism (B), and glucose oxidation (C).

For time-course experiments (A) soleus strips were incubated in the presence or absence of AICAR (2 mM) and muscle strips were freeze-clamped at the time-points indicated, for further analysis of AMPKα1 and AMPKα2 activities, pyruvate dehydrogenase activation (PDHa) and pyruvate concentration. For FA metabolism (B), rodent soleus muscle strips were incubated (30°C) in modified Kreb's-Henseleit buffer (KHB) through four stages: PREINCUBATION (PREINC); PULSE, ([9,10-^{3}H]palmitate; WASH; and CHASE, ([1-^{14}C]palmitate) to monitor exogenous and endogenous FA metabolism. During the WASH and CHASE (last 60 min), soleus strips were incubated in the presence or absence of AICAR (2 mM), in KHB with low-fatty acid (LFA, 0.2 mM) or high-fatty acid (1 mM) concentration. For glucose oxidation (C), soleus strips were incubated in the presence or absence of AICAR (2 mM), in KHB with low-fatty acid (LFA, 0.2 mM) or high-fatty acid (1 mM) concentration throughout the protocol (60 min) and glucose oxidation was monitored during the last 30 min.

Time-Course for AMPK Activation

Muscle Incubations. AMPKα1 and AMPKα2 activities were examined after 30, 40 and 60 min of AICAR treatment (*Figure 4A*). Briefly, muscle strips were incubated in KHB with or without the addition of 2 mM AICAR (Toronto Research Chemicals, Toronto, ON, Canada). At the end of the incubation period, the muscle strips were quickly freeze-clamped and stored in liquid nitrogen until further analysis.

Immunoprecipitation and AMPK Activity. Muscle strips (~25 – 30 mg) were homogenized in buffer (50 mM Tris · HCl, pH 7.5, 1 mM EDTA, 1 mM EGTA, 1 mM dithiothreitol, 50 mM NaF, 5 mM Na pyrophosphate, 10% glycerol, 1% Triton X-100, 10 μg/ml trypsin inhibitor, 2 μg/ml aprotinin, 1 mM benzamidine, 1 mM phenylmethylsulfonyl fluoride). The homogenates were incubated with AMPKα1 and AMPKα2 (Upstate, Charlottesville, VA) antibody-bound protein A beads (Sigma, St. Louis, MI) each for 2 h at 4°C. Immunocomplexes were washed with PBS and suspended in 60 μl dilution buffer (50 mM Tris (pH 7.5), 1 mM DTT, 10 % Glycerol, 0.1% Triton-X) for AMPK activity assay (34). Briefly, 20 μl of sample was combined with 20 μl of reagent mixture (5mM Hepes pH 7.5, 1 mM $MgCl_2$, 0.5% glycerol, 1 mM DTT, 100 μM SAMS peptide (Upstate Scientific, Charlottesville, VA), 250 μM ATP with $^{32}P\gamma$-ATP (Amersham Biosciences, QC, Canada), 100 μM AMP). The reaction proceeded for 15 min, after which 23 μl of reaction mixture was spotted onto p81 filter paper (Upstate Scientific, Charlottesville, VA) and washed three times in 1% phosphoric acid. Filter papers were dried and placed in organic scintillant for counting.

Lipid Metabolism (Pulse-Chase Experiments, Figure 4B)

Pulse and Wash. After an initial preincubation period (30 min), the buffer was drained from the reservoir and 7 mL KHB with 2 μCi [9,10-^{3}H]palmitate (Amersham Biosciences, QC, Canada) was added to the reservoir. Strips were pulsed for 30 min to prelabel the endogenous lipid pools (intramuscular DAG and TAG). After the pulse phase, the buffer was drained and the muscles were washed for 30 min in the absence of radiolabeled palmitate to allow for the removal of non-incorporated [^{3}H]palmitate. During the wash, the buffer either remained at 1 mM palmitate (HFA) or was decreased to 0.2 mM palmitate (LFA). During this period, some strips were exposed to 2 mM AICAR to ensure sufficient time for AICAR to diffuse into the muscle and activate AMPK prior to the *Chase Phase*. At the end of the wash phase, one strip from each pair was removed and extracted for endogenous lipids to determine prelabeling.

Chase Phase (Experimental Phase). The remaining muscle strips continued to be incubated for 30 min in pre-gassed, modified KHB containing 0.5 μCi [1-^{14}C]palmitate (Amersham Biosciences, QC, Canada). Strips were incubated in the presence or absence of 2 mM AICAR, either at HFA or LFA. During this phase the gas was turned off to prevent the escape of $^{14}CO_2$. Exogenous palmitate oxidation and esterification were monitored by the production of $^{14}CO_2$ and incorporation of [1-^{14}C]palmitate into intramuscular lipids, respectively. Intramuscular lipid hydrolysis and oxidation were monitored simultaneously by measuring the net change in lipid [^{3}H]palmitate content and the production of ^3H_2O, respectively.

Palmitate Oxidation. Exogenous [1-^{14}C]palmitate oxidation was determined as outlined previously (50) with minor modifications. At the end of the chase phase, a 3.5 mL aliquot of buffer was transferred to a 50 mL Erlenmeyer flask, which was quickly sealed with a rubber stopper fitted with a stopcock and needle. The buffer was acidified with 3 mL of 1 M H_2SO_4 and the $^{14}CO_2$ was captured over 120 min in a 0.5-mL microcentrifuge tube containing 400 μl of 1 M benzethonium hydroxide (Sigma, Oakville, ON, Canada) suspended from the stopper. The microcentrifuge tube was placed in a scintillation vial and counted using standard liquid scintillation techniques. Loss of ^{14}C through isotopic exchange at the level of Kreb's cycle was accounted for by collecting a 0.5 mL aliquot of the aqueous phase produced during the muscle lipid extraction as previously described (50). Endogenous [9,10-^{3}H]palmitate oxidation was quantified by measuring $^{3}H_2O$ production. Two milliliters of the chase incubation buffer was transferred to a 13 mL plastic centrifuge tube containing 5 mL of 2:1 chloroform-methanol (vol/vol). Samples were shaken for 15 min before adding 2 mL of 2 M KCl-HCl and were shaken for an additional 15 min. The samples were then centrifuged at 5,000 *x g*, at 4°C for 10 min. A 1 mL aliquot was removed from the upper aqueous phase and quantified by liquid scintillation counting.

Extraction of Muscle Lipids. After incubation, the muscles were removed, blotted and weighed, and placed in 13 mL plastic centrifuge tubes containing 5 mL ice-cold 2:1 chloroform-methanol (vol/vol) and homogenized using a Polytron homogenizer. Connective tissue was weighed and subtracted from the initial wet weight of the muscle. Samples were then centrifuged at 5000 *x g*, 4°C for 10 min. The supernatant was removed and transferred to a clean centrifuge tube. Distilled water (2 mL) was added and the samples were shaken for 10 min and centrifuged at 5,000 *x g*, 4°C for 10 min to separate the aqueous and lipophilic phases.

The chloroform phase was transferred to glass centrifuge tubes and gently evaporated under a stream of N_2. The samples were redissolved in 100 μl 2:1 chloroform-methanol containing internal standards of dipalmitin and tripalmitin (Sigma, Oakville, ON, Canada) to ensure proper lipid identification. Fifty microliters of each sample was spotted on a silica gel plate that had been oven-dried overnight. Silica gel plates were placed in a sealed tank containing solvent (60:40:3 heptane-isopropyl ether-acetic acid) for 60 min. Plates were then removed, permitted to dry and sprayed with dichlorofluorescein dye (0.02% wt/vol in ethanol) and visualized using long-wave ultraviolet light. The DAG and TAG bands were scraped into scintillation vials for counting.

Glucose Oxidation

Glucose oxidation (*Figure 4C*) was determined in a separate set of experiments. The preincubation period utilized 7 mL KHB (LFA or HFA, 10 mM glucose) as described in the pulse-chase experiments, either in the presence or absence of 2 mM AICAR. After the 30 min preincubation, the buffer was drained and 7 mL of pre-gassed, modified KHB containing 2 μCi of [U-^{14}C]glucose was added to the reservoir. The muscle strips were incubated for an additional 30 min in the presence or absence of 2 mM AICAR. Gaseous $^{14}CO_2$ was captured as described previously.

Time-Course for PDH Activation and Pyruvate Content

In a separate series of experiments, we investigated the effect of AICAR on PDH activation after 30, 40 and 60 min by incubating muscle strips in the absence or presence of AICAR (*Figure 4A*). Freeze-clamped soleus (10 - 15 mg) was used for the determination of PDHa, as described previously (143). The remainder of the muscle was freeze-dried, powdered, and dissected free of all visible blood and connective tissue and analyzed for pyruvate concentration. Briefly, freeze-dried muscle (~5 mg) was extracted with 0.5 M perchloric acid containing 1 mM EDTA and neutralized with 2.2 M $KHCO_3$. Pyruvate was analyzed fluorometrically (138).

Calculations and Statistics

AMPK activity was expressed as picomoles ^{32}P transferred to SAMS peptide per minute per milligram protein. To calculate palmitate (nmol/g wet weight) oxidized or incorporated into lipid pools, the specific activity of the incubation buffer (dpm radiolabeled palmitate/nmol total palmitate) was used. Intramuscular TAG hydrolysis was calculated as the net loss of preloaded [^3H]palmitate (nmol/g) from lipid pools (DAG and TAG) between paired soleus strips. Glucose oxidation was calculated with the specific activity of labeled glucose in KHB in the same manner as palmitate.

Results are presented as mean ± SEM. One-way ANOVA tests were used to analyze muscle viability data over the two-hour incubation. Two-way ANOVA followed by Student-Newman Keuls post-hoc analyses were used to assess statistical significance between time points for AMPK activity, with and without AICAR. Students' *t*-tests were used to analyze the effect of AICAR on FA and glucose metabolism. Two-way repeated measures ANOVA followed by Student-Newman Keuls post-hoc analyses were used to assess statistical significance between time points for PDHa and pyruvate, with and without AICAR. Significance was accepted at $P \leq 0.05$.

Results

Viability of Incubated Muscle

There were no significant differences in ATP, PCr and Cr (*Table 1*), and most importantly, all measured parameters remained stable after the initial 30 min when measurements for glucose oxidation and lipid metabolism were made.

Time-Course for AMPK Activation with AICAR

AICAR treatment had no effect on AMPKα1 activity (*Figure 5A*). However, over 60 min, AICAR resulted in significant increases in AMPKα2 activity (*Figure 5B*). By 60 min of incubation with AICAR, AMPKα2 activity in soleus strips was higher (+192%; $P < 0.05$) than strips not treated with AICAR.

Effects of AICAR on FA Metabolism

Exogenous FA Metabolism. AICAR treatment significantly increased exogenous FA oxidation in both LFA (+33%; $P < 0.05$; *Figure 6A*) and HFA conditions (+36%; $P < 0.05$; *Figure 6B*). Although incorporation into TAG was not significantly different with AICAR (*Figure 6C, 6D*), there was an increase in the amount of FA partitioned toward oxidation relative to TAG esterification at both LFA (+15%; $P < 0.05$; *Figure 6E*) and HFA (+49%; $P < 0.05$; *Figure 6F*). There were no significant differences in palmitate incorporation into DAG with AICAR (*Table 2*).

Endogenous FA Metabolism. There were no significant effects on DAG or TAG hydrolysis with AICAR treatment in the LFA condition. Correspondingly, there was also no effect on endogenous oxidation with AICAR. These results were not different at HFA with AICAR treatment (*Table 2*).

Effects of AICAR on Glucose Oxidation

AICAR increased glucose oxidation, both in the LFA (+105%; $P < 0.05$; *Figure 7A*) and HFA conditions (+170%; $P < 0.0001$; *Figure 7B*).

Changes in Calculated ATP Production with AICAR

Calculated total ATP production (*Table 3*) increased with AICAR both with LFA (+89%; $P < 0.05$) and HFA (+131%; $P < 0.001$) as a result of increased ATP production from glucose (LFA: +104%; $P < 0.05$; HFA: +165%; $P < 0.001$) and FA oxidation (LFA: +17%; $P < 0.05$; HFA: +30%; $P < 0.05$).

Time-Course for PDHa and Pyruvate Content with AICAR

Over 60 min, AICAR treatment resulted in significant increases in PDHa (*Figure 8A*). By 60 min of incubation with AICAR, PDHa was higher than strips not treated with AICAR (+71%; $P < 0.005$), and also significantly different from AICAR treatment after 30 min (+126%; $P < 0.05$). Muscle pyruvate was not significantly different during 60 min of AICAR treatment (*Figure 8B*).

Table 1: Muscle viability (ATP, phosphocreatine (PCr), and creatine (Cr)) in isolated SOL incubated in modified Kreb's Henseleit buffer over 120 minutes.

Values are mean ± SEM, mmol/kg dry mass, n = 4 - 6 per time point.

	ATP	**PCr**	**Cr**
0 min (Fresh)	24.3 ± 2.0	45.7 ± 6.4	57.2 ± 5.3
30 min	19.3 ± 1.8	35.0 ± 5.0	60.2 ± 3.0
90 min	19.8 ± 2.4	35.1 ± 5.4	50.4 ± 6.9
120 min	19.6 ± 3.1	36.8 ± 7.9	47.5 ± 5.0

Table 2: Intramuscular diacylglycerol (DAG) esterification and hydrolysis, intramuscular triacylglycerol (TAG) hydrolysis and endogenous oxidation at rest in the presence (+) and absence (-) of AICAR (2 mM) for 60 min.

Values are means ± SEM, nmol g wet wt^{-1}, n = 7.

	DAG				**TAG**			
	LFA, 0.2 mM		**HFA, 1 mM**		**LFA, 0.2 mM**		**HFA, 1 mM**	
	Esterification	Hydrolysis	Esterification	Hydrolysis	Hydrolysis	Endogenous Oxidation	Hydrolysis	Endogenous Oxidation
- AICAR	2.9 ± 0.5	1.5 ± 1.0	8.4 ± 0.7	1.4 ± 0.4	20.6 ± 3.1	14.0 ± 1.0	6.6 ± 2.8	15.9 ± 1.8
+ AICAR	2.8 ± 0.3	1.1 ± 0.4	8.9 ± 0.8	1.9 ± 0.7	14.3 ± 3.2	13.7 ± 1.5	6.1 ± 4.8	17.4 ± 2.1

Table 3: Calculated ATP production from glucose and FA oxidation in the presence (+) or absence (-) of AICAR (2 mM) for 60 min. Values are means ± SE, μmol g wet wt^{-1}, n = 6-8 per group. ⋆Significantly different from No AICAR within the same FA concentration ($P \leq 0.05$); †Sum of exogenous and endogenous FA oxidation.

	ATP Production (LFA, 0.2 mM)			**ATP Production (HFA, 1.0 mM)**		
	Glucose Oxidation	**FA Oxidation†**	**Total**	**Glucose Oxidation**	**FA Oxidation†**	**Total**
- AICAR	19.6 ± 2.5	4.0 ± 0.2	23.6 ± 2.5	22.6 ± 2.6	8.3 ± 0.4	31.1 ± 2.6
+ AICAR	40.1 ± 7.4⋆	4.7 ± 0.3⋆	44.8 ± 7.2⋆	61.1 ± 2.9⋆	10.8 ± 0.8⋆	71.9 ± 3.2⋆

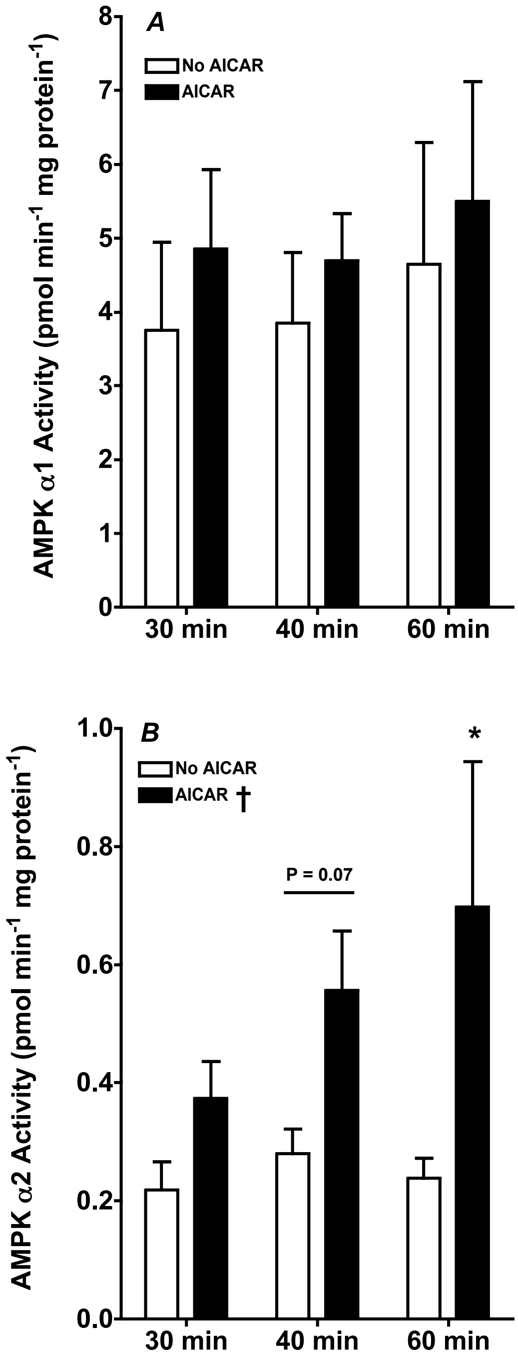

Figure 5: Time-course for AMPKα1 (A) and AMPKα2 (B) activity in the presence or absence of AICAR in isolated rat soleus muscle.

Values are means ± SEM, pmol min $^{-1}$ mg protein^{-1}, n = 5 - 8 per group. *Significantly different from 30 min of same condition ($P \leq 0.05$); †Treatment effect of AICAR significantly different from No AICAR ($P \leq 0.05$).

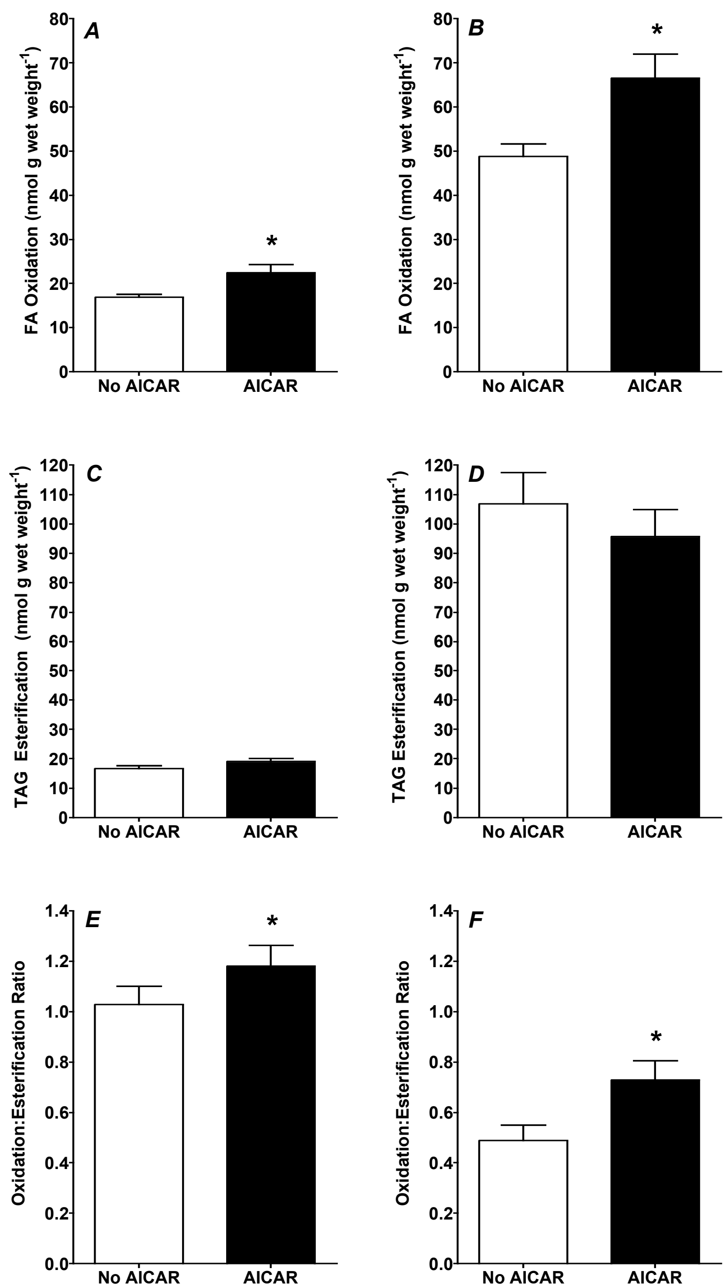

Figure 6: Effect of AICAR on fatty acid oxidation and TAG esterification in isolated rat soleus muscle

Effect of AICAR on fatty acid oxidation in low fatty acid (0.2 mM, LFA: A) or high fatty acid (1 mM, HFA: B) modified KHB; TAG esterification (LFA: C; HFA: D); and oxidation:TAG esterification ratio (LFA: F; HFA: G) in isolated rat soleus muscle. Values are means ± SEM, nmol g wet wt^{-1}, n = 7 per group. *Significantly different from No AICAR ($P \leq 0.05$).

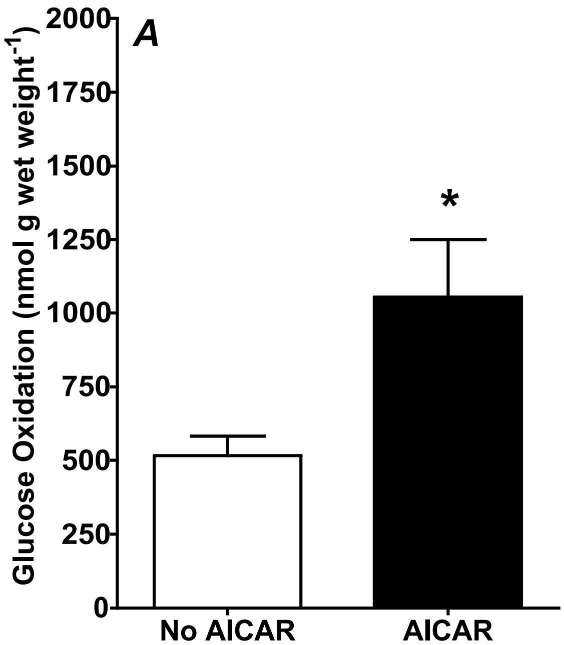

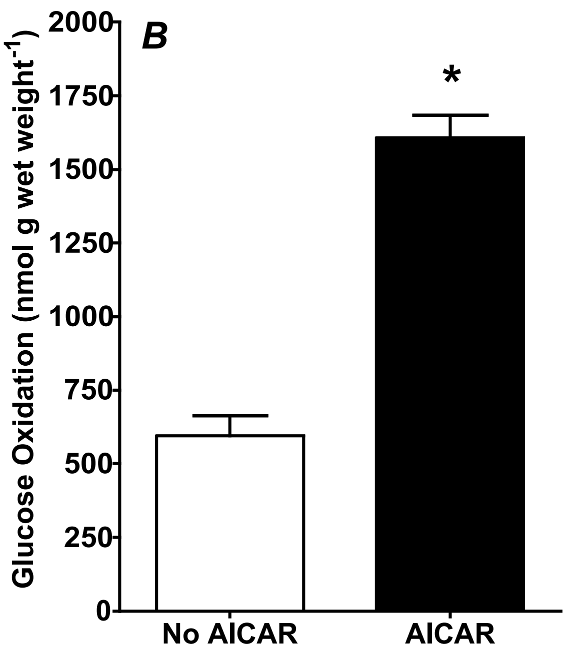

Figure 7: Effect of AICAR on glucose oxidation in isolated rat soleus muscle

Effect of AICAR on glucose oxidation in low fatty acid (0.2 mM, LFA: A), or high fatty acid (1 mM, HFA: B) modified KHB in isolated rat soleus muscle. Values are means ± SEM, n = 6-8 per group. *Significantly different from No AICAR ($P \leq 0.05$).

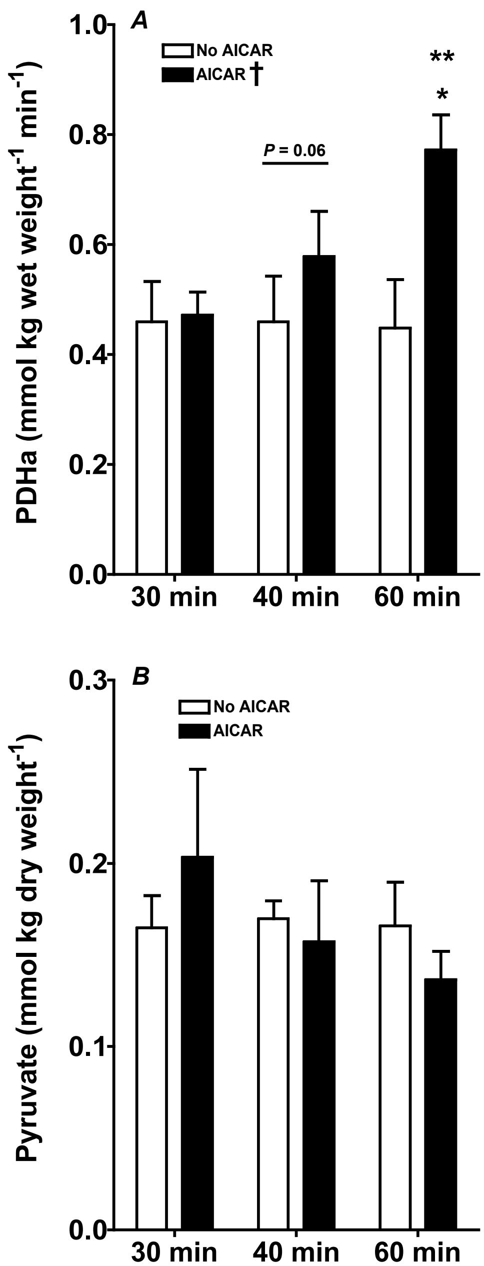

Figure 8: Effect of AICAR on time course for pyruvate dehydrogenase activation and pyruvate content in isolated rat soleus muscle

Time-Course for pyruvate dehydrogenase activation (PDHa, A) and pyruvate content (B) in the presence or absence of AICAR in isolated rat soleus muscle. Values are means ± SEM, n = 6 – 8 per group. ★Significantly different from 30 min of same condition ($P \leq 0.05$); **Significantly different from 30 min of different condition ($P \leq 0.05$); †Trial effect of AICAR being significantly different from No AICAR ($P \leq 0.05$).

Discussion

With the use of palmitate and glucose tracers, we were able to directly examine the acute effects of AICAR on FA and glucose metabolism in isolated rodent soleus muscle. We confirmed previous results that in resting muscle AICAR activates AMPKα2 activity (97, 145) leading to stimulation of FA oxidation (125, 130, 145). In addition, several novel observations were made in this investigation: 1) AICAR increased glucose oxidation regardless of the level of FA available to the muscle, indicating an increase in total energy provision; 2) PDHa increased during 60 min of AICAR treatment, supporting the observed increase in glucose oxidation; however, this was not due to an increase in pyruvate; and 3) AICAR had no independent effects on resting endogenous FA metabolism (TAG hydrolysis, oxidation).

Effect of AICAR on Skeletal Muscle FA Metabolism

Exogenous Oxidation. In agreement with previous studies (100, 125, 130, 145), we show that AICAR increased FA oxidation ~40%, demonstrating that AMPK is a key regulator of FA oxidation in soleus. Indeed, 60 min of AICAR administration activated AMPKα2 ~2-fold, which has been previously demonstrated in this muscle (1.5- to 3-fold; (97, 204)). Increases in FA oxidation are presumably due to the downstream effects of AMPK activation, including inhibition of ACC (202), increases in MCD (154), ultimately decreasing malonyl-CoA levels (3) with subsequent relief of the inhibition on CPT-I, a rate-limiting step in FA oxidation in muscle.

TAG Esterification and Endogenous Hydrolysis. The regulation of intramuscular lipid metabolism, both at rest and during contraction, is poorly understood. To our surprise, we failed to see a significant decrease in TAG esterification with AICAR in both fat conditions. These findings are in direct contrast to those of Muoio *et al.* (130), who demonstrated a decrease in TAG esterification in mouse soleus. Mitochondrial *sn*-glycerol-3-phosphate acyltransferase (GPAT) is a rate-limiting step in TAG esterification and has been suggested to be the likely mechanism by which AMPK may be regulating TAG esterification (130). However, the degree by which AMPK-mediated mitochondrial GPAT activity plays a role in altering TAG esterification is a matter of debate. Indeed, regulation of mitochondrial GPAT in skeletal muscle has been difficult to determine (137, 193) and the current study does not support an AMPK-mediated effect on GPAT for TAG esterification. Differences in TAG esterification may be due to time-course of exposure to AICAR [60 minutes (present study) vs. 180 minutes (130)], or a species difference. Murine muscle has a higher metabolic rate, is highly oxidative (130) and may respond more quickly to AICAR. However, even with no changes observed in TAG esterification, we did observe an increase in the ratio of FA oxidized relative to TAG esterification, which has been suggested to play a role in increased insulin sensitivity in skeletal muscle (139). The oxidation:TAG ratio provides a reasonable index of the relative partitioning of FA toward storage or oxidation, however, a more complete analysis of FA partitioning would include rates of FA uptake. AICAR has been shown to increase AMPK activity and FAT/CD36 translocation from intracellular vesicles to the sarcolemmal membrane in cardiac myocytes, which is associated with initial increases in FA uptake rates (118), suggesting that AMPK regulates FA uptake through the translocation of of FAT/CD36 to the plasma membrane. Rates of FA uptake were not measured in this study, however total uptake into DAG, TAG and through oxidation was not different with AICAR treatment (*data not shown*), suggesting that AMPK activation is indeed involved in FA partitioning in skeletal muscle.

Intuitively, one would expect that AICAR-induced AMPK activation would stimulate TAG hydrolysis and subsequent oxidation in muscle to provide energy for ATP production, similar to that observed during contraction (49). Regulation of intramuscular TAG hydrolysis is poorly understood in skeletal muscle. Hormone sensitive lipase, a key enzyme involved in TAG hydrolysis, has been identified in muscle (110, 140) and is stimulated by epinephrine and contraction by at least partially distinct mechanisms (109). However, TAG hydrolysis is inhibited by AICAR in soleus (3) and in C_2C_{12} myotubes (130), demonstrating a similar anti-lipolytic effect as observed in adipocytes (40, 181). Therefore, we expected to observe a similar anti-lipolytic effect with AICAR in resting soleus. However, AICAR had no effect on resting TAG hydrolysis rates, likely as these were already very low. To our surprise, reducing the FA substrate was not a strong enough stimulus to drive TAG hydrolysis to investigate potential AICAR mediation of this process. It is also possible that the duration of this protocol (AICAR treatment over 60 min) may have been too short to observe any differences in lipolytic rate with AICAR. It should also be noted that with HFA, there was a slight mismatch between TAG hydrolysis and endogenous oxidation. This discrepancy may be due to possible reincorporation (recycling) of a small amount of ^3H tracer which may ultimately underestimate TAG hydrolysis, and also because calculated endogenous oxidation may be overestimated, as it is based on the specific activity of the TAG pool. In addition, the calculation of TAG hydrolysis is derived from paired muscle strips from one soleus muscle, which could increase variability. Nonetheless, AICAR had no effect on endogenous FA oxidation in resting soleus, which may be the more accurate measure of endogenous metabolism, as this is measured in a single muscle strip.

Effects of AICAR on Skeletal Muscle Glucose Metabolism

To our knowledge, this is the first study in isolated rat skeletal muscle to show that glucose oxidation is increased in the presence of AICAR and that this effect is independent of the increase in FA availability and oxidation. In fact, we observe even higher rates of glucose oxidation at HFA than at LFA in the presence of AICAR, results that argue against a glucose-fatty acid cycle phenomena and reinforce the idea that activation of FA oxidation through AMPK does not lead to concomitant decreases in glucose oxidation. Previous studies have shown conflicting results for the role that AICAR-stimulated AMPK activation plays in regulating glucose oxidation. It has been proposed that increased FA oxidation may inhibit the uptake and subsequent oxidation of glucose in resting muscle (ie. the glucose-fatty acid cycle). Dagher *et al.* (41) subjected isolated human endothelial cells to AICAR and found that AMPK activity was increased 5-fold by 30 min and remained elevated for the duration of the two-hour incubation period, which correlated with a significant increase in glucose oxidation. However, Kaushik *et al.* (100) found that a 60 min incubation with AICAR decreased glucose oxidation by 44% in soleus muscle isolated from fed but not from fasted rats. In this study, FA oxidation increased 90% with AICAR, suggesting that the AICAR-inhibited glucose oxidation was secondary to an increase in FA oxidation (100). Surprisingly, increases in AMPK activity could not be demonstrated or linked to changes in FA and glucose metabolism over 60 min (100). However, in the present study there were significant increases in AMPKα2 activity and we did not observe a concomitant decrease in glucose oxidation secondary to the increase in FA oxidation. Thus, the current data indicates that due to increases in both exogenous FA and glucose substrate oxidation, there is an overall doubling in the increase in calculated ATP provision at rest with AICAR-mediated AMPK activation. Previous data suggests that ATP, AMP and ADP do not change with AICAR (125). Although not measured in this study, actual rates of ATP and PCr content with AICAR would have been helpful in determining whether ATP was actually accumulating or being buffered to PCr through the near-equilibrium enzyme, creatine kinase. Furthermore, due to questionable specificity of AICAR, it cannot be discounted that AICAR may be increasing overall energy expenditure through the regulation of ion pumps, uncoupling proteins and substrate cycling, therefore indirectly affecting FA and glucose metabolism.

The resulting increase in PDHa over 60 min of AICAR exposure supports AMPK as being a stimulator of glucose oxidation. However, we cannot establish an allosteric regulatory mechanism for the increase in PDHa, as pyruvate content was not different in the presence of AICAR. Pyruvate is both a substrate and a negative allosteric inhibitor of PDH kinase, which phosphorylates and inactivates PDH (167). We did not observe any changes in phosphagens involved in the regulation of AMPK (ATP, PCr, Cr) and due to the fact that AICAR is phosphorylated to ZMP, there are no expected changes in endogenous adenine nucleotides (ATP, ADP, AMP) (125), which are involved in allosteric regulation of PDH kinase (167). It is then tempting to speculate that the PDH complex may be a direct target of AMPK which may be interacting to regulate PDH directly or to regulate the relative activities of the kinase and phosphatase that determine the amount of PDH in its active form. However, there are no known covalent regulators of the kinase and phosphatase in skeletal muscle (167).

Summary

The results from the present study demonstrate that AMPKα2 activation by AICAR is an important mediator of FA and glucose metabolism in skeletal muscle. There were simultaneous increases in FA and glucose oxidation, independent of FA availability. Taken together, AMPK activation increases exogenous substrate oxidation to increase energy provision in skeletal muscle. Stimulation of PDHa appears to be responsible for the AMPK-activated increase in glucose oxidation, but this is not due to increases in pyruvate.

CHAPTER 4: AICAR FURTHER INCREASES FATTY ACID OXIDATION AND BLUNTS TRIACYLGLYCEROL HYDROLYSIS IN CONTRACTING RAT SOLEUS MUSCLE

As published, with minor modifications:

Angela C. Smith, Clinton R. Bruce, and David J. Dyck. AMP kinase activation with AICAR further increases fatty acid oxidation and blunts triacylglycerol hydrolysis in contracting rat soleus muscle. *J Physiol* 565(2): 547-553, 2005.

Introduction

Muscle contraction increases glucose uptake (78) and FA metabolism (49, 112) in isolated rat skeletal muscle. AMPK was first shown to be activated during treadmill exercise in rat skeletal muscle, leading to decreased malonyl-CoA through inhibition of ACC (200), and increased FA oxidation. The coordinated regulation of AMPK, ACC and malonyl-CoA content in rats during treadmill exercise is intensity-dependent, with the greatest AMPK activation observed during short-term, high-intensity exercise (146). In tetanic contraction protocols, AMPK activity increases 3- to 5-fold in glycolytic epitrochlearis muscle (2) and 2- to 3-fold in oxidative soleus muscle (78) during short-term (~10 min) protocols.

Although AMPK is activated during contraction, its exact role in regulating substrate (glucose, exogenous FA, intramuscular TAG) metabolism is controversial. AICAR is a pharmacological activator of AMPK, demonstrating similar effects to exercise for increasing glucose uptake (13, 125, 156) and FA oxidation (130) in skeletal muscle at rest. However, isolated muscle from mice with a dominant inhibitory mutant of AMPK, demonstrate full inhibition of AICAR- and hypoxia-stimulated glucose uptake, but only a partial reduction (-40%) in contraction-stimulated glucose uptake (128), suggesting that AMPK is only partially involved in the regulation of contraction-induced glucose uptake. Recent evidence in perfused rat hindquarters subjected to a combination of AICAR and low intensity muscle contraction suggests that small increases in AMPK activity (+34%) did not account for the synergistic increase in FA oxidation (+175%) (145). This leads to the possibility of AMPK-independent mechanisms regulating substrate oxidation in skeletal muscle.

Regulation of intramuscular TAG is poorly understood in both resting and contracting skeletal muscle. In isolated muscle preparations, TAG hydrolysis is increased during tetanic contraction in soleus, leading to increased TAG oxidation rates (49). Contraction- and AICAR-stimulated AMPK activation have therefore been suggested to be involved in the regulation of TAG hydrolysis and oxidation in skeletal muscle. However, in adipocytes, AICAR inhibits isoprenaline-induced lipolysis (40, 181), apparently by phosphorylating and inhibiting HSL (64). Similarly, AICAR has an anti-lipolytic effect in resting soleus (3) and C_2C_{12} myotubes (130) and recent evidence suggests that activating AMPK with AICAR can over-ride and inhibit epinephrine-induced HSL activation in non-contracting L6 myotubes (193).

To gain further insight into the role of AMPK in the regulation of substrate use during contraction, we utilized tracer methodologies to examine FA metabolism and glucose oxidation in isolated contracting soleus muscle, in the absence or presence of AICAR. With the use of different buffer concentrations of palmitate (low-fatty acid

(LFA; 0.2 mM) and high-fatty acid (HFA; 1.0 mM)), we also examined the role that FA availability had on both exogenous and endogenous FA metabolism with contraction and AICAR. We wished to determine whether 1) AICAR would increase AMPK activity above the threshold set by high intensity, tetanic contraction; 2) the combination of AICAR and contraction would result in additional increases in FA and glucose oxidation; and 3) AICAR inhibited TAG hydrolysis and oxidation during contraction.

Methods

Animals and Preparation of Muscle Strips

Female Sprague-Dawley rats (Charles River Laboratory, QC; wt: 215 ± 2 g) were used for all experiments. Animals were housed in a controlled environment on a 12:12-h reversed light-dark cycle and fed Purina rat chow and water *ad libitum*. All procedures were approved by the Animal Care Committee at the University of Guelph. Animals were anesthetized with an intraperitoneal injection of pentobarbital sodium (6mg/100g body mass) prior to all experimental procedures. Longitudinal soleus muscle strips were carefully dissected with tendons intact, using a 27-gauge needle. Each strip was sutured, removed and suspended on brass hooks in a 7-mL incubation reservoir, in order to maintain resting tension, as previously described (49). Seven milliliters of warmed (30°C), pre-gassed (95% O_2-5% CO_2) modified Kreb's-Henseleit buffer (KHB) containing 4% FA-free bovine serum albumin (Boehringer, QC, Canada), 10 mM glucose, and 1 mM palmitate, was immediately added to the incubation reservoir. This was the base buffer for all experiments and was maintained at 30°C by an exterior circulating water system, and continuously gassed during all stages except the ***Chase Phase*** (*see below*). A layer of heavy mineral oil was placed on top of the incubation buffer at all stages of the procedure in order to maintain gassing pressures. At the termination of the dissection procedure, the rats were humanely euthanized with an intracardiac injection of pentobarbital sodium.

Time-Course for AMPK Activation

Muscle Incubations. AMPKα1 and AMPKα2 activities were examined at rest and following 10 and 30 min of contraction, with or without the addition of AICAR. Muscle strips were pre-incubated for 30 min either in KHB or KHB with the addition of 2 mM AICAR (Toronto Research Chemicals, Toronto, ON, Canada). At the end of this preincubation, one muscle strip was removed and freeze-clamped, while other muscles were stimulated to contract (150-ms trains comprised of 0.5-ms impulses (20-40 V; 60 Hz) at 20 tetani/min) for 10 or 30 min, with or without the addition of AICAR in the medium. At the end of the incubation period, the muscle strips were quickly freeze-clamped and stored in liquid nitrogen until further analysis.

Immunoprecipitation and AMPK Activity. Muscle strips (~25 – 30mg) were homogenized and incubated with AMPKα1 and AMPKα2 (Upstate, Charlottesville, VA) antibody-bound protein A beads (Sigma, St. Louis, MI) as previously described (*See* **CHAPTER 3**). Immunocomplexes were used for the AMPK activity assay as previously described (*See* **CHAPTER 3**).

Lipid Metabolism (Pulse-Chase Experiments)

Pulse and Wash. After an initial 30 min preincubation period, the buffer was drained from the reservoir and 7 mL KHB with 2 μCi [9,10-^{3}H]palmitate (Amersham Life Science, Oakville, ON, Canada) was added to the reservoir. Muscles were pulsed for 30 min to prelabel the endogenous lipid pools (intramuscular DAG and TAG). After the pulse phase, the buffer was drained and the muscles were washed for 30 min in the absence of radiolabeled palmitate to allow for the removal of non-incorporated [^{3}H]palmitate. During the wash, the buffer either remained at 1 mM palmitate (HFA) or was decreased to 0.2 mM palmitate (LFA) (see *Chase Phase*). During this period, some muscles were exposed to 2 mM AICAR (Toronto Research Chemicals, Toronto, ON, Canada). At the end of the wash phase, one soleus strip from each pair was removed and extracted for endogenous lipids to determine prelabeling.

Chase Phase (Experimental Phase). The remaining muscle strips continued to be incubated for 30 min in pre-gassed, modified KHB containing 0.5 μCi [1-^{14}C]palmitate (Amersham Life Science, Oakville, On, Canada) and stimulated to contract (150-ms trains comprised of 0.5-ms impulses (20-40 V; 60 Hz) at 20 tetani/min) for 30 min in the presence or absence of 2 mM AICAR, either at HFA or LFA (as in *Wash Phase*) and glucose concentration remained at 10 mM. During this phase the gas was turned off to prevent the escape of $^{14}CO_2$. Exogenous palmitate oxidation and esterification were monitored by the production of $^{14}CO_2$ and incorporation of [1-^{14}C]palmitate into intramuscular lipids, respectively. Intramuscular lipid hydrolysis and oxidation were monitored simultaneously by measuring the net change in lipid [^{3}H]palmitate content and the production of $^{3}H_2O$, respectively.

Palmitate Oxidation. Endogenous [9,10-^{3}H]palmitate and exogenous [1-^{14}C]palmitate oxidation was determined as outlined previously (50) with minor modifications (*See* **CHAPTER 3**).

Extraction of Muscle Lipids. After incubation, the muscles were removed, blotted and weighed, and placed in 13 mL plastic centrifuge tubes containing 5.0 mL ice-cold 2:1 chloroform-methanol (vol/vol), homogenized and lipids (intramuscular DAG and TAG) were extracted as previously described (*See* **CHAPTER 3**).

Muscle Triacylglycerol Content. In previous studies, we have determined that the endogenous radiolabel tracks only a small portion of the TAG pool in resting muscle (51). Therefore, it is important to determine the relationship between changes in ^{3}H-radiolabeled TAG pool and enzymatically-measured TAG content during contraction. In a separate set of experiments, net TAG utilization was analyzed on freeze-dried tissue (~5 mg dry) from resting and contracted (30 min) muscles, which was dissected free of all visible blood and connective tissue. Muscle TAG was measured enzymatically as previously described (51).

Glucose Oxidation

Glucose oxidation was determined in a separate set of experiments. Muscle strips were preincubated as outlined previously (*See* **CHAPTER 3**), in the absence or presence of 2 mM AICAR. After the preincubation, the gas was turned off to prevent the escape of $^{14}CO_2$, the buffer was drained and 7 mL of pre-gassed, modified KHB containing 2 μCi of [U-^{14}C]glucose (Amersham Life Science, Oakville, On, Canada) was added to the reservoir. The muscle strips were incubated in the absence or presence of 2 mM AICAR and were stimulated to contract (150-ms trains comprised of 0.5-ms impulses (20-40 V; 60 Hz) at 20 tetani/min). After this phase, buffer was drained and a 3.5 mL aliquot of the incubation medium was transferred to a 50 mL Erlenmeyer flask, and was acidified as described previously (*See* **CHAPTER 3**) to capture $^{14}CO_2$.

Calculations and Statistics

Specific activity of the incubation buffer (dpm radiolabeled palmitate/nmol total palmitate) was used to calculate palmitate (nmol/g wet weight) incorporated into lipid pools or oxidized. With enzymatic analysis of net TAG utilization during contraction, we were able to determine the relationship between the changes in the radiolabeled TAG pool and the total (enzymatically determined) TAG pool. Each nmol of [^{3}H]palmitate represented 83 nmol (LFA) and 37 nmol (HFA) of total FA in the TAG pool. This ratio was used to calculate the rates of net TAG hydrolysis (net loss of preloaded [^{3}H]palmitate (nmol/g) from lipid pools (TAG and DAG) between paired soleus strips) and endogenous lipid oxidation during muscle contraction. Glucose oxidation was calculated with the specific activity of labeled glucose in KHB in the same manner as palmitate.

Results are presented as mean ± SEM. Two-way ANOVA followed by Student-Newman Keuls post-hoc analyses were used to assess statistical significance between time points for AMPK activity, with and without AICAR. Students' *t*-tests were used to analyze the effect of AICAR on FA and glucose metabolism during contraction. Significance was accepted at $P \leq 0.05$.

Results

Time-Course for AMPK activation with Contraction and AICAR

Contraction and AICAR had no effect on AMPKα1 activity (*Figure 9A*). However, with contraction alone, AMPKα2 activity (*Figure 9B*) was significantly increased at 30 min compared to 10 min (+67%; $P < 0.05$) and 0 min (+195%; $P < 0.05$). The combination of contraction and AICAR resulted in significant further increases in AMPKα2 activity ($P < 0.01$; treatment effect). With contraction and AICAR combined, AMPKα2 activity was significantly increased at 30 min compared to 10 min (+71%; $P < 0.05$) and 0 min (+154%; $P < 0.001$). At 30 min of contraction and AICAR, AMPKα2 activity was significantly greater than contraction alone (+45%; $P < 0.05$).

Effects of AICAR on FA Metabolism During Contraction

Exogenous FA Metabolism. The combination of contraction and AICAR significantly increased exogenous FA oxidation at both LFA (+71%; $P < 0.05$; *Figure 10A*) and HFA (+46%; $P < 0.05$; *Figure 10B*). Incorporation into TAG was not significantly different with AICAR (*Figure 10C and 10D*), but there was an increase in the amount of FA partitioned toward oxidation relative to TAG esterification at LFA (+65%; $P < 0.05$; *Figure 10E*), while no significant increase in this ratio was observed at HFA (+28%; $P = 0.30$; *Figure 10F*). There were no significant differences in palmitate esterification into DAG with AICAR (*Table 4*).

Endogenous FA Metabolism. AICAR resulted in significant blunting of TAG hydrolysis during 30 min of contraction at both LFA (-294%; $P < 0.001$; *Figure 11A*), and HFA (-117%; $P < 0.05$; *Figure 11B*) conditions. There were no significant effects of AICAR treatment on endogenous oxidation at LFA or HFA. There were no significant effects on DAG hydrolysis (*Table 4*) with AICAR treatment during contraction.

Effects of AICAR on Glucose Oxidation in Isolated Soleus Muscle

AICAR had no significant effect on glucose oxidation during contraction, both with LFA (*Figure 12A*) and HFA (*Figure 12B*).

Table 4: Intramuscular diacylglycerol (DAG) esterification and hydrolysis in the presence (+) and absence (-) of AICAR in isolated contracting rat soleus muscle.

Values are means ± SEM, nmol g wet wt^{-1}, n = 7.

	LFA, 0.2 mM		**HFA, 1 mM**	
	DAG Esterification	DAG Hydrolysis	DAG Esterification	DAG Hydrolysis
- AICAR	4.6 ± 0.3	0.6 ± 1.3	11.2 ± 0.6	0.8 ± 0.9
+ AICAR	3.9 ± 0.4	0.7 ± 0.8	9.5 ± 0.9	0.9 ± 0.5

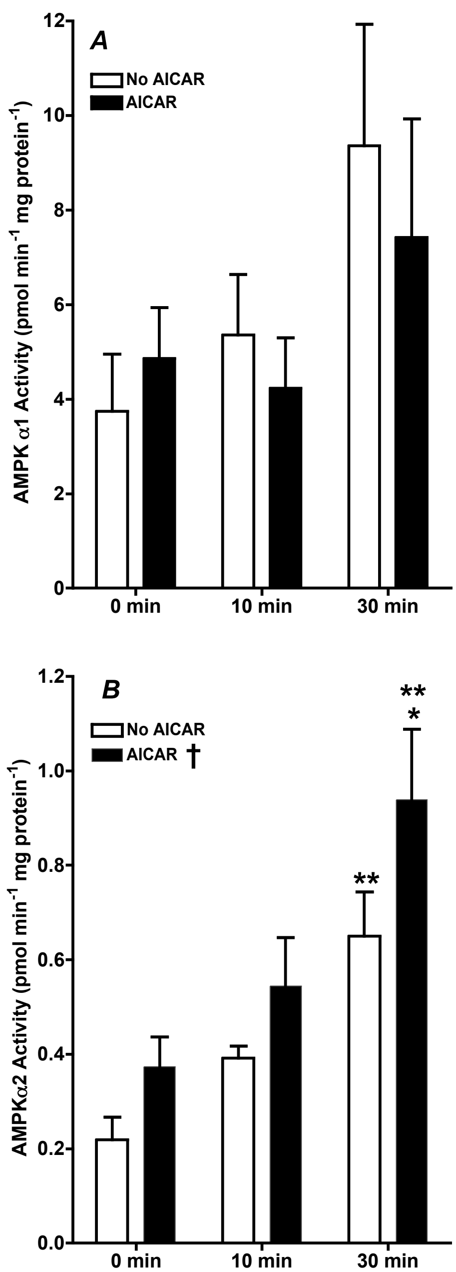

Figure 9: Time-course for AMPKα1 (A) and AMPKα2 (B) activity in the presence or absence of AICAR in isolated contracting rat soleus muscle.

Values are means ± SEM, pmol min $^{-1}$ mg protein^{-1}, n = 5 - 8 per group. *Significantly different from 30 min contraction alone ($P \leq 0.05$); **Significantly different from 0 and 10 min of same condition; †Treatment effect of AICAR significantly different from No AICAR ($P \leq 0.05$).

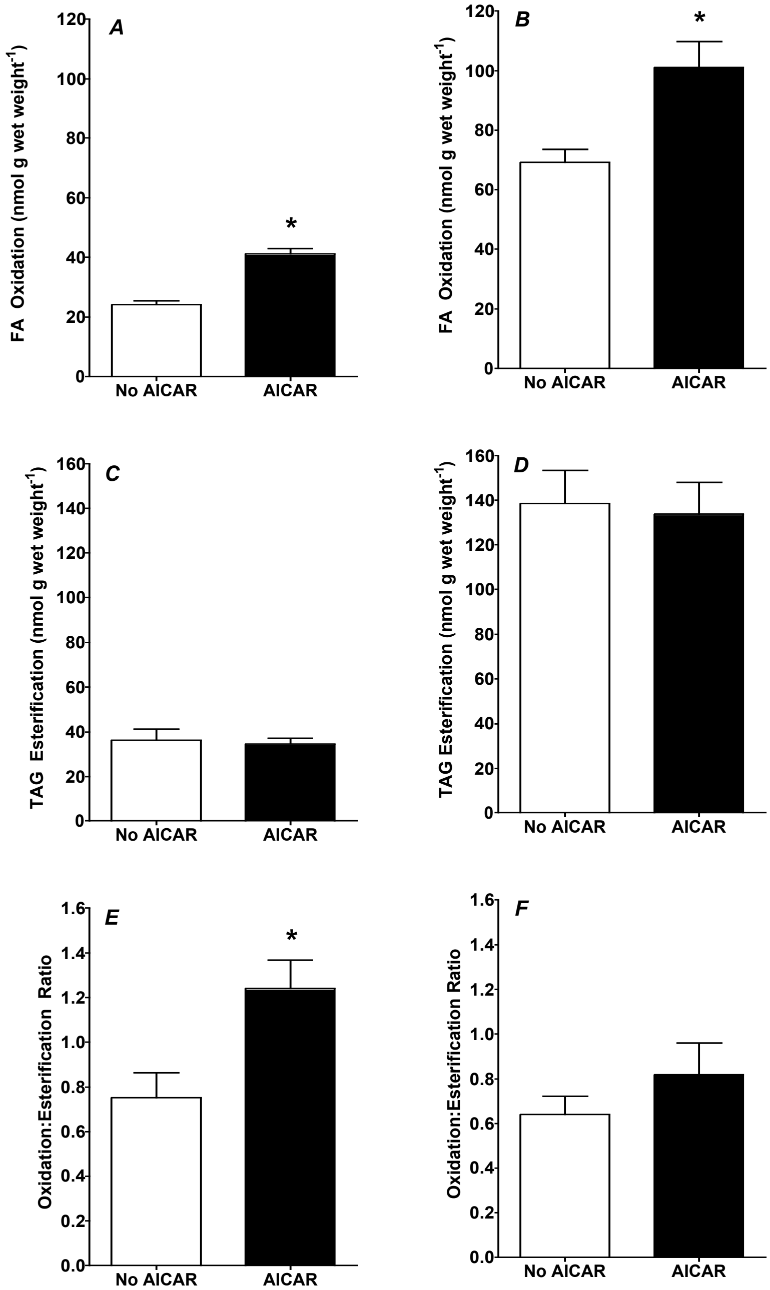

Figure 10: Effect of AICAR on fatty acid oxidation and triacylglycerol (TAG) esterification in isolated contracting rat soleus muscle

Effect of AICAR on fatty acid oxidation in low fatty acid (0.2 mM, LFA: A) or high fatty acid (1 mM, HFA: B) modified KHB; TAG esterification (LFA: C; HFA: D); and oxidation:TAG esterification ratio (LFA: F; HFA: G) in isolated contracting rat soleus muscle. Values are means ± SEM, nmol g wet wt^{-1}, n = 7 per group. ⋆Significantly different from No AICAR ($P \leq 0.05$).

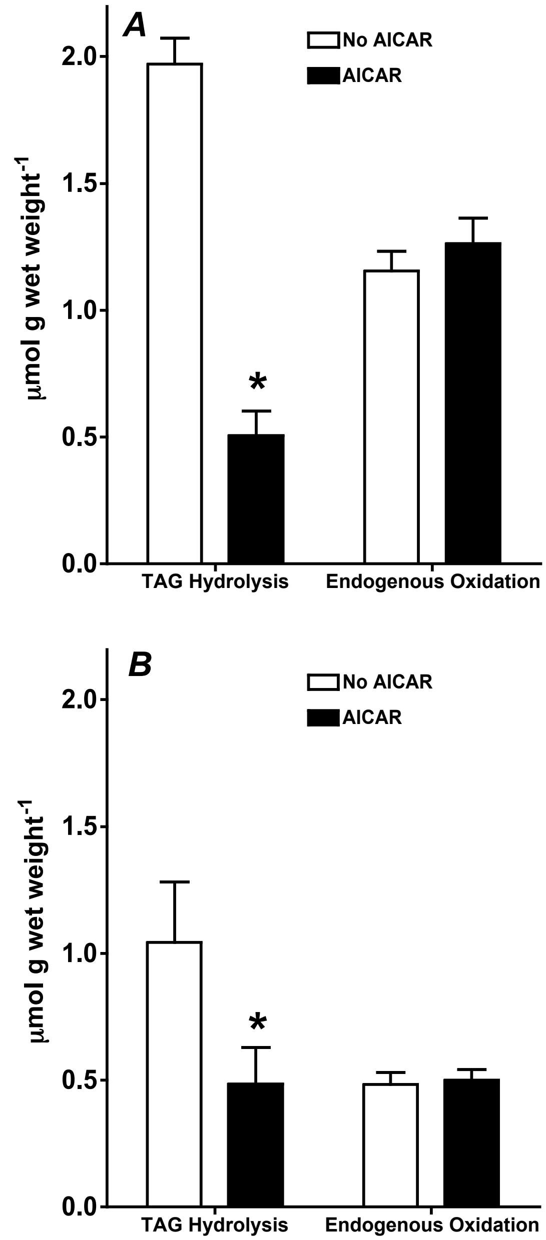

Figure 11: Effect of AICAR on TAG hydrolysis and endogenous fatty acid oxidation in isolated contracting rat soleus muscle

Effect of AICAR on triacylglycerol (TAG) hydrolysis and endogenous fatty acid oxidation in low fatty acid (0.2 mM, LFA: A) or high fatty acid (1 mM, HFA: B) modified KHB in isolated contracting rat soleus muscle. Values are means ± SEM, nmol g wet wt^{-1}, n = 7 per group. ⋆Significantly different from No AICAR ($P \leq 0.05$).

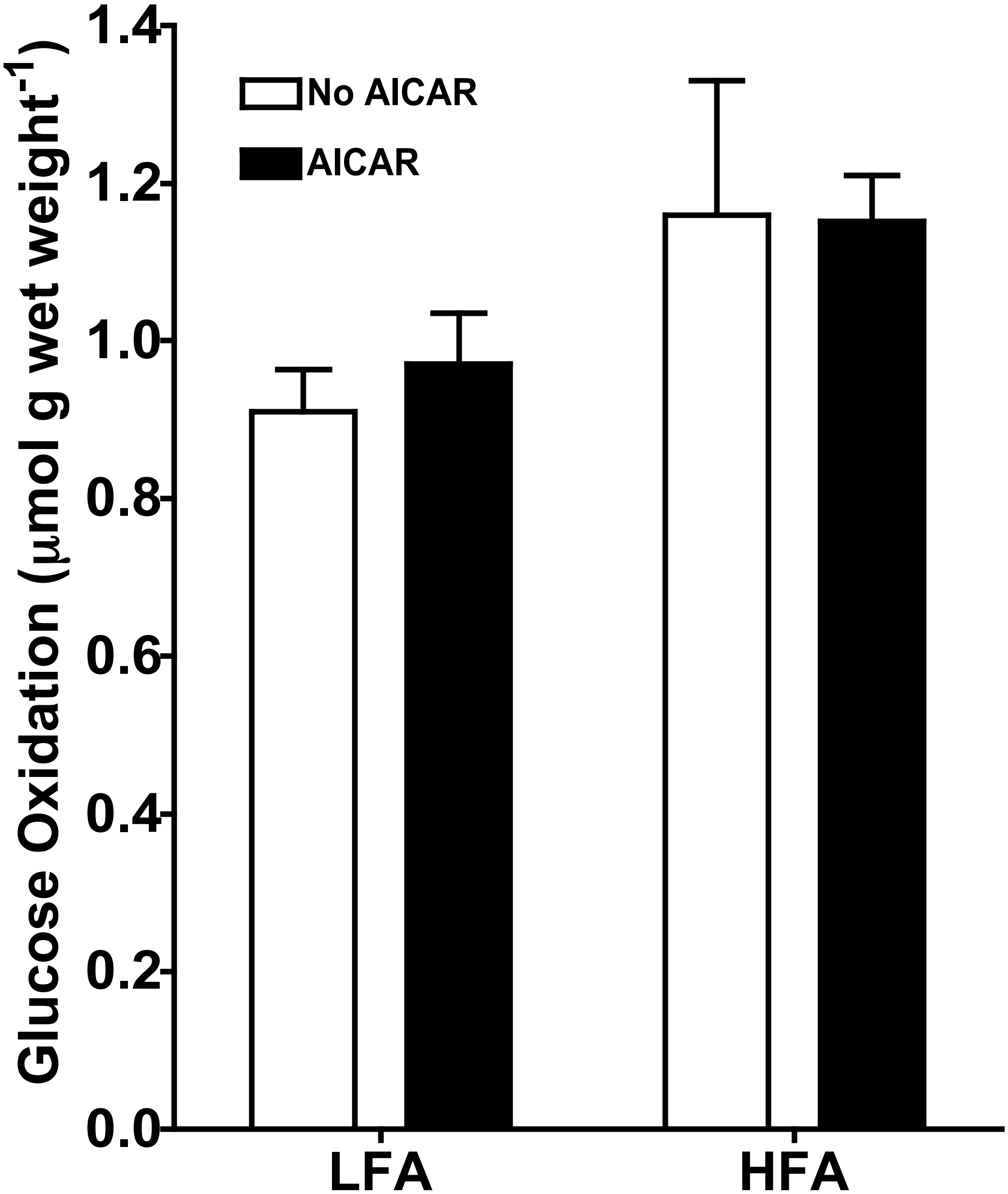

Figure 12: Effect of AICAR on glucose oxidation in low fatty acid (0.2 mM, LFA: A), or high fatty acid (1 mM, HFA: B) modified KHB in isolated contracting (last 30 min) rat soleus muscle

Values are means ± SEM, n = 6-8 per group. *Significantly different from No AICAR (*P* ≤0.05).

Discussion

With the use of palmitate and glucose tracers, we were able to directly examine the effects of AICAR on FA metabolism and glucose oxidation during high intensity tetanic contraction. Several novel observations were made: 1) incubation with AICAR further increased AMPKα2 activity above that seen with contraction alone; 2) AICAR further increased FA oxidation during contraction, independent of FA availability; 3) AICAR blunted TAG hydrolysis during contraction, independent of FA availability, while 4) having no effect on endogenous oxidation; and 5) AICAR had no effect on glucose oxidation during contraction. Therefore, our data suggest that FA substrate metabolism is much more sensitive than glucose to AMPKα2 stimulation during muscle contraction.

Effect of AICAR on Skeletal Muscle Lipid Metabolism During Contraction

To our knowledge, this is the first study to examine AICAR's effect on exogenous and endogenous lipid metabolism during contraction. With AICAR, there was an increase in exogenous FA oxidation above that seen with contraction alone, which could be due to a further increase in AMPKα2 activity. Previous evidence has shown that 15 minutes of hindlimb perfusion with AICAR-containing medium (at rest; 0.5, 1.0, 2.0 mM) significantly increased ZMP content in gastrocnemius-plantaris muscles, while having no effect on endogenous high-energy phosphates (ATP, ADP, AMP). This was associated with a significant increase in AMPK activity, leading to downstream effects of decreased ACC activity and decreased malonyl-CoA (125). Our previous resting protocol (*See* **CHAPTER 3**) certainly supports this AICAR-mediated increase in AMPK activity, which may be due to an initial increase in ZMP content. This further activation indicates that in our isolated tetanic contraction preparation, AMPK activation is a major regulator of FA oxidation. Recent evidence in AICAR-perfused rat hindquarters using a low intensity contraction protocol demonstrated that the increase in FA oxidation above that seen with contraction could not be attributed to the small increase in AICAR-induced AMPK activity, suggesting that with contraction, there are AMPK-independent mechanisms regulating FA metabolism (145). In this study, we used a higher intensity tetanic contraction protocol that has previously shown maximal stimulation of FA metabolism (49). The current data indicate that at high intensity tetanic contraction, AICAR can lead to further activation of AMPK, with further downstream effects on exogenous FA oxidation. Alternatively, AICAR may be targeting other additional regulatory enzymes resulting in an increase in FA oxidation. We also observed an increase in the partitioning of exogenous FA to oxidation at LFA during contraction, demonstrating an increased provision of FA to oxidative processes with AICAR. We did not observe a significant increase in FA partitioning with AICAR at HFA. However, this may not be surprising, as with increased FA substrate available during contraction proportionately more FA is available to be oxidized as well as esterified to TAG (49).

Regulation of TAG hydrolysis in resting and contracting skeletal muscle is poorly understood. In this study, treatment with AICAR during tetanic contraction significantly blunted TAG hydrolysis, independent of FA availability, while having no effect on endogenous-derived TAG oxidation. Indeed, exposing soleus strips to LFA did increase the provision of FA from TAG hydrolysis during contraction (+89% vs. HFA), with AICAR attenuating this effect in both conditions. It appears that AMPK regulation of TAG hydrolysis can occur during contraction and it is possible that AICAR reduced TAG hydrolysis during contraction by inhibiting the activation of HSL. Hormone sensitive lipase is an important enzyme in the hydrolysis of TAG. Recently, it has been shown that stimulation of AMPK prevents activation of HSL (193). Thus, it is possible that pharmacological stimulation of AMPK combined with contraction prevented the activation of HSL as would be expected with contraction alone, resulting in a reduction in TAG hydrolysis. However, further work is required to investigate the effect of AMPK activation on the regulation of HSL and TAG hydrolysis.

Importantly, although AICAR attenuated TAG hydrolysis, there was no significant effect on endogenous oxidation in contracting soleus muscle. It is possible that during contraction, there is an excess of FA released from the endogenous TAG pool which may be reincorporated if the oxidative needs of the cell are met (49). Regulatory mechanisms that hydrolyze the TAG molecule might allow for an excess of FA to be broken down during contraction, but the energy required by the cell would govern actual oxidation. This attenuation with AICAR suggests a better matching of TAG hydrolysis with the oxidative needs of the cell. Even with a slight mismatch between TAG hydrolysis and endogenous oxidation at LFA with AICAR, the results show that AICAR had no effect on the amount of FA oxidized from endogenous stores during contraction. Furthermore, if AICAR does markedly inhibit endogenous TAG hydrolysis and creates a better match between hydrolysis and oxidation, this could greatly reduce the accumulation of reactive lipid intermediates (DAG, ceramide) and any fatty acyl-CoA accumulating in the cytosol may be oxidized or re-esterified to TAG post-contraction (ie. reduction in DAG and ceramide content). The current pulse-chase protocol does not allow for the assessment of endogenous FA re-esterified into intramuscular TAG; however, rates of exogenous DAG and TAG esterification are not different during contraction with AICAR, suggesting that during contraction, when there are high rates of TAG hydrolysis, reactive lipid intermediates may be accumulating in the cytosol and AICAR may attenuate this increase. Further investigation of the accumulation of fatty acyl-CoA, DAG and ceramide after a contraction protocol to assess post-contraction insulin signaling is warranted.

Effect of AICAR on Muscle Glucose Oxidation During Contraction

AICAR had no further effect on already high rates of glucose oxidation in our tetanic contraction protocol. Much research has demonstrated that AMPK is involved in contraction-stimulated glucose uptake (78, 131), but it is likely not the sole mediator (128). Indeed, the combination of AICAR and contraction does not have an additive effect on glucose uptake (13, 78), which supports the current data on glucose oxidation rates. Importantly, it is also possible that factors other than AMPK regulate glucose uptake and oxidation. Muscle from mice with a dominant negative form of AMPK, were found to have full inhibition of AICAR- and hypoxia-induced glucose uptake, but only a partial (-40%) reduction in contraction-stimulated glucose uptake (128), suggesting that AMPK is only partially involved in the signaling mechanism to regulate glucose uptake and subsequent metabolism during contraction. It should also be noted that only one glucose concentration (10 mM) was used throughout these experiments. Thus, as was the case with FA oxidation, it is possible that an AICAR-induced stimulation of glucose oxidation may have been observed during contraction in the presence of a lower glucose concentration.

Summary

The results from the present study demonstrate that AICAR-mediated AMPKα2 activation is intimately involved in the regulation of FA metabolism during contraction, while having no effects on the already high rates of glucose oxidation in skeletal muscle. Incubation with AICAR during tetanic contraction 1) leads to synergistic increases in AMPKα2 activity; 2) further increases exogenous FA oxidation; and 3) blunts TAG hydrolysis, both at LFA and HFA. Further studies investigating AMPK regulation of HSL and TAG hydrolysis during contraction are warranted.

Chapter 5: Reduced Fatty Acid Uptake and Lipid Accumulation as Potential Mechanisms for Metformin and Exercise in the Prevention of Diabetes in High-Fat Fed Female Zucker Diabetic Rats

Introduction

The mechanisms that link acute FA exposure and obesity to insulin resistance are poorly understood. Acute and chronic (obesity) FA exposure are suggested to inhibit insulin-stimulated glucose transport and/or glucose phosphorylation in muscle (19, 149). It is becoming increasingly clear that derangements in skeletal muscle FA metabolism that relate to insulin resistance in obesity include increased FA transporters and FA transport rates (21, 32, 117), reduced FA oxidation in morbidly obese subjects (102, 105) and a resultant accumulation of various reactive lipid species, including DAG and ceramides (25).

Of particular interest is whether interventions that stimulate the AMPK-axis may play a role in improving glucose homeostasis and preventing the progression of obesity-related insulin resistance and T2DM. Acute activation of AMPK with AICAR in skeletal muscle stimulates glucose uptake (125) and partitions FA to oxidation (125, 130), while chronic activation leads to improved insulin-stimulated glucose uptake (27, 97), increased GLUT4 protein expression (84, 97, 201), PGC-1α protein content (184) and increased mitochondrial biogenesis (201). Previous studies have shown that AMPK is not down-regulated in obese human skeletal muscle (175) and that AMPK is capable of being activated during an acute exercise bout in muscle from subjects with T2DM (132). The antidiabetic agent metformin acutely activates AMPK in muscle (38, 61, 216), and liver (216). The dose and time of chronic metformin treatment may be an important determinant of the extent of AMPK activation in various tissues. One week of metformin treatment in rats prevented acute lipid-induced insulin resistance, but was shown to be associated with activation of AMPK in liver and not skeletal muscle (37). However, 4-10 weeks of metformin treatment activates AMPKα2 in skeletal muscle of subjects with T2DM (132). Longitudinal studies have shown that lifestyle changes (diet, exercise) and metformin reduce the development of T2DM in subjects with impaired glucose tolerance (107), which may be related to AMPK regulation of substrate use in skeletal muscle.

The male ZDF rat has traditionally been used as a model of obesity-related insulin resistance and diabetes for a number of years. In the insulin resistant stage, male ZDF rats have reduced AMPK activity (213); chronic AICAR treatment and exercise prevent the progression of diabetes in this model (142). In addition, treatment of male ZDF rats with troglitazone, a member of the TZD class of anti-diabetic drugs which also activates AMPK (113), improves soleus muscle FA oxidation (93) and insulin-stimulated glucose transport (168). The female Zucker diabetic fatty (ZDF) rat is an obese model of HF diet-induced T2DM. Within 4-8 weeks of being placed on a HF (48 kcal % fat) diet, these rats consistently develop overt diabetes that parallels the progression of T2DM seen in humans (39). Whether exercise and anti-diabetic drugs such as metformin regulate AMPK in skeletal muscle of female ZDF rats is not known.

Therefore, the aims of the current study were to determine whether 8 weeks of metformin and exercise, alone or in combination, would prevent derangements in glucose homeostasis in the female ZDF rats; and further, to determine whether improvements may be related to changes in skeletal muscle FA metabolism and AMPK regulation. We hypothesized that metformin and exercise, alone or in combination, would improve systemic glycemic control and skeletal muscle insulin-stimulated glucose transport. Furthermore, we hypothesized that improvements would be related to decreased markers of FA uptake (the putative FA transport proteins FAT/CD36 and FABpm) and improved partitioning of FA to oxidation and away from accumulation in skeletal muscle.

Methods

Animals

Female Zucker lean (+/?) or diabetic fatty (ZDF, *fa/fa*) rats were obtained from Charles River Laboratories (Charles River Laboratories, St. Constant, QC, Canada) at the age of 5 weeks. The animals were housed individually upon arrival, in a controlled environment with a reversed 12:12-hr light-dark cycle. Animals were fed standard rat chow (Purina Formulab® 5008) known to maintain normoglycemia in female ZDF rats (39) for an acclimation period of 5-7 days. Lean rats were maintained on standard rat chow, while ZDF rats were randomly assigned to either standard rat chow (16.7 kcal% fat, Purina Formulab® 5008) or HF-diet (60 kcal % fat, mainly animal fat (Research Diets C13004, New Brunswick, NJ, USA, *Appendix 3*)) alone or with one of the following interventions: metformin (HF-Met), exercise (HF-Ex) or the combination of exercise and metformin (HF-E+M). All protocols were approved by the Animal Care Committee, University of Guelph.

Feeding and Training Protocol

Rats were fed their respective diets *ad libitum* for 8 weeks (*Figure 13*). Metformin was dissolved in water (50mg/ml) and supplemented in the diet at an initial dose of 250 mg/kg body weight for one week and was increased to 500 mg/kg body weight for the duration of the study. Rats randomized to HF-Ex and HF-E+M were initially given two acclimation sessions on a motorized treadmill at 13m/min (0% grade) for a maximum of 5 min. Training took place 5 days per week and began with the rats running for 15 min, 15m/min, 0% grade, with duration and intensity gradually increasing to 2 hr, 18-19 m/min on a 10% grade by the end of 4 weeks. This duration and intensity was maintained for the subsequent 4 weeks, for a total of 8 weeks of training. To prevent any acute effects of the last training bout, experimental procedures were carried out 48 hours after the last training session. Animals were anaesthetized with an intraperitoneal injection of pentobarbital sodium (15 mg/kg body weight) before all experimental procedures.

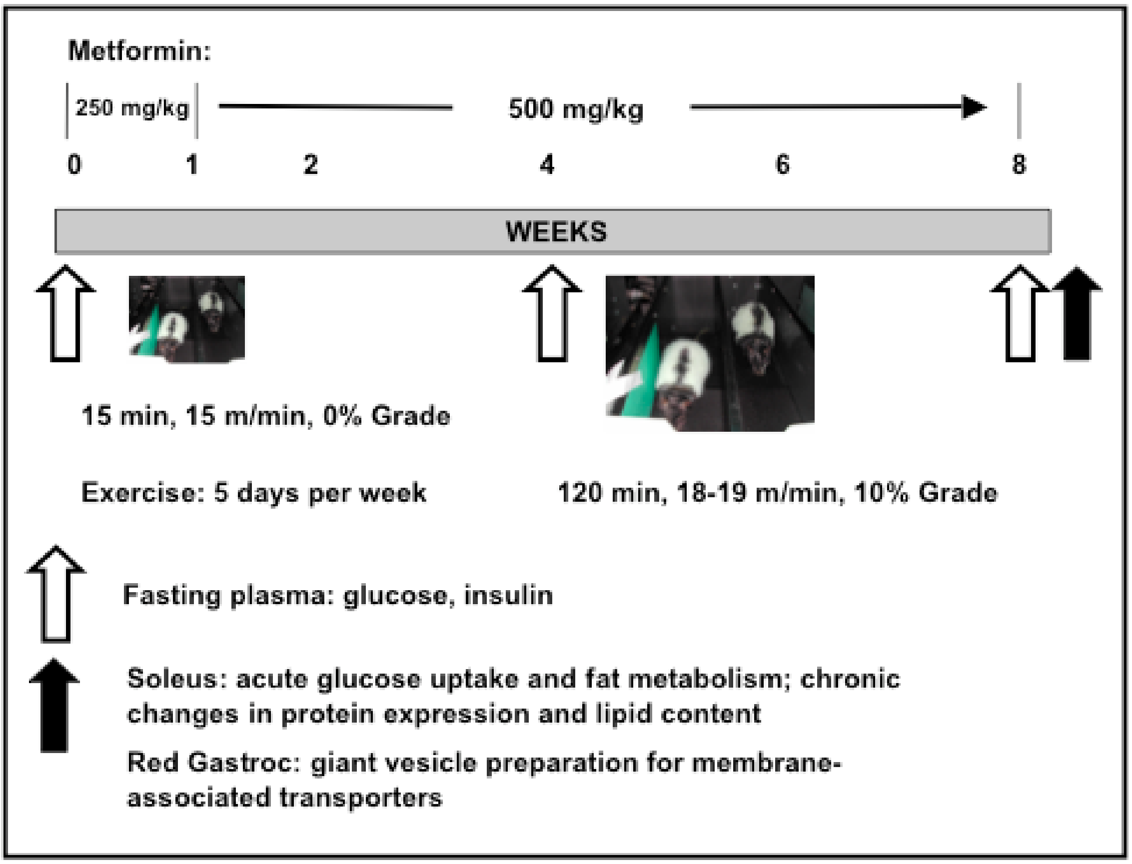

Figure 13: Experimental Protocol

Female Zucker Lean (+/?) or diabetic fatty (ZDF, *fa/fa*) were placed on an 8-week protocol. Lean rats were maintained on standard rat chow (Purina Lab Formula 5008), while ZDF rats were randomly assigned to either Purina Formulab® 5008 (does not induce hyperglycemia, 16.7 kcal% fat; n = 12) or HF-diet (48 kcal% fat) alone (n = 12) or in combination with metformin (HF-Met, up to 500 mg/kg; n = 12), exercise (HF-Ex, n = 12) or the combination of exercise and metformin (HF-E+M; n = 12). The exercise protocol took place 5 days per week and began with the rats running for 15 min, 15 m/min, 0% grade with duration and intensity gradually increasing to 2 hr, 18-19 m/min, 10% grade by the end of 4 weeks. This protocol was maintained for the duration of the 8-week protocol. At the end of the protocol, animals were anaesthetized and blood and tissue were collected as described in **Methods**.

Blood and tissue sampling

Fasting blood was collected pre-trial, and after four weeks, from the tail artery of animals anaesthetized with isofluorine inhalant. At the completion of the feeding and exercise protocol rats were fasted overnight and blood was collected via cardiac puncture after the excision of all tissues. Blood was transferred to heparinized tubes and kept on ice until being centrifuged (10,000 x *g*, 5 min) and plasma was collected. Fasting plasma insulin was assayed using a rat RIA kit (Linco, St. Charles, MO). Fasting plasma glucose was analyzed by Ascensia Elite Glucometer (Bayer, Inc.). Quality control analyses were performed with blood samples from healthy Sprague Dawley rats, consisting of multiple glucometer samples and verification with standard fluorometric analysis (*Appendix 4*).

Soleus muscle was carefully dissected into longitudinal strips from tendon to tendon with a 27-gauge needle, which were used for the determination of basal- and insulin-stimulated glucose uptake, and FA metabolism and muscle protein analysis (*See below*). Due to the tissue constraints of soleus muscle, protein expression of glucose and FA transporters were determined in whole tissue and giant sarcolemmal vesicles prepared from RG muscle. Vesicles were prepared without any exposure to physiological buffers containing agents that would alter sarcolemmal membrane protein content, such as insulin (116).

Basal- and insulin-stimulated skeletal muscle glucose uptake

Glucose uptake consisted of three incubation stages, as described previously (24). Briefly, soleus strips were equilibrated for 30 min in 2 ml warmed (30°C) pregassed

(95% O_2/5% CO_2) Kreb's-Henseleit buffer (KHB) containing 8 mM glucose and 32 mM mannitol, in the absence or presence of insulin (10 mU/ml). The concentration of insulin was maintained in all subsequent steps. Muscle strips were then washed in two 10-min incubations with glucose-free KHB containing 4 mM pyruvate and 36 mM mannitol. In the experimental phase, solei were incubated for 20 min (insulin-stimulated) or 40 min (basal) in KHB containing 4 mM pyruvate, 8 mM 3-O-[^{3}H]methyl-D-glucose (800 μCi/mmol), 28 mM [^{14}C]mannitol (60 μCi/mmol). After incubation, muscles were blotted of excess fluid, weighed and digested by boiling at 95°C in 1 ml NaOH for 10 min with intermittent vortexing. Glucose uptake was analyzed from a 200μl aliquot of muscle digest to quantify the accumulation of intracellular 3-O-[^{3}H]methyl-D-glucose.

Skeletal muscle fatty acid oxidation and quantification of skeletal muscle lipids incorporated during incubation

Soleus strips were placed in 2 ml of warmed (30°C) pregassed (95% O_2/5% CO_2) KHB containing 4% fatty acid-free bovine serum albumin (Serologicals, Norcross, GA), 1 mM palmitate, and 5.5 mM glucose in a gentle shaking bath. After an equilibration phase of 30 min, muscles were transferred to the experimental phase and incubated for 60 minutes in the same medium described above with the addition of 0.5 μCi/ml [1-^{14}C]palmitate (Amersham, QC, Canada), permitting the determination of exogenous palmitate oxidation and incorporation into endogenous lipid pools.

Gaseous $^{14}CO_2$ produced from exogenous oxidation of [1-^{14}C]palmitate was determined as outlined in **CHAPTER 3 AND 4** (164, 165) with minor modifications. A 0.5

ml microcentrifuge tube containing 250 μl of 1 M benzethonium hydroxide (Sigma, Oakville, ON, Canada) was placed within a 1.5 ml microcentrifuge tube and was incubated along with solei within the incubation vial to quantify gaseous $^{14}CO_2$ produced during the incubation. At the end of the experimental phase a 1.0 ml aliquot of buffer was transferred to a 50 ml Erlenmeyer flask, which was quickly sealed with a rubber stopper fitted with a stopcock and needle. The buffer was acidified with 1 ml of 1 M H_2SO_4 and $^{14}CO_2$ was captured and quantified as previously described. Quantification of skeletal muscle lipids incorporated during incubation was determined as previously described in **CHAPTER 3 AND 4**.

Whole tissue lipid content analysis

Soleus muscle (~50-80 mg) was freeze-dried, powdered and cleaned of any visible connective tissue. Skeletal muscle lipids were graciously analyzed by Dr. Adrian Chabowski, Medical University of Bialystok (Bialystok, POLAND), as previously described (25). Briefly, lipids were extracted in chloroform-methanol (2:1 v/v) according to the Folch method of lipid extraction (59) with the addition of 0.01% butyrated hydroxytoluene (Sigma-Aldrich, St. Louis, MO) as an anti-oxidant. Lipids were separated by chromatography on thin layer silica gel plates. The total lipid extract was separated to isolate DAG and ceramide (46) using heptane-isopropyl ether-acetic acid (60:40:3 v/v/v) solvent. Briefly, samples were developed to one-third of the total length of the plate in chloroform-methanol-25% NH_3 (20:5:0.2 v/v/v) solvent, dried and rechromatographed in heptane-isopropyl ether-acetic acid (60:40:3 v/v/v) solvent. Plates were then dried, sprayed with dichlorofluorescein dye (0.2% wt/vol in methanol), and visualized under long-wave ultraviolet light. Standards for DAG and ceramide were run along with the plates to facilitate identification of lipid bands. The individual lipid bands were marked on the plate and scraped into vials. After lipid separation, samples with methylpentadecanoic acid (internal standard, Sigma-Aldrich, Oakville, ON, Canada) were transmethylated in the presence of 1 ml 14% boron fluoride in methanol at 100°C for 90 min. The samples were cooled to room temperature, and 1 ml pentane and 0.5 ml water were added. After centrifugation, the upper pentane phase was evaporated under N_2. The methyl esters were dissolved in 40 μl hexane and analyzed by gas-liquid chromatography. A Hewitt-Packard 5890 Series II and a fused HP-INNOWax (50 m x 0.53 mm) capillary column were used. Injector and detector temperatures were set at 250°C each. The oven temperature was increased linearly from 160 to 250°C at a rate of 5°C/min. Individual FA methyl esters were quantified using the area corresponding to the internal standards. Total DAG and ceramide contents were estimated as the sum of the particular FA content of the assessed fraction and was expressed in nanomoles per gram dry weight (*See Calculations and Statistics, below*).

Preparation of giant sarcolemmal vesicles

Giant sarcolemmal vesicles were graciously prepared by Jennifer Nickerson, M.Sc., Department of Human Health and Nutritional Sciences, University of Guelph, from fresh tissue samples of RG muscle as described previously (173). Briefly, 1-3 mm thick slices of muscle were obtained by slicing with a scalpel blade in 140 mM KCl-10 mM MOPS (KCl-MOPS, pH 7.4). The muscle preparation was then incubated for 1-1.5 hr in 140 mM KCl-10 mM MOPS (pH 7.4), aprotonin (1.0 mg/ml) and collagenase type

VII (150 U/ml) in a shaking water bath maintained at 34°C. The medium was then filtered through cheesecloth to obtain the supernatant fraction, with the remaining tissue being rinsed in KCl-MOPS with 10 mM EDTA and the resulting second supernatant fraction was filtered through cheesecloth and pooled with the first supernatant to a volume of 7.5 ml. Percoll (16% v/v) and aprotinin (1 mg/ml) were added (1.7 ml) and the resulting suspension was placed at the bottom of a density gradient consisting of a 1 ml upper layer and a 3 ml middle layer of 4% Nycodenz (wt/vol). The suspension was centrifuged at 60 x *g* for 45 min at room temperature and the vesicles were harvested from the interface separating the upper and middle phases, diluted with KCl-MOPS and recentrifuged at 1200 x *g* for 5 min. The resulting pellets were resuspended with KCl-MOPS to protein concentrations of 0.3-0.8 mg/ml and frozen at -80°C until protein content analysis (*See below*).

Preparation of tissue lysates for protein content and activity assays

Muscle tissue (~50 mg, soleus and RG) was homogenized (5000μl/g tissue, 1:5 dilution) in ice-cold buffer suitable for protein extraction and preserving phosphorylation states of proteins, containing 50 mM Tris (pH 7.5), 1 mM EDTA, 1 mM EGTA, 50 mM NaF, 5 mM Na pyrophosphate, 10% (v/v) glycerol, 1% (v/v) Triton X-100, 2 mg/ml leupeptin, 2 mg/ml aprotinin, 2 mg/ml pepstatin, 1 mM DTT, and 1 mM phenylmethylsulfonyl fluoride. Homogenates were centrifuged at 20,000 x *g* for 20 min at 4°C and the supernatant was removed and protein content was determined with the Pierce method, using BSA as standards.

Western blot analysis

Fifty micrograms of tissue lysate protein (for Thr172 phosphorylated AMPK (pAMPK), total AMPKα (tAMPK), AMPKα1, AMPKα2, Ser-79 phosphorylated ACC (pACC)) or 10 μg of lysate protein from the preparation of giant sarcolemmal vesicles (for FAT/CD36, FABPpm, GLUT4) were solubilized in 4x Laemmeli's buffer and boiled at 95°C for 5 min, resolved by SDS-PAGE and wet transferred to PVSF membranes (*See Appendix 5 for protocols for each protein*). The membranes were blocked for one hour and then incubated with the specific primary antibodies. After incubation with the appropriate secondary antibody and final wash, the immune complexes were detected using the ECL method and immunoreactive bands were quantified with densiometry.

Measurement of oxidative enzyme activity in soleus muscle homogenates

Citrate synthase activity was determined spectrophotometrically in aliquots of homogenized whole muscle, according to Srere (169), with minor modifications. Briefly, soleus muscle lysates containing Triton X-100 were diluted to 1:20 and repeatedly freeze-thawed (at least two times) to ensure lyzing of mitochondria. The diluted homogenate was mixed with (final concentrations) 60 mM TRIS buffer (pH 8.3), 0.32 mM acetyl-CoA, 0.1 mM 5,5-dithiobis-2-nitrobenzoate (DTNB), 0.04% (vol/vol) Triton X-100. The reaction was initiated with the addition of 0.6 mM oxaloacetate (OAA) and citrate synthase activity was quantified as the enzymatic release of CoASH from acetyl-CoA linked to a linear colour change in DTNB at a wavelength of 412 nm.

β-hydroxyacyl-CoA dehydrogenase activity was assayed spectrophotometrically as the reverse reaction converting a four-carbon alcohol to the four-carbon beta-oxidation intermediate acetoactetyl-CoA in diluted whole muscle homogenates as for the citrate synthase assay (37°C, 340nm) by measuring the linear disappearance of NADH. The assay mixture (final concentrations) consisted of 50 mM TRIS-HCl (pH 7.0), 2 mM EDTA, 0.25 mM NADH, 0.02% Triton X-100 and the initiation of the reaction with 0.1 mM acetoacetyl-CoA (115).

Calculations and Statistics

To calculate palmitate oxidized or incorporated into lipid pools (nanomoles per gram wet wt), the specific activity of the incubation buffer (dpm. radiolabeled palmitate/nmol total palmitate) was used. Glucose uptake into soleus muscle was calculated by the accumulation of intracellular 3-O-[^{3}H]methyl-D-glucose analogue after correcting for extracellular volume with the determination of [^{14}C]mannitol and expressed as nmol glucose analogue accumulated per gram wet tissue per 5 min. Protein expression quantification utilized samples from Lean controls and were allocated a value of 100% protein content and were not included in statistical analyses.

Results are presented as mean ± SEM. For the analyses of individual DAG and ceramide species, the sum of the means were determined (n = 8-12 per group, due to the removal of data points giving non-detectable (ND) species in some samples), whereas for analyses of total saturated, monounsaturated and polyunsaturated DAG and ceramide contents, the mean of the sums were used in the calculation (n = 12). The samples with

ND species were not removed from the data set, as FA were re-distributed to other species and/or pools. Therefore, due to differences in the individual lipid species sample size, there were slight differences in the reported mean ± SEM for the total saturated, monounsaturated and polyunsaturated DAG and ceramide contents, compared to the summation of the reported mean ± SEM for individual DAG and ceramide species. For example:

Summation of the Individual Saturated Lipid Species:

$$\text{Sum of Means} = \frac{\sum(C14:0)}{8} + \frac{\sum(C16:0)}{10} + \ldots + \frac{\sum(C22:0)}{11} + \frac{\sum(C24:0)}{12} \qquad [\textit{Eq 1}]$$

Whereas:

Mean of the Total Saturated Lipid Species:

$$\text{Mean of the Sums} = \frac{\sum(C14:0 + C16:0 + \ldots + C22:0 + C24:0)}{12} \qquad [\textit{Eq 2}]$$

Therefore, due to different denominators as the number of observations, the summation of the individual lipid species do not equate to the total of each respective lipid pool, but rather are an approximation of each other (*Table 7 and 8*).

Two-way ANOVA analyses were performed for plasma glucose and insulin, with time and treatment as factors, followed by Fisher least square differences (LSD) *post-hoc* analyses to assess statistical differences between groups. For all endpoint measurements, one-way ANOVA analyses were performed to analyze significant differences, followed by Fisher LSD *post-hoc* analyses to assess statistical significance between groups. Statistical significance was accepted at $P \leq 0.05$, with note of any trends ($P \leq 0.10$), marked with the letter in parentheses.

Results

Body Composition

Body mass of Lean and ZDF rats are shown in *Table 5*. Body mass in all of the ZDF groups were significantly elevated compared to Lean rats at the beginning of the trial (+50%, $P < 0.01$), at Wk 4 (+70-80%, $P < 0.001$) and Wk 8 (+80-90%, $P < 0.001$). The final body mass of all ZDF groups were not different at the end of the trial.

Plasma insulin and glucose

Insulin. Pre-trial, there were no differences in fasting plasma insulin between any of the groups (*Table 5*). By week 4, plasma insulin levels were significantly higher than pre-trial in all ZDF HF-fed rats ($P < 0.05$), however, the increase in plasma insulin was greatest in rats fed the HF diet alone (ie. no intervention). After 8 weeks, all HF rats were hyperinsulinemic compared to Lean rats ($P < 0.001$).

Glucose. Pre-trial, there were no differences in fasting plasma glucose between any of the groups (*Table 5*). By week 4, plasma glucose in HF rats were increased compared to Lean (+144%), C (+80%), HF-Ex (+80%), HF-E+M (+60%) ($P < 0.05$). By week 8, HF rats developed overt hyperglycemia (24.38 ± 2.12 mM), which was significantly higher than Lean (+193%, $P < 0.001$) and all ZDF groups (+42-120%, $P < 0.01$).

Basal and insulin-stimulated glucose uptake

Basal glucose uptake. There were no significant differences in basal glucose uptake between any of the groups (*Figure 14A*).

Insulin-stimulated glucose uptake. All ZDF groups exhibited impaired insulin-stimulated glucose uptake (-40-80%, $P < 0.001$) compared to Lean rats. In addition, HF (-32%, $P < 0.001$) and HF-Met (-35%, $P < 0.001$) exhibited impaired insulin-stimulated glucose uptake compared to C, HF-Ex ($P = 0.068$) and HF-E+M. Insulin-stimulated glucose uptake was partially normalized in HF-Ex and HF-E+M rats, as there were no differences observed between C, HF-Ex and HF-E+M groups (*Figure 14B*).

Chronic changes in whole muscle and plasma membrane GLUT4 protein expression in skeletal muscle

Plasma membrane-associated changes in GLUT4 levels were assessed in RG muscle after the preparation of giant sarcolemmal vesicles. Both HF-Ex and HF-E+M exhibited increases in whole muscle (HF-Ex: +23-26%, $P < 0.05$; HF-E+M: +31-35%, $P < 0.01$) and plasma membrane-associated (HF-Ex: +45-55%, $P < 0.05$; HF-E+M: +70-80%, $P < 0.001$) GLUT4 protein content (*Figure 15*).

Fatty Acid Metabolism in Skeletal Muscle

Exogenous FA Metabolism. All ZDF groups exhibited depressed exogenous FA oxidation (-24-43%, P<0.01, *Figure 16A*) and increased TAG esterification (+47-51%, P<0.01, *Figure 16B*) compared to Lean rats, and no acute changes in FA oxidation were observed between any of the ZDF (C or HF) groups.

Chronic changes in Skeletal Muscle FAT/CD36 and FABPpm Membrane Protein Expression

Whole muscle and plasma membrane-associated changes in FAT/CD36 and FABPpm levels were assessed in RG muscle after the preparation of giant sarcolemmal vesicles (*Figure 17*). Whole muscle (+40%, P < 0.001) and plasma membrane-associated (+56%, P < 0.001) FAT/CD36 was increased in ZDF HF compared to C. All treatments resulted in significant reductions in whole muscle and plasma membrane-associated FAT/CD36 protein expression compared to HF-fed rats (HF-Met: -15-27%, $P < 0.05$; HF-Ex: -18-29%, $P = 0.006$; HF-E+M: -21-33%, $P < 0.01$). Linear regression revealed a significant negative correlation between plasma membrane-associated FAT/CD36 and plasma membrane-associated GLUT4 (P = 0.05, r = 0.94) in rats fed the HF diet. No changes in whole muscle or plasma membrane-associated FABPpm were observed in the ZDF groups.

Skeletal muscle lipid content

Diacylglycerol. ZDF HF rats had increased total DAG content (*Figure 18A*) compared to both Lean (+72%, $P < 0.001$) and C (+20%, $P = 0.028$) rats. Reductions in total DAG content were observed with HF-Met (-53%, $P < 0.001$) and both HF-Ex and HF-E+M rats (-110-130%, $P < 0.001$) compared to ZDF HF rats. Interestingly, total DAG content was decreased in all HF treatments (HF-Met, HF-Ex, HF-E+M, $P < 0.005$) compared to C rats on a low-fat diet. There were further reductions in total DAG content in both HF-Ex ($P = 0.021$) and HF-E+M ($P = 0.008$) compared to HF-Met treatment alone.

ZDF HF rats also had significantly more total saturated DAG content compared to Lean rats and C ($P < 0.001$), as well as more monounsaturated ($P < 0.001$) and polyunsaturated ($P = 0.019$) DAG content (*Table 6*) compared to Lean rats. Stearoyl-CoA (C18:0) and eicosanoyl-CoA (22:0) were significantly increased in ZDF HF-fed rats (C18:0: $P < 0.001$ vs Lean and C; C22:0: $P < 0.01$ vs Lean and C). Reductions in total saturated ($P < 0.001$), monounsaturated ($P < 0.01$) and polyunsaturated ($P < 0.05$) DAG content were seen in ZDF HF-Met, HF-Ex and HF-E+M rats, due to decreases in some (C14:0, C:16:0, C16:1, C18:0, C22:0; C:18:1; C20:4, 20:5, $P < 0.05$) but not all DAG species. Furthermore, the C16:0, C18:0, C18:1 and C20:5 species were significantly lower in HF-Met, HF-Ex and HF-E+M than the ZDF C rats on a lower-fat diet. Interestingly, the sum of the saturated DAG species ($P < 0.05$), a number of saturated species (C14:0, C16:0, C18:0 C22:0, $P < 0.05$), and C16:1 ($P < 0.06$) were further reduced in HF-Ex and HF-E+M compared to HF-Met.

Ceramide. ZDF HF rats had increased total ceramide content (*Figure 18B*) compared to both Lean (+111%, P <0.001) and C (+71%, P < 0.001). Reductions in total ceramide were observed with ZDF HF-Met (-68%, P < 0.001) and both HF-Ex and HF-E+M rats (-109-225%, P < 0.001) compared to ZDF HF rats. Further reductions in total ceramide content were observed with combined HF-E+M rats compared to C and HF-Met rats (-90%, P < 0.01). Furthermore, a synergistic effect was observed as HF-E+M had less total ceramide species compared to HF-Ex (-55%, P = 0.05).

ZDF HF rats also had significantly more total saturated, monounsaturated and polyunsaturated ceramide content compared to Lean and ZDF-C rats (P < 0.001, *Table 7*). Most (P < 0.05), but not all (C20:0, C22:0 *not significant*) ceramide species were increased in the ZDF HF compared to C. Virtually all ceramide species were elevated in ZDF HF fed rats in comparison to Lean rats (P < 0.05). There were significant reductions in total saturated (P < 0.001), monounsaturated (P < 0.001) and polyunsaturated (P < 0.05) ceramide content in ZDF HF-Met, HF-Ex and HF-E+M treatments that were attributed to decreases in all ceramide species. Interestingly, the sum of the saturated (P < 0.01), monounsaturated (P < 0.01) and polyunsaturated (P < 0.05) ceramide species were further reduced with the combination HF-E+M, compared to HF-Met.

Skeletal muscle AMPK signaling

AMPK Protein Expression. There were no significant differences in total protein expression of AMPK (*Figure 19A*) or the phosphorylation state of AMPK (*Figure 19B*). There were modest increases in AMPKα1 protein expression (*Figure 19C*) with HF-Met treatment (+ 30%, $P < 0.05$), and AMPKα2 protein expression (*Figure 19D*) in HF-Ex (+12-17%, $P < 0.05$) and the combination HF-E+M (+15-21%, $P < 0.05$) compared to ZDF HF and HF-Met rats.

AMPK "Target" Proteins. There were no significant differences in the phosphorylation state of the downstream target ACC (*Figure 20A*). However, PGC-1α protein content tended to increase in HF-Met rats (+15%, $P = 0.06$), and was increased in HF-Ex (+22-26%, $P = 0.01$) and HF-E+M (+20-25%, $P = 0.01$), compared to C and HF rats (*Figure 20B*).

Oxidative Enzyme Activity

There was an increase in the activity of citrate synthase (*Table 8*) with both HF-Ex (+12-15%, $P < 0.05$) and HF-E+M (+21-24%, $P < 0.05$). There was also an increase in β-HAD with HF-Ex (+20-24%, $P < 0.05$) and HF-E+M (+30-35%, $P < 0.01$).

Table 5: Body weight and fasting plasma insulin and glucose from Lean and ZDF rats on Control (C) or high-fat (HF) diet

Values are expressed as mean ± SEM, [a]: Significantly different from Lean ($P \leq 0.05$); [b]: Significantly different from Control ($P \leq 0.05$); [c]: Significantly different from HF ($P \leq 0.05$); [d]: Significantly different from HF-Met ($P \leq 0.05$); [e]: Significantly different from HF-Ex ($P \leq 0.05$); [f]: Significantly different from Week 0 ($P \leq 0.05$); [g]: Significantly different from Week 4 ($P \leq 0.05$).

		ZDF				
	Lean	C	HF	HF-Met	HF-Ex	HF-E+M
n	12	12	12	12	12	12
Body Weight, g						
Week 0	100 ± 1	146 ± 5[a]	146 ± 4[a]	153 ± 6[a]	137 ± 5[a]	139 ± 4[a]
Week 4	160 ± 2	274 ± 4[a]	286 ± 8[a]	290 ± 7[a]	285 ± 3[a]	273 ± 4[a]
Week 8	188 ± 3	358 ± 6[a]	345 ± 8[a]	350 ± 7[a]	339 ± 3[a]	337 ± 4[a]
Fasting Plasma Insulin, ng/ml						
Week 0	0.3 ± 0.1	2.6 ± 1.2	2.2 ± 0.5	1.4 ± 0.3	1.8 ± 0.3	3.0 ± 0.8
Week 4	0.4 ± 0.1	3.4 ± 0.4	13.9 ± 1.4[abf]	7.0 ± 1.3[acf]	7.7 ± 0.8[acf]	2.5 ± 0.4[ac]
Week 8	1.9 ± 0.3	13.2 ± 0.8[fg]	16.2 ± 1.6[abf]	17.2 ± 2.2[afg]	18.10 ± 1.2[afg]	14.2 ± 1.3[afg]
Fasting Plasma Glucose, mM						
Week 0	2.6 ± 0.3	6.7 ± 0.8	5.5 ± 0.5	7.8 ± 3.3	6.6 ± 0.9	6.6 ± 1.1
Week 4	4.1 ± 0.5	5.6 ± 0.5	10.1 ± 2.9[ab]	7.1 ± 1.3	5.6 ± 0.6[c]	6.5 ± 0.5
Week 8	8.3 ± 1.10[fg]	13.3 ± 1.4[fg]	24.4 ± 2.1[afg]	17.7 ± 2.7[acfg]	11.1 ± 0.9[acfg]	14.7 ± 1.7[acfg]

Table 6: Soleus muscle diacylglycerol (DAG) content from Lean and ZDF rats on Control (C) or high-fat (HF) diet

Values are expressed as mean ± SEM, nmol/g dry weight ^{a}: Significantly different from Lean ($P \leq 0.05$); ^{b}: Significantly different from Control ($P \leq 0.05$); ^{c}: Significantly different from HF ($P \leq 0.05$); ^{d}: Significantly different from HF-Met ($P \leq 0.05$). Letters in parentheses denote a trend ($0.05 < P \leq 0.10$).

		ZDF				
DAG Species	Lean	C	HF	HF-Met	HF-Ex	HF-E+M
Saturated						
14:0	121 ± 24	150 ± 23	168 ± 25$^{(a)}$	115 ± 23^{c}	64 ± 8$^{abc(d)}$	70 ± 8$^{(a)bc(d)}$
16:0	1087 ± 93	1559 ± 179^{a}	1812 ± 151^{a}	1203 ± 106^{bc}	884 ± 63$^{bc(d)}$	812 ± 74^{bcd}
18:0	1254 ± 91	1385 ± 115	2091 ± 250^{ab}	1217 ± 155^{bc}	827 ± 83^{abcd}	691 ± 88^{abcd}
20:0			ND			
22:0	11 ± 2	11 ± 2	18 ± 2^{ab}	13 ± 1.4^{c}	7 ± 1^{cd}	8 ± 1^{cd}
24:0			ND			
Sum Saturated*	**2367 ± 213**	**3092 ± 251^{a}**	**3885 ± 434^{ab}**	**2548 ± 265.6^{c}**	**1783 ± 139^{bcd}**	**1581 ± 164^{abcd}**
Monounsaturated						
16:1	74 ± 23	230 ± 22^{ac}	159 ± 22^{a}	140 ± 19	88 ± 9^{cd}	84 ± 15^{cd}
18:1	506 ± 65	925 ± 129^{a}	949 ± 104^{a}	686 ± 53^{bc}	537 ± 46^{bc}	529 ± 58^{bc}
24:1			ND			
Sum Monounsaturated	**574 ± 76**	**1117 ± 143^{a}**	**1231 ± 176^{a}**	**751 ± 79^{bc}**	**581 ± 62^{bc}**	**613 ± 71^{bc}**
Polyunsaturated						
18:2	189 ± 31	240 ± 32	253 ± 31	216 ± 22	172 ± 16	159 ± 16
20:4	54 ± 12	94 ± 21$^{(a)}$	115 ± 29^{a}	50 ± 8$^{(b)c}$	50 ± 11$^{(b)c}$	38 ± 4^{bc}
20:5	19 ± 3	29 ± 6$^{(a)}$	35 ± 5^{a}	17 ± 2^{bc}	10 ± 2$^{(a)bc}$	12 ± 1^{bc}
22:6	17 ± 2	28 ± 2	20 ± 7	13 ± 2	15 ± 3	17 ± 1
Sum Polyunsaturated	**275 ± 35**	**381 ± 32^{a}**	**388 ± 51^{a}**	**291 ± 29$^{(b)c}$**	**239 ± 24^{bc}**	**224 ± 16^{bc}**

Table 7: Soleus muscle ceramide content from Lean and ZDF rats on Control (C) or high-fat (HF) diet

Values are expressed as mean ± SEM, nmol/g dry weight [a]: Significantly different from Lean ($P \le 0.05$); [b]: Significantly different from Control ($P \le 0.05$); [c]: Significantly different from HF ($P \le 0.05$); [d]: Significantly different from HF-Met ($P \le 0.05$); [e]: Significantly different from HF-Ex ($P \le 0.05$). Letters in parentheses denote a trend ($0.05 < P \le 0.10$).

		ZDF				
Ceramide Species	Lean	C	HF	HF-Met	HF-Ex	HF-E+M
Saturated						
14:0	111 ± 16	116 ± 11	222 ± 27[ab]	106 ± 10[c]	58 ± 6[abcd]	54 ± 5[abcd]
16:0	208 ± 18	259 ± 17	413 ± 42[ab]	220 ± 17[c]	183 ± 9[bc]	142 ± 11[abcd]
18:0	200 ± 15	265 ± 18[a]	441 ± 43[ab]	242 ± 21[c]	207 ± 13[c]	158 ± 13[bcd]
20:0	15 ± 1	22 ± 3[a]	25 ± 2[a]	16 ± 1[bc]	16 ± 1[bc]	14 ± 1[bc]
22:0	18 ± 2	26 ± 4	41 ± 6[a]	20 ±1[c]	18 ± 2[c]	15 ± 1[bc]
24:0	75 ± 9	77 ± 5	116 ± 11[ab]	68 ± 5[c]	49 ± 6[abcd]	44 ± 3 [abcd]
Total Saturated*	**576 ± 51**	**712 ± 76**	**1168 ± 126[ab]**	**674 ± 60[c]**	**547 ± 44[c]**	**371 ± 33[abcd]**
Monounsaturated						
16:1	11 ± 1	15 ± 2	24 ± 3[ab]	16 ± 2[ac]	8 ± 1[bcd]	7 ± 1[bcd]
18:1	66 ± 7	106 ± 18[a]	160 ± 18[ab]	78 ± 6[c]	57 ± 5[bc]	38 ± 5[bcd]
24:1	32 ± 4	38 ± 5	57 ± 5[ab]	33 ± 3[c]	20 ± 3[abc]	22 ± 2[abcd]
Total Monounsaturated	**104 ± 12**	**129 ± 14**	**208 ± 29[ab]**	**127 ± 8[c]**	**89 ± 16[c]**	**63 ± 8[bcd]**
Polyunsaturated						
18:2	54 ± 10	92 ± 15	148 ± 30[ab]	91 ± 13[c]	85 ± 11[c]	41 ± 6[bcd(e)]
20:4	43 ± 6	63 ± 9	145 ± 30[ab]	87 ± 10[c]	84 ± 14[c]	41 ± 6[cde]
20:5	19 ± 2	17 ± 3	38 ± 4[ab]	15 ± 1[c]	12 ± 1[ac]	11 ± 1[ac]
22:6	35 ± 6	31 ± 6	43 ± 6[(b)]	31 ± 3[(c)]	22 ± 3[c]	12 ± 2[bcd]
Total Polyunsaturated	**128 ± 18**	**165 ± 24**	**330 ± 67[ab]**	**216 ± 23[c]**	**181 ± 30[c]**	**91 ± 15[cd(e)]**

Table 8: Soleus muscle citrate synthase and β-HAD from ZDF rats on high-fat (HF) diet

Values are expressed as mean ± SEM, μmol/min/g wet wt. [c]: Significantly different from HF ($P \leq 0.05$); [d]: Significantly different from HF-Met ($P \leq 0.05$).

	ZDF			
	HF	HF-Met	HF-Ex	HF-E+M
Citrate Synthase Activity, μmol/min/g wet wt	43.8 ± 1.8	44.8 ±1.6	50.5 ± 1.3[cd]	54.2 ± 3.2[cd]
β-HAD Activity, μmol/min/g wet wt	12.1 ± 1.1	12.6 ± 0.9	15.0 ± 0.8[cd]	16.3 ± 0.7[cd]

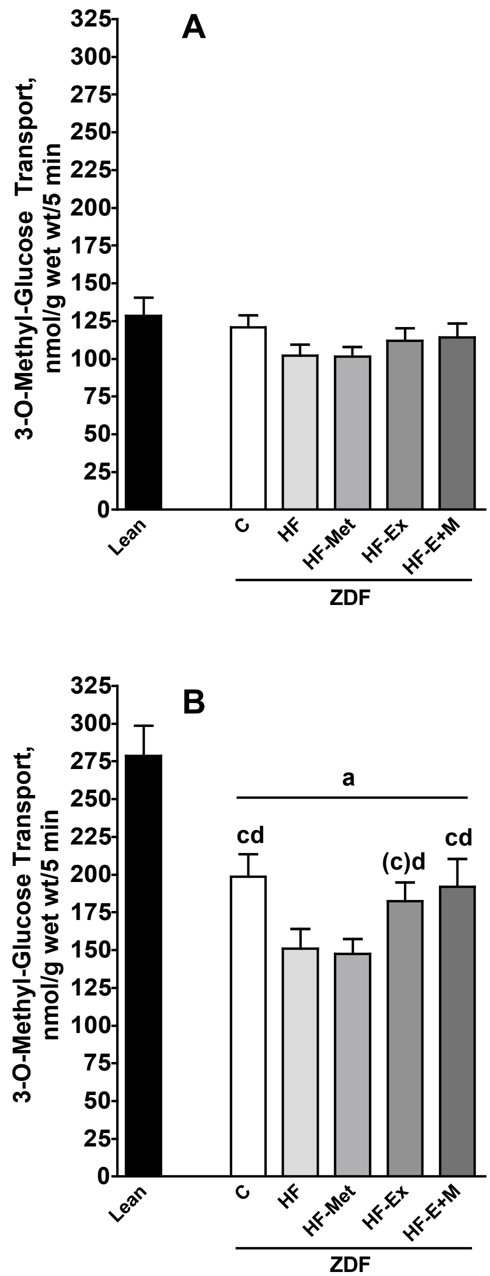

Figure 14: Basal (A) and insulin-stimulated (B) glucose transport in soleus muscle from Lean and ZDF rats on Control (C) or high-fat (HF) diet

Glucose transport rates were monitored over 40 min for basal and 20 min for insulin-stimulated conditions. Values are mean ± SEM, nmol/g wet weight/60 min. [a]: Significantly different from Lean ($P \leq 0.05$); [c]: Significantly different from HF ($P \leq 0.05$); [(c)]: trend observed ($P = 0.068$); [d]: Significantly different from HF-Met ($P \leq 0.05$).

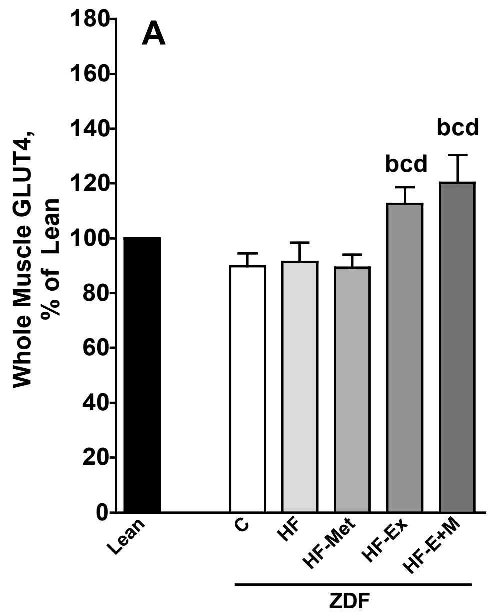

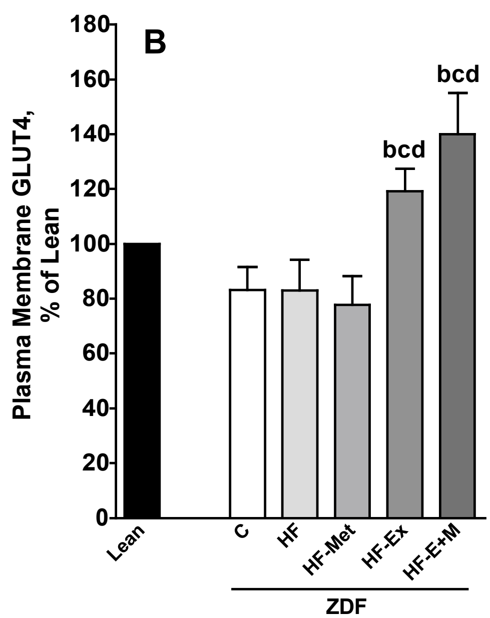

Figure 15: Whole muscle (A) and plasma membrane (B) GLUT4 glucose transporter protein expression in RG muscle from Lean and ZDF rats on Control (C) or high-fat (HF) diet

Values are mean ± SEM, expressed as % of Lean control (set to 100%). [b]: Significantly different from Control ($P \leq 0.05$); [c]: Significantly different from HF ($P \leq 0.05$); [d]: Significantly different from HF-Met ($P \leq 0.05$).

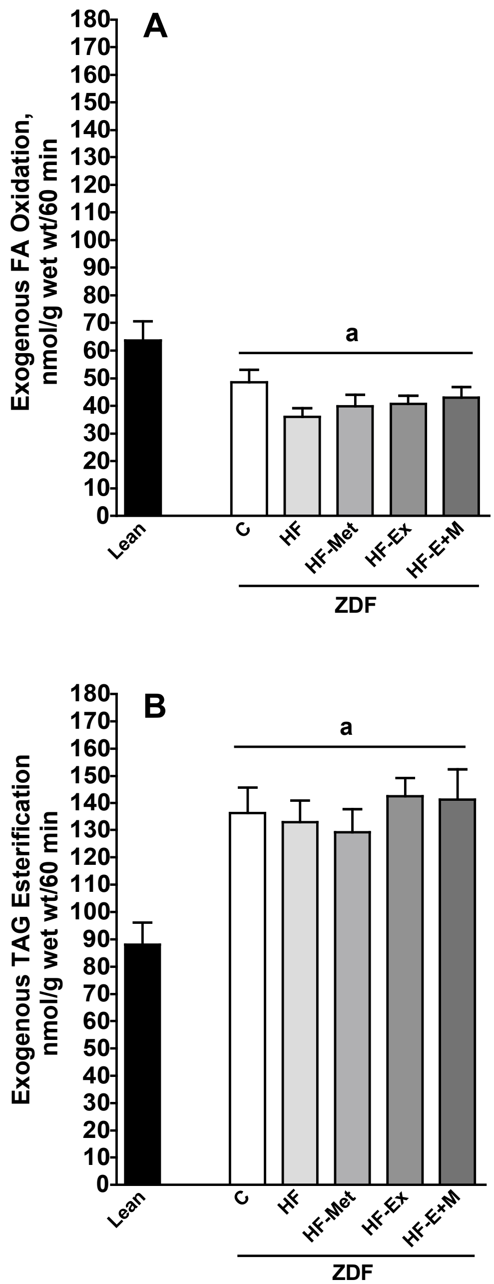

Figure 16: Soleus muscle exogenous FA oxidation (A) and TAG esterification (B) from Lean and ZDF rats on Control (C) or high-fat (HF) diet

Metabolism was monitored over an acute 60 minute incubation. Values are mean ± SEM, nmol/g wet weight/60 min. [a]: Significantly different from Lean ($P \leq 0.05$).

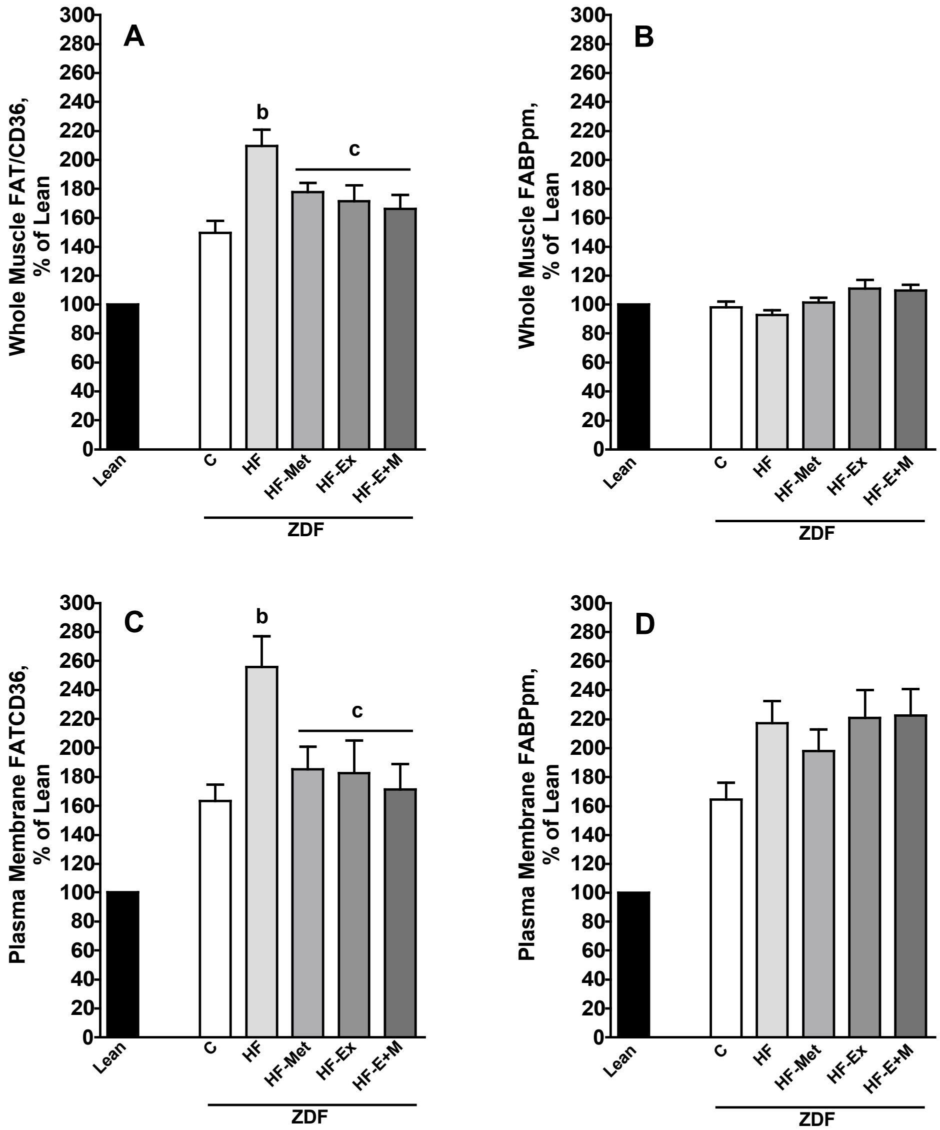

Figure 17: Whole RG muscle FAT/CD36 (A) and FABPpm (B), and plasma membrane FAT/CD36 (C) and FABPpm (D) protein expression in RG muscle from Lean and ZDF rats on Control (C) or high-fat (HF) diet

Values are mean ± SEM, expressed as % of Lean control (set to 100%). [b]: Significantly different from Control ($P \leq 0.05$); [c]: Significantly different from HF ($P \leq 0.05$).

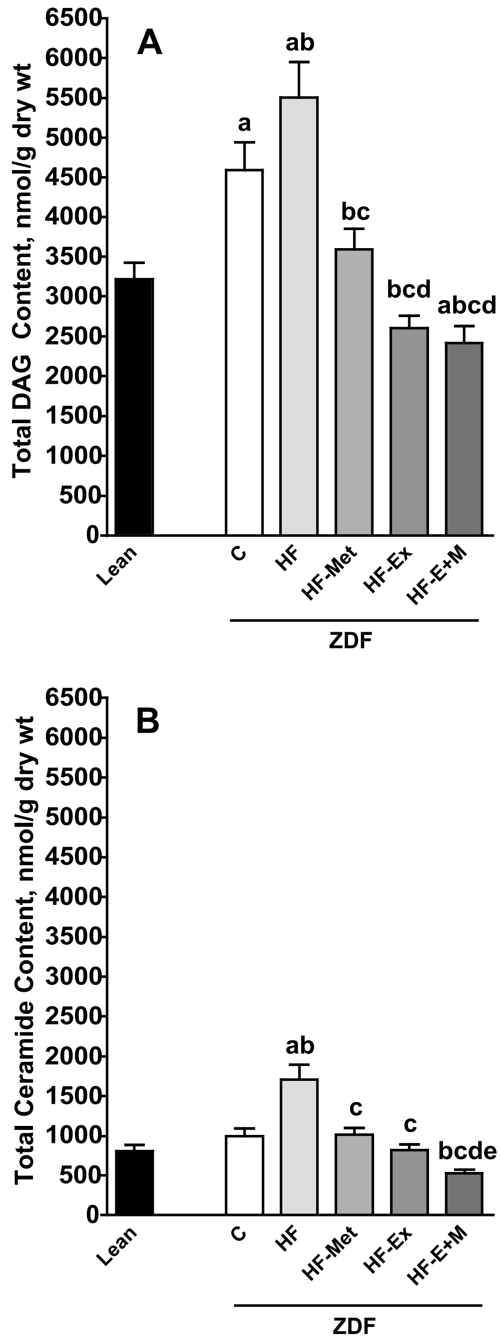

Figure 18: Soleus muscle total diacylglycerol (DAG) content (A) and total ceramide content (B) from Lean and ZDF rats on Control (C) or high-fat (HF) diet

Values are mean ± SEM, nmol/g dry weight. [a]: Significantly different from Lean ($P \leq 0.05$); [b]: Significantly different from Control ($P \leq 0.05$); [c]: Significantly different from HF ($P \leq 0.05$); [d]: Significantly different from HF-Met ($P \leq 0.05$); [e]: Significantly different from HF-Ex ($P \leq 0.05$).

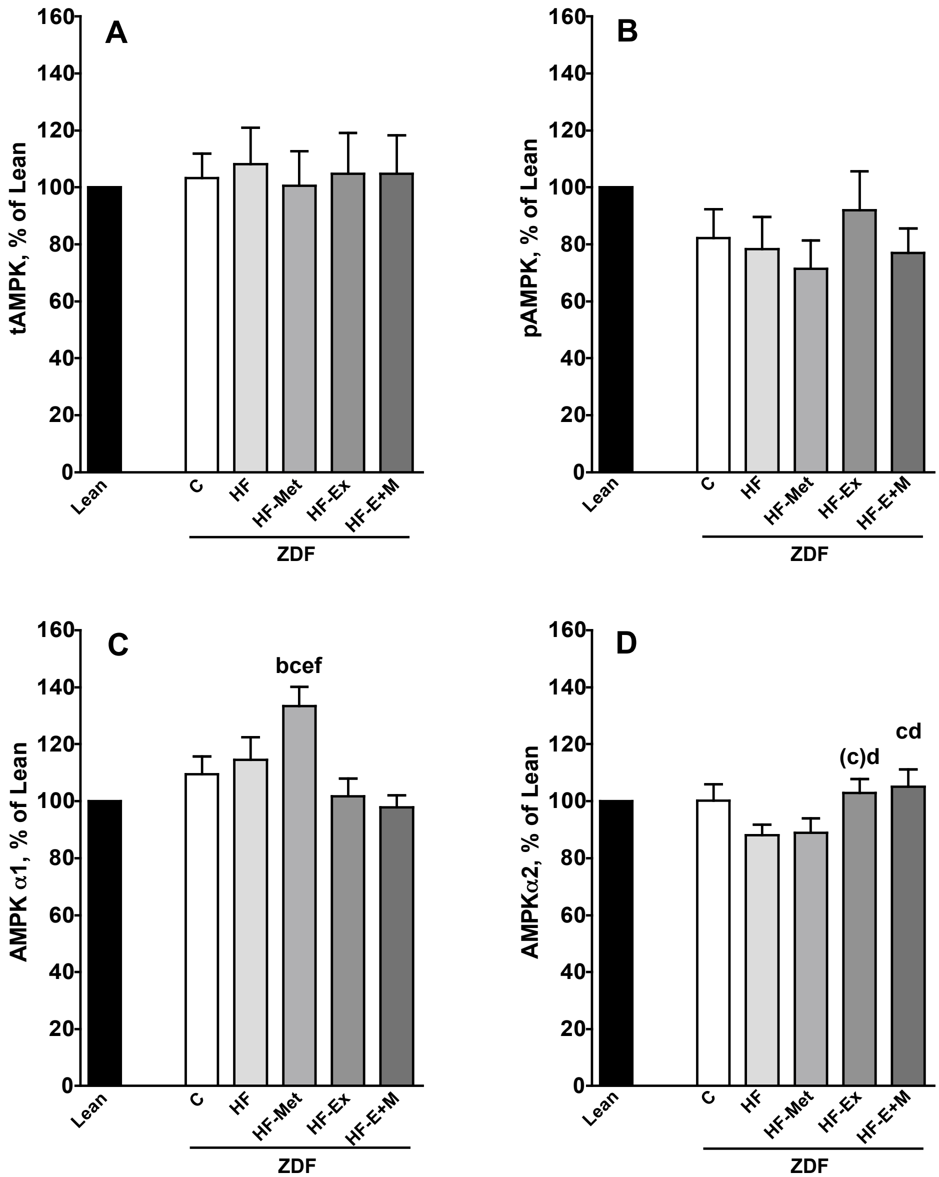

Figure 19: Soleus muscle total AMPK (A), phosphorylated AMPK (pAMPK, B), AMPKα1 (C) and AMPKα2 (D) protein expression from Lean and ZDF rats on Control (C) or high-fat (HF) diet

Values are mean ± SEM, expressed as % of Lean Control (set to 100%). [b]: Significantly different from Control ($P \leq 0.05$); [c]: Significantly different from HF ($P \leq 0.05$); [(c)]: trend observed ($P = 0.068$); [d]: Significantly different from HF-Met ($P \leq 0.05$); [e]: Significantly different from HF-Ex ($P \leq 0.05$); [f]: Significantly different from HF-E+M ($P \leq 0.05$).

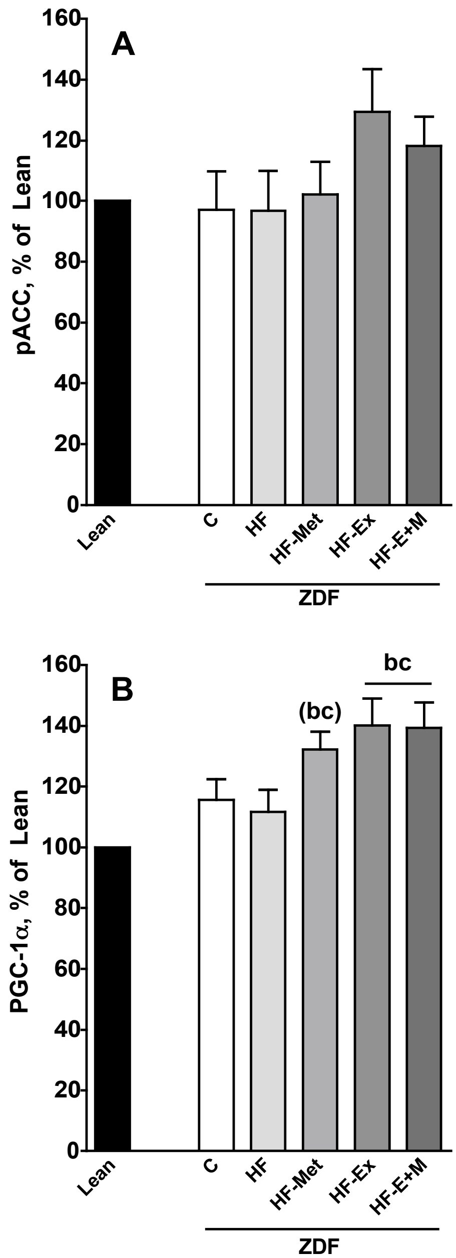

Figure 20: Soleus muscle phosphorylated ACC (pACC), A), and PGC-1α (B) protein expression from Lean and ZDF rats on Control (C) or high-fat (HF) diet

Values are mean ± SEM, expressed as % of Lean Control (set to 100%). [b]: Significantly different from Control ($P \leq 0.05$); [c]: Significantly different from HF ($P \leq 0.05$); (bc): trend toward a difference from Control and HF observed ($P = 0.06$).

Discussion

It has been postulated that treatments that stimulate the AMPK-axis may increase glucose uptake and partition FA to oxidation in skeletal muscle, and therefore may be an important therapeutic means to target the pathogenesis of insulin resistance. Very few studies have been performed with the female ZDF rat, as it was originally thought that while they exhibited obesity and insulin resistance, they did not develop diabetes on a conventional rodent diet. In comparison, the male ZDF rat is a spontaneous model, consistently developing insulin resistance by 7-8 weeks of age and overt diabetes by 12 weeks of age (58, 141). We confirmed previous findings that female ZDF rats fed a HF-diet (48 kcal% fat) developed diabetes (39), as indicated by overt fasting hyperglycemia and hyperinsulinemia (39, 196).

A number of novel observations were made in this study, including that the overt hyperglycemia observed in ZDF HF-fed rats was accompanied by impaired insulin-stimulated glucose transport in skeletal muscle; metformin, exercise, and their combination prevented the progression of overt diabetes in female ZDF HF-fed rats; and the beneficial effects on systemic glycemia were related to enhanced skeletal muscle insulin-stimulated glucose uptake and increased whole muscle and plasma membrane GLUT4 expression with exercise and the combination of exercise and metformin, but NOT with metformin treatment on its own. In relation to lipid metabolism, no treatment altered FA oxidation or TAG synthesis; however, whole muscle and plasma membrane-associated FAT/CD36 protein expression was reduced with all treatments, which was likely at least partially responsible for the observed reduction in DAG and ceramide contents. Finally, modest changes in AMPK were observed, as metformin increased AMPKα1 and downstream PGC-1α protein expression, while exercise and the combination of exercise and metformin increased AMPKα2 and PGC-1α protein expression, suggesting differential effects of pharmacological treatment versus exercise training on the AMPK-axis in skeletal muscle.

Effects of metformin and exercise on glucose metabolism and the prevention of diabetes in the female ZDF rat

In this study, improvements in hyperglycemia induced by metformin were not related to improvements in insulin-stimulated glucose transport or changes in GLUT4 protein expression in skeletal muscle of HF-fed rats. The exact mechanism by which metformin exerts its antidiabetic effects is poorly understood. The main site of metformin action appears to be the liver, via a reduction in hepatic glucose output through inhibition of gluconeogenesis (90, 180). However, limited evidence also suggests that metformin may have direct effects on skeletal muscle. Specifically, metformin has been shown to activate AMPK (38, 216) and stimulate glucose uptake in isolated rat EDL muscle (216). Metformin has also been shown to enhance insulin-stimulated glucose transport in soleus muscle from healthy Sprague-Dawley rats (22). The effects of metformin stimulation of skeletal muscle insulin-stimulated glucose uptake have been shown in studies of insulin resistant human subjects (63) but not in subjects with newly diagnosed diabetes (99). Therefore, it is possible that metformin-mediated effects on the reduction of hyperglycemia in female ZDF rats were related to reductions in hepatic glucose output.

It is well established that acute exercise bouts, as well as chronic training improve muscle insulin sensitivity, particularly by increasing GLUT4 expression (97) and translocation to the plasma membrane (57). Indeed, exercise training has been shown to improve skeletal muscle insulin-stimulated glucose uptake in obese Zucker rats (36, 96) up to 7 days after the last exercise bout (36). In the current study, the progression of overt hyperglycemia was prevented with exercise and this was related to enhanced insulin-stimulated glucose uptake, as well as increased basal whole muscle and plasma membrane-associated GLUT4 protein expression. This suggests that with exercise training, there was a chronic upregulation of total muscle GLUT4 protein expression, which was likely translocated to the sarcolemmal membrane during insulin stimulation, contributing to the increased insulin sensitivity and reductions in fasting glycemia. The effects of the last exercise bout on insulin sensitivity cannot be discounted, however, as it is possible that glycogen levels may have been lower in exercised animals on a high-fat diet. We did not have enough soleus to assess glycogen levels, but soleus muscle is an oxidative tissue, resistant to glycogen breakdown. It is therefore unlikely that large reductions in soleus muscle glycogen due to the last exercise bout occurred in the trained rats (training protocol completed 48 hours before measurements taken) and is likely not a mechanism related to increased insulin-stimulated glucose transport in this ZDF model. Regardless, these findings suggest that metformin and exercise may be exerting distinct effects on glucose metabolism in different tissues (ie. liver and skeletal muscle).

Effects of metformin and exercise on skeletal muscle fatty acid oxidation and oxidative capacity

Evidence is accumulating that strongly suggests that defects in skeletal muscle FA metabolism are involved in the pathogenesis of insulin resistance in obesity. Previous data have shown that during the progression to diabetes, male ZDF rats display increased fasting RQ values, suggesting impairments in whole body fasting FA oxidation (58). Indeed, in obese humans, FA oxidation is impaired in muscle homogenates (105) and from increased fasting leg RQ values, despite similar FA uptake across the leg compared to lean subjects (101). These findings suggest that FA oxidation is reduced, possibly leading to lipid accumulation in skeletal muscle (*See below*).

Female ZDF rats have reduced acute exogenous FA oxidation and an increase in TAG esterification compared to lean rats. Surprisingly, no treatment (HF-Met, HF-Ex, HF-E+M) had any effect on acute FA metabolism in this HF model. However, it is tempting to speculate that differences in FA oxidative capacity caused by metformin and exercise, or their combination, may have been revealed if soleus muscle strips had been subjected to a contraction paradigm that stimulates FA oxidation. Indeed, 8 weeks of endurance training in Sprague-Dawley rats has been shown to increase FA oxidation in isolated contracting, but not resting soleus muscle, which was associated with increased citrate synthase and β-HAD activities (50). Isoform-specific AMPK protein content increases with HF-Met (α1), and HF-Ex and HF-E+M (α2) were associated with increased PGC-1α protein content in all three treatments. Modest increases in citrate synthase and β-HAD activities occurred in both exercising HF groups. However, the changes in these markers of oxidative capacity were not profound, suggesting that improvements in oxidative capacity may not be a requirement. Rather, reductions in FA uptake and storage as reactive lipid species may be underlying mechanisms in the prevention of diabetes in this model.

Effects of metformin and exercise on skeletal muscle fatty acid transporters and accumulation of lipid species

It has been suggested that dysregulation of FA metabolism in obese, insulin resistant states predispose muscle to increase FA transport and reduce oxidation. Indeed, red oxidative skeletal muscle from obese Zucker rats (117), and male ZDF rats (32), and in *rectus abdominus* muscle from obese humans (21) display increased rates of palmitate transport, which is correlated with increased FAT/CD36 protein content located at the plasma membrane. Due to tissue limitations, we were not able to measure actual rates of FA transport with giant sarcolemmal vesicles, however it has been consistently shown that the abundance of membrane-bound FA transporter proteins correlate well with initial rates of FA uptake measured in giant sarcolemmal vesicles (20, 32, 118). However, our results are in agreement with these studies in obese states (21, 32, 117), demonstrating that FAT/CD36 protein content is chronically increased at the plasma membrane in HF-fed diabetic ZDF female rats. Interestingly, in obese Zucker rats, total protein content does not change but rather increased amounts of FAT/CD36 are observed to be permanently translocated to the sarcolemmal membrane (117). Whereas in male ZDF (32) and female HF-fed ZDF rats in the current study, both whole muscle and plasma membrane-associated FAT/CD36 are increased in RG muscle chronically. This a novel finding that suggests increased whole muscle and plasma membrane-associated FAT/CD36 may exacerbate the diabetic condition in both the male ZDF and the HF-fed female ZDF model. Furthermore, this is the first known study to show that metformin and exercise, alone or in combination, reduced whole muscle and plasma membrane-associated FAT/CD36 in the ZDF HF groups, suggesting that metformin, and exercise may each regulate FA uptake chronically in skeletal muscle. Interestingly, these results raise an apparent conflict between acute versus chronic AMPK regulation of FA uptake, which we cannot decipher conclusively from the results of the current study. Contraction and AICAR has been shown to acutely stimulate AMPK activity, which is associated with increased sarcolemmal translocation of FAT/CD36 and FA uptake in cardiac myocytes (118), whereas chronic metformin treatment and exercise training in female ZDF rats reduces skeletal muscle plasma membrane-associated FAT/CD36. It may be that the apparent dysregulation of increased FA transporters and subsequent FA uptake in obese/insulin resistant states may be regulated by increased systemic FA, with metformin and exercise leading to an “appropriate” regulation of translocation of FA transporters between intramuscular depots and the sarcolemmal membrane in skeletal muscle.

Neither metformin or exercise, or their combination, had effects on the elevated rates of TAG esterification in ZDF rats. Additionally, there were no differences in rates of TAG esterification between insulin resistant ZDF rats on C diet and ZDF rats on HF diet, suggesting that TAG storage may not be a mechanism associated with the progression of diabetes in this model. Alternatively, previous data suggested that DAG content is increased in chronic insulin resistant states such as HF-fed rats (11, 160), obese

Zucker rats (190) and obese humans (25). Also, ceramides are increased in obese Zucker rats (190) and humans (1, 25) and are negatively associated with insulin sensitivity (179). It is thought that DAG are allosteric activators of certain PKC isoforms which translocate to the plasma membrane and interrupt insulin signaling through Ser/Thr phosphorylation of IRS-1, while ceramides inhibit more distal components of the insulin signaling pathway, including Akt/PKB (161, 182). In ZDF HF-fed female rats, total DAG and ceramides were increased almost 2-fold, while all interventions resulted in reductions in both total DAG and ceramide content. This suggested that decreases in reactive lipid intermediates may be a potential mechanism for reduced fasting glycemia and inhibited progression to diabetes in this model. This is in agreement with previous studies that have shown reductions in the accumulation of DAG after training (25) and ceramides with both acute prolonged exercise (46) and chronic training (25, 47).

Also important were the findings that the sum of the individual saturated, monounsaturated and polyunsaturated DAG and ceramide species were increased in ZDF HF-fed rats. It has been suggested that the saturated:unsaturated FA ratio is important in the regulation of cell growth and differentiation and would therefore have effects on membrane fluidity and signal transduction (ie. insulin signaling) (45). In addition, it is possible that stearoyl-CoA desaturase 1 (SCD1) may be involved in the regulation of the degree of desaturation of individual lipid species in skeletal muscle and may be a contributing factor to obesity and insulin resistance. Stearoyl-CoA desaturase 1 catalyzes the desaturation of saturated fatty acyl-CoA, with its preferred substrates being palmitoyl-CoA and stearoyl-CoA. In soleus muscle from healthy rats, saturated palmitoyl-CoA

(C16:0) and stearoyl-CoA (C18:0) make up the majority (~65-70%) of ceramide, with monounsaturated oleoyl-CoA (C18:1) only making up ~5% of ceramide species (46). In this study, saturated palmitoyl-CoA (C16:0) and stearoyl-CoA (C18:0) also made up the majority of ceramide and DAG species. However, in male ZDF rats (192) and obese humans (88), there is an increase in *Scd1* gene expression, suggesting that there may be increased SCD1 protein content that may increase synthesis of monounsaturated oleoyl-CoA. Furthermore, in myocytes cultured from obese humans, increased SCD1 expression and activity are correlated with low FA oxidation, increased TAG and increased monounsaturated lipid species, suggesting abnormal lipid partitioning when oleoyl-CoA is elevated (88). In the current study, the HF C13004 diet is made up of 48 kcal% fat, mainly from animal sources, and ~25% of fat being palmitic acid (C16:0) and stearic acid (C18:0) (*Appendix 3*). Although we did not measure SCD1 protein expression in this study, it is likely that SCD1 is elevated in ZDF HF rats, leading to an ~1.9- to 2.4-fold increase in oleoyl (C18:1) DAG and ceramide compared to lean insulin sensitive rats. Taken together, the increase in saturated DAG and ceramide species, along with enhanced desaturation to yield monounsaturated DAG and ceramide species is a novel finding in this female ZDF HF model.

Another novel finding of this study was that metformin and exercise, alone or in combination, decreased saturated palmitoyl (C16:0) and stearoyl (C18:0), as well as monounsaturated oleoyl (C18:1) DAG and ceramide content in ZDF HF rats. In addition, both exercise treatments reduced palmitoyl (C16:0) and stearoyl DAG species significantly more than with metformin alone. These results suggest that although we did not observe any chronic increases in pAMPK, presumably daily exercise training upregulated the AMPK-axis and increased FA oxidation in skeletal muscle. Indeed, moderate increases in AMPKα2 were observed with exercise and the presumed increase in FA oxidation, along with decreased FAT/CD36 would be the likely mechanism to attribute the large decreases in DAG and ceramide species. Although metformin treatment did not reduce DAG and ceramide content to the same extent as exercise intervention, there were significant decreases compared to HF diabetic rats, in the majority of DAG and ceramide species detected. Metformin increased AMPKα1 protein expression, which was associated with increased PGC-1α, a likely mechanism in increased mitochondrial biogenesis (184).

Summary

In conclusion, we show that the female ZDF rat is a good model of HF diet-induced diabetes. The overt hyperglycemia observed in the ZDF HF-fed rat was accompanied by impaired insulin-stimulated glucose transport. The progression of diabetes was prevented with metformin and exercise, or their combination, indicated by reductions in fasting glucose levels. Only the exercise treatments were associated with improved skeletal muscle insulin-stimulated glucose uptake and increased whole muscle and plasma membrane-associated GLUT4 protein expression. Reductions in whole muscle and plasma membrane FAT/CD36, and total and monounsaturated DAG and ceramide may be mechanisms related to the alleviation of FA-induced insulin resistance and diabetes in female ZDF rats. Modest changes in AMPK isoform-specific protein content and PGC-1α protein content may have been related to preventing the progression of diabetes and whether the stimulation of the AMPK-axis had direct effects on reductions in FAT/CD36 protein content, DAG and ceramide content remains to be elucidated.

CHAPTER 6: GENERAL SUMMARY

The proposed role of AMPK as a regulator of FA and glucose metabolism made this enzyme a candidate therapeutic target for the alleviation of insulin resistance. In recent years, a great deal of research has investigated the regulation of skeletal muscle metabolism by AMPK; however the extent of its involvement has been a matter of much debate. Initial rodent experiments suggesting that the AMPK-axis was regulating FA oxidation during treadmill exercise never measured the functional endpoint of FA oxidation (198-200), as this is technically difficult *in vivo* in rodents. AMPK-mediated effects on FA oxidation were not shown until *in vitro* experiments in rodent skeletal muscle were performed with the AMPK activator, AICAR. AICAR allowed for the examination of the regulation of substrate utilization both *in vitro* and *in vivo* in rodent skeletal muscle, demonstrating increased glucose uptake (13, 125, 130) and partitioning of FA to oxidation (130).

Considering that AMPK is sensitive to decreases in the energy charge of the cell, and that its activation results in increased ATP provision, it is surprising that very few studies have actually examined the effect of AMPK activation on the oxidation of glucose. Although it would seem intuitive that stimulation of AMPK would result in the simultaneous increase in oxidation of both FA and glucose substrates for the purposes of restoring ATP concentrations, the initial findings of Kaushik *et al.* (100) were that glucose oxidation actually decreased in resting muscle in the presence of AICAR, presumably a secondary effect to the observed increase in FA oxidation (i.e. glucose-fatty acid cycle). This suggests that the actual effect of AMPK activation on glucose oxidation may depend on the availability of FA substrates for enhanced oxidation. Furthermore, AICAR treatment in isolated hepatocytes and adipocytes had an anti-lipolytic effect during β-adrenergic stimulation (29, 40, 181). Collectively, these effects seem counter-intuitive, as from a teleological viewpoint, AMPK would be thought to regulate pathways of FA and glucose metabolism to supply substrate for ATP production in times of energy need, regardless of the source (ie. exogenous FA and glucose, endogenous TAG stores).

Therefore, the purpose of the acute studies of this thesis (**CHAPTER 3 AND CHAPTER 4**) was to examine the effects of AICAR on FA metabolism and glucose oxidation at rest and during contraction in isolated rat soleus muscle *in vitro*. The results of these studies demonstrated that at rest, AMPKα2 activation with AICAR simultaneously increased FA and glucose oxidation, regardless of the level of FA availability. PDHa increased acutely, supporting the observed increase in glucose oxidation. Ultimately, these effects would have increased total ATP production. With AICAR, we observed a significant increase in calculated ATP production from both glucose and FA oxidation, which may be well in excess of what would be estimated in resting muscle. However, it is possible that the excess ATP could be converted to PCr through the near-equilibrium enzyme creatine kinase, which was not measured in these studies and warrants further investigation. Alternatively, it is not known if AICAR may also stimulate other energy-requiring processes, such as the regulation of ion pumps, uncoupling proteins and substrate cycling that may be consuming ATP with AICAR treatment. Additionally, AICAR had no independent effects on *endogenous* FA metabolism (TAG hydrolysis and subsequent endogenous oxidation), as had been previously shown in mouse soleus muscle with longer incubation times (3 hours, (130)). During contraction, AICAR further increased the activity of AMPKα2 above that seen with contraction alone, which led to further increases in FA oxidation regardless of FA availability. Furthermore, AICAR blunted TAG hydrolysis, but had no effect on endogenous oxidation during contraction. There were no effects on glucose oxidation during contraction, as these rates were already likely to be at or near maximal during intense tetanic stimulation.

The results of first two thesis studies suggest that AMPK is an important regulator of FA metabolism in both resting and contracting skeletal muscle. However, over 40 years after the conceptualization of the glucose fatty-acid cycle hypothesis by Randle *et al.* (144), we still do not have a good understanding of the regulation of fat-carbohydrate interaction in contracting skeletal muscle. Indeed, we understand that the intensity of muscle contraction and exercise changes the relative proportion of glucose or FA substrate used by muscle (151), but the mechanisms regulating these relative proportions are not fully understood. Important rate-limiting steps in FA uptake and metabolism are known, such as the membrane-associated fatty acid transport proteins FAT/CD36 and FABPpm, mitochondrial CPT-I and HSL. However, recent evidence suggests that FAT/CD36 may be associated with *both* the sarcolemmal and the mitochondrial membrane, possibly co-localizing with CPT-I (16, 159). Also, the exact role of malonyl-CoA in regulating CPT-I activity at rest and during exercise in rat and human skeletal muscle is not known. The IC_{50} concentrations for CPT-I suggests that CPT-I is maximally inhibited even at rest and whole muscle malonyl-CoA levels decrease in exercising rodent (134, 198, 199), but not human (134) muscle, suggesting possible compartmentalization.

There is also much debate regarding the extent to which AMPK regulates FA oxidation during muscle contraction and exercise. AMPK is activated during exercise in an intensity-dependent manner in both rats (146) and humans (35, 206), with increases in activity only seen at higher intensity protocols, when energy provision is predominantly from glycogen. Therefore, AMPK has been suggested not to be critical for increased FA oxidation in rodent skeletal muscle during lower intensity *in vitro* contraction (145), as large increases in FA uptake and oxidation were not correlated to modest activation of AMPK. AMPK-independent mechanisms for the regulation of glucose uptake during contraction have already been shown in mice expressing a dominant inhibitory mutant of AMPK (128), and it is also possible that AMPK is only part of the mechanism regulating FA metabolism during contraction. To add to the controversy of AMPK regulation, in a recent study of moderately trained men and women cycling during prolonged (90 min) moderate-intensity exercise (60% VO_{2max}), the higher FA oxidation rates observed in females could not be explained by greater AMPK activation (150).

Therefore, many questions still remain as to the importance of AMPK in the regulation of fat metabolism during contraction/exercise. The role of AMPK in regulating contraction-mediated FA metabolism is, for the most part, poorly understood. There is a need for more specific AMPK "activators" similar to AICAR. The development of novel AMPK activators will advance the study of the metabolic effects of AMPK activation. Current studies with AICAR are limited due to possible activation of other kinases and AICAR's sustained, artificial increase in ZMP does not allow for the system to use homeostatic mechanisms to "turn off" metabolic processes. Also, specific AMPK "inhibitors" will help to advance our understanding of AMPK's role in the regulation of FA oxidation during contraction. The specificity of iodotubercidin and araA as AMPK inhibitors has been questioned; however, a newer class of AMPK inhibitor, **compound C** (6-[4-(2-Piperidin-1-yl-ethoxy)-phenol)]-3-pyridin-4-yl-pyrrazolo[1,5-a]-pyrimidine; Calbiochem), is a potent, selective, reversible ATP-competitive inhibitor of AMPK (216) that does not affect the activity of other kinases (ie. PKA, PKC). Compound C blocks ACC inactivation by both AICAR and metformin in hepatocytes (216) and presumably would have effects on FA oxidation. To our knowledge, compound C has not been used in resting or contracting skeletal muscle to evaluate the role that AMPK may be playing in skeletal muscle. AMPK inhibition with compound C during muscle contraction or exercise would provide strong evidence as to how necessary AMPK is for observed increases in FA oxidation. Also, knockout models have generally been used to examine contraction-mediated effects on glucose uptake (128), with no known examination of FA oxidation.

The potent acute effects that AMPK activation had on FA oxidation in resting and contracting skeletal muscle in the current thesis led to the hypothesis that AMPK regulation may have effects on FA metabolism and therefore increase insulin sensitivity in female ZDF rats, a HF diet model of inducible diabetes (**CHAPTER 5**). The female ZDF rat may be a more appropriate model compared to the male ZDF for the study of insulin resistance and diabetes, as diabetes is diet-induced and progressive as opposed to spontaneous, and the females have prolonged hyperinsulinemia prior to the decline in β-cell function (39). This characteristic allows for the prolonged study of potential preventative treatments, such as metformin and exercise that may activate AMPK and/or alter skeletal muscle lipid content or oxidative capacity and prevent the progression of diabetes. It is important to note that all treatments (metformin, exercise and the combination of exercise and metformin) used in this model were in combination with the HF diet, allowing for the study of AMPK regulation and fat metabolism in a diabetogenic model.

The results of these studies suggest that improvements in FA oxidation may not be necessary for correcting insulin resistance. Rather, reductions in whole muscle and plasma membrane-associated FAT/CD36 may be sufficient to alter intramuscular lipid content and profile and prevent the progression of T2DM in female ZDF rats. The reductions in whole muscle and plasma membrane-associated FAT/CD36 and whole muscle ceramide and DAG content were much more pronounced than the modest increases in markers of oxidative capacity, namely the activity of citrate synthase and β-HAD, and the protein expression of AMPKα1 (metformin), AMPKα2 (exercise) and PGC-1α. Therefore, verification of these results in other models of insulin resistance and the study of the underlying mechanisms for the observed reduction in FAT/CD36, DAG and ceramide species is required to gain a better understanding of ways to alleviate FA-induced insulin resistance.

The study of the underlying mechanisms for the reduction in FAT/CD36 and reactive lipid species should include both acute and chronic methods. Cell culture assays can test whether acute metformin treatment reduces plasma membrane-associated FAT/CD36 at the cell membrane with the development of stable cell lines expressing an FAT/CD36*myc* epitope, thereby allowing for microscopic imaging techniques to follow subcellular localization of FAT/CD36. The *in vitro* use of the specific FAT/CD36 inhibitor sulfo-N-succimidyl-oleate (SSO, (16)) and specific inhibitors of ceramide and DAG synthesis (33), alone or in combination, in soleus muscle from both non-diabetic and ZDF rats would help to ascertain the extent to which FA uptake alters DAG and ceramide synthesis acutely. Additionally, a restoration in insulin-stimulated glucose uptake with the exposure of these inhibitors can be evaluated. Chronically, the contribution of different types of fat in the pathogenesis of insulin resistance is warranted. Recent evidence suggests that saturated FA induce insulin resistance in muscle of HF-fed Sprague-Dawley rats, which was associated with increased DAG content (114). Indeed, the composition of the diabetogenic HF diet in our studies suggests that saturated FA may be exacerbating insulin resistance in female ZDF rats.

Importantly, the study of the underlying mechanisms of metformin and exercise linking the reduction in DAG and ceramide species to increased insulin sensitivity requires further study. Reductions in the activity and/or protein expression of PKC as well as serine palmitoyl transferase and ceramide synthase may be associated with the observed reductions in DAG and ceramide, respectively, and with improvements in the insulin signaling pathway (IRS-1, IRS-1-associated PI3-kinase activity, Akt/PKB) in insulin resistant models.

Ultimately, we need to better establish the importance of various tissues (ie. adipose tissue, liver, skeletal muscle) as targets in the pharmacological and lifestyle treatment of diabetes. Metformin and exercise may be exerting distinct effects on glucose and FA metabolism in different tissues. In addition, there is still much debate as to the extent to which metformin activates AMPK in muscle, with this being the first known study to establish metformin as a potential therapeutic for reducing skeletal muscle reactive lipid accumulation. With a main body of literature supporting metformin's primary effects of decreasing hepatic glucose output (90, 180), the prolonged time-frame of AMPK activation in skeletal muscle with metformin (132) and strong effects of exercise to increase insulin sensitivity at the level of the muscle, the focus of future research will need to include the combination of both exercise and pharmacological treatment. It appears that lifestyle intervention, including exercise and diet, as well as pharmacological treatment may be important in the treatment of insulin resistance and the progression of diabetes.

REFERENCES

1. **Adams JM, 2nd, Pratipanawatr T, Berria R, Wang E, DeFronzo RA, Sullards MC, and Mandarino LJ.** Ceramide content is increased in skeletal muscle from obese insulin-resistant humans. *Diabetes* 53: 25-31, 2004.

2. **Ai H, Ihlemann J, Hellsten Y, Lauritzen HP, Hardie DG, Galbo H, and Ploug T.** Effect of fiber type and nutritional state on AICAR- and contraction- stimulated glucose transport in rat muscle. *Am J Physiol Endocrinol Metab* 282: E1291-1300, 2002.

3. **Alam N and Saggerson ED.** Malonyl-CoA and the regulation of fatty acid oxidation in soleus muscle. *Biochem J* 334: 233-241, 1998.

4. **American Diabetes Association.** 2006 Clinical Practice Recommendations: Diagnosis and Classification of Diabetes Mellitus. *Diabetes Care* 29: S43-48, 2006.

5. **Arita Y, Kihara S, Ouchi N, Takahashi M, Maeda K, Miyagawa J, Hotta K, Shimomura I, Nakamura T, Miyaoka K, Kuriyama H, Nishida M, Yamashita S, Okubo K, Matsubara K, Muraguchi M, Ohmoto Y, Funahashi T, and Matsuzawa Y.** Paradoxical decrease of an adipose-specific protein, adiponectin, in obesity. *Biochem Biophys Res Commun* 257: 79-83, 1999.

6. **Aschenbach WG, Hirshman MF, Fujii N, Sakamoto K, Howlett KF, and Goodyear LJ.** Effect of AICAR treatment on glycogen metabolism in skeletal muscle. *Diabetes* 51: 567-573, 2002.

7. **Baar K.** Involvement of PPAR gamma co-activator-1, nuclear respiratory factors 1 and 2, and PPAR alpha in the adaptive response to endurance exercise. *Proc Nutr Soc* 63: 269-273, 2004.

8. **Balon TW and Jasman AP.** Acute exposure to AICAR increases glucose transport in mouse EDL and soleus muscle. *Biochem Biophys Res Commun* 282: 1008-1011, 2001.

9. **Bavenholm P, Pigon J, Saha A, Ruderman N, and Efendic S.** Fatty acid oxidation and the regulation of malonyl-CoA in human muscle. *Diabetes* 49: 1078-1083, 2000.

10. **Beg ZH, Allmann DW, and Gibson DM.** Modulation of 3-hydroxy-3-methylglutaryl coenzyme A reductase activity with cAMP and wth protein fractions of rat liver cytosol. *Biochem Biophys Res Commun* 54: 1362-1369, 1973.

11. **Bell KS, Schmitz-Peiffer C, Lim-Fraser M, Biden TJ, Cooney GJ, and Kraegen EW.** Acute reversal of lipid-induced muscle insulin resistance is associated with rapid alteration in PKC-theta localization. *Am J Physiol Endocrinol Metab* 279: E1196-1201, 2000.

12. **Bergeron R, Previs SF, Cline GW, Perret P, Russell RR, 3rd, Young LH, and Shulman GI.** Effect of 5-aminoimidazole-4-carboxamide-1-beta-D-ribofuranoside infusion on in vivo glucose and lipid metabolism in lean and obese Zucker rats. *Diabetes* 50: 1076-1082, 2001.

13. **Bergeron R, Russell RR, III, Young LH, Ren J-M, Marcucci M, Lee A, and Shulman GI.** Effect of AMPK activation on muscle glucose metabolism in conscious rats. *Am J Physiol Endocrinol Metab* 276: E938-944, 1999.

14. **Bevilacqua S, Bonadonna R, Buzzigoli G, Boni C, Ciociaro D, Maccari F, Giorico MA, and Ferrannini E.** Acute elevation of free fatty acid levels leads to hepatic insulin resistance in obese subjects. *Metabolism* 36: 502-506, 1987.

15. **Bevilacqua S, Buzzigoli G, Bonadonna R, Brandi LS, Oleggini M, Boni C, Geloni M, and Ferrannini E.** Operation of Randle's cycle in patients with NIDDM. *Diabetes* 39: 383-389, 1990.

16. **Bezaire V, Bruce CR, Heigenhauser GJ, Tandon NN, Glatz JF, Luiken JJ, Bonen A, and Spriet LL.** Identification of fatty acid translocase on human skeletal muscle mitochondrial membranes: essential role in fatty acid oxidation. *Am J Physiol Endocrinol Metab* 290: E509-515, 2006.

17. **Bianchi A, Evans JL, Iverson AJ, Nordlund AC, Watts TD, and Witters LA.** Identification of an isozymic form of acetyl-CoA carboxylase. *J Biol Chem* 265: 1502-1509, 1990.

18. **Boden G, Chen X, Ruiz J, White JV, and Rossetti L.** Mechanisms of fatty acid-induced inhibition of glucose uptake. *J Clin Invest* 93: 2438-2446, 1994.

19. **Boden G, Jadali F, White J, Liang Y, Mozzoli M, Chen X, Coleman E, and Smith C.** Effects of fat on insulin-stimulated carbohydrate metabolism in normal men. *J Clin Invest* 88: 960-966, 1991.

20. **Bonen A, Luiken JJ, and Glatz JF.** Regulation of fatty acid transport and membrane transporters in health and disease. *Mol Cell Biochem* 239: 181-192, 2002.

21. **Bonen A, Parolin ML, Steinberg GR, Calles-Escandon J, Tandon NN, Glatz JF, Luiken JJ, Heigenhauser GJ, and Dyck DJ.** Triacylglycerol accumulation in human obesity and type 2 diabetes is associated with increased rates of skeletal muscle fatty acid transport and increased sarcolemmal FAT/CD36. *Faseb J* 18: 1144-1146, 2004.

22. **Borst SE, Snellen HG, and Lai HL.** Metformin treatment enhances insulin-stimulated glucose transport in skeletal muscle of Sprague-Dawley rats. *Life Sci* 67: 165-174, 2000.

23. **Bruce CR, Anderson MJ, Carey AL, Newman DG, Bonen A, Kriketos AD, Cooney GJ, and Hawley JA.** Muscle oxidative capacity is a better predictor of insulin sensitivity than lipid status. *J Clin Endocrinol Metab* 88: 5444-5451, 2003.

24. **Bruce CR, Mertz VA, Heigenhauser GJ, and Dyck DJ.** The stimulatory effect of globular adiponectin on insulin-stimulated glucose uptake and fatty acid oxidation is impaired in skeletal muscle from obese subjects. *Diabetes* 54: 3154-3160, 2005.

25. **Bruce CR, Thrush AB, Mertz VA, Bezaire V, Chabowski A, Heigenhauser GJ, and Dyck DJ.** Endurance training in obese humans improves glucose tolerance and mitochondrial fatty acid oxidation and alters muscle lipid content. *Am J Physiol Endocrinol Metab* 291: E99-E107, 2006.

26. **Brunmair B, Staniek K, Gras F, Scharf N, Althaym A, Clara R, Roden M, Gnaiger E, Nohl H, Waldhausl W, and Furnsinn C.** Thiazolidinediones, Like Metformin, Inhibit Respiratory Complex I: A Common Mechanism Contributing to Their Antidiabetic Actions? *Diabetes* 53: 1052-1059, 2004.

27. **Buhl ES, Jessen N, Pold R, Ledet T, Flyvbjerg A, Pedersen SB, Pedersen O, Schmitz O, and Lund S.** Long-term AICAR administration reduces metabolic disturbances and lowers blood pressure in rats displaying features of the insulin resistance syndrome. *Diabetes* 51: 2199-2206, 2002.

28. **Buhl ES, Jessen N, Schmitz O, Pedersen SB, Pedersen O, Holman GD, and Lund S.** Chronic treatment with 5-aminoimidazole-4-carboxamide-1-beta-D-

ribofuranoside increases insulin-stimulated glucose uptake and GLUT4 translocation in rat skeletal muscles in a fiber type-specific manner. *Diabetes* 50: 12-17, 2001.

29. **Caballero AE.** Endothelial dysfunction in obesity and insulin resistance: a road to diabetes and heart disease. *Obes Res* 11: 1278-1289, 2003.

30. **Carling D, Clarke PR, Zammit VA, and Hardie DG.** Purification and characterization of the AMP-activated protein kinase. Copurification of acetyl-CoA carboxylase kinase and 3-hydroxy-3-methylglutaryl-CoA reductase kinase activities. *Eur J Biochem* 186: 129-136, 1989.

31. **Carling D, Zammit VA, and Hardie DG.** A common bicyclic protein kinase cascade inactivates the regulatory enzymes of fatty acid and cholesterol biosynthesis. *FEBS Lett* 223: 217-222, 1987.

32. **Chabowski A, Chatham JC, Tandon NN, Calles-Escandon J, Glatz J, Luiken JJ, and Bonen A.** Fatty acid transport and FAT/CD36 are increased in red but not in white skeletal muscle of ZDF rats. *Am J Physiol Endocrinol Metab* 291: E675-682, 2006.

33. **Chavez JA, Knotts TA, Wang LP, Li G, Dobrowsky RT, Florant GL, and Summers SA.** A role for ceramide, but not diacylglycerol, in the antagonism of insulin signal transduction by saturated fatty acids. *J Biol Chem* 278: 10297-10303, 2003.

34. **Chen Z-P, McConell GK, Michell BJ, Snow RJ, Canny BJ, and Kemp BE.** AMPK signaling in contracting human skeletal muscle: acetyl-CoA carboxylase and NO synthase phosphorylation. *Am J Physiol Endocrinol Metab* 279: E1202-1206, 2000.

35. **Chen Z-P, Stephens TJ, Murthy S, Canny BJ, Hargreaves M, Witters LA, Kemp BE, and McConell GK.** Effect of Exercise Intensity on Skeletal Muscle AMPK Signaling in Humans. *Diabetes* 52: 2205-2212, 2003.

36. **Christ CY, Hunt D, Hancock J, Garcia-Macedo R, Mandarino LJ, and Ivy JL.** Exercise training improves muscle insulin resistance but not insulin receptor signaling in obese Zucker rats. *J Appl Physiol* 92: 736-744, 2002.

37. **Cleasby ME, Dzamko N, Hegarty BD, Cooney GJ, Kraegen EW, and Ye J-M.** Metformin Prevents the Development of Acute Lipid-Induced Insulin Resistance in the Rat Through Altered Hepatic Signaling Mechanisms. *Diabetes* 53: 3258-3266, 2004.

38. **Collier CA, Bruce CR, Smith AC, Lopaschuk G, and Dyck DJ.** Metformin counters the insulin-induced suppression of fatty acid oxidation and stimulation of triacylglycerol storage in rodent skeletal muscle. *Am J Physiol Endocrinol Metab* 291: E182-189, 2006.

39. **Corsetti JP, Sparks JD, Peterson RG, Smith RL, and Sparks CE.** Effect of dietary fat on the development of non-insulin dependent diabetes mellitus in obese Zucker diabetic fatty male and female rats. *Atherosclerosis* 148: 231-241, 2000.

40. **Corton JM, Gillespie JG, Hawley SA, and Hardie DG.** 5-Aminoimidazole-4-carboxamide riboside: A specific method for activating AMP-activated protein kinase in intact cells? *Eur J Biochem* 229: 558-565, 1995.

41. **Dagher Z, Ruderman N, Tornheim K, and Ido Y.** The effect of AMP-activated protein kinase and its activator AICAR on the metabolism of human umbilical vein endothelial cells. *Biochem Biophys Res Commun* 265: 112-115, 1999.

42. **Davies SP, Carling D, and Hardie DG.** Tissue distribution of the AMP-activated protein kinase, and lack of activation by cyclic-AMP-dependent protein kinase, studied using a specific and sensitive peptide assay. *Eur J Biochem* 186: 123-128, 1989.

43. **Dean D, Daugaard JR, Young ME, Saha A, Vavvas D, Asp S, Kiens B, Kim KH, Witters L, Richter EA, and Ruderman N.** Exercise diminishes the activity of acetyl-CoA carboxylase in human muscle. *Diabetes* 49: 1295-1300, 2000.

44. **Derave W, Ai H, Ihlemann J, Witters L, Kristiansen S, Richter E, and Ploug T.** Dissociation of AMP-activated protein kinase activation and glucose transport in contracting slow-twitch muscle. *Diabetes* 49: 1281-1287, 2000.

45. **Dobrzyn A, Dobrzyn P, Lee SH, Miyazaki M, Cohen P, Asilmaz E, Hardie DG, Friedman JM, and Ntambi JM.** Stearoyl-CoA desaturase-1 deficiency reduces ceramide synthesis by downregulating serine palmitoyltransferase and increasing beta-oxidation in skeletal muscle. *Am J Physiol Endocrinol Metab* 288: E599-607, 2005.

46. **Dobrzyn A and Gorski J.** Ceramides and sphingomyelins in skeletal muscles of the rat: content and composition. Effect of prolonged exercise. *Am J Physiol Endocrinol Metab* 282: E277-285, 2002.

47. **Dobrzyn A, Zendzian-Piotrowska M, and Gorski J.** Effect of endurance training on the sphingomyelin-signalling pathway activity in the skeletal muscles of the rat. *J Physiol Pharmacol* 55: 305-313, 2004.

48. **Durante PE, Mustard KJ, Park S-H, Winder WW, and Hardie DG.** Effects of endurance training on activity and expression of AMP-activated protein kinase isoforms in rat muscles. *Am J Physiol Endocrinol Metab* 283: E178-186, 2002.

49. **Dyck DJ and Bonen A.** Muscle contraction increases palmitate esterification and oxidation and triacylglycerol oxidation. *Am J Physiol* 275: E888-896, 1998.

50. **Dyck DJ, Miskovic D, Code L, Luiken JJ, and Bonen A.** Endurance training increases FFA oxidation and reduces triacylglycerol utilization in contracting rat soleus. *Am J Physiol Endocrinol Metab* 278: E778-785, 2000.

51. **Dyck DJ, Peters SJ, Glatz J, Gorski J, Keizer H, Kiens B, Liu S, Richter EA, Spriet LL, van der Vusse GJ, and Bonen A.** Functional differences in lipid metabolism in resting skeletal muscle of various fiber types. *Am J Physiol Endocrinol Metab* 272: E340-351, 1997.

52. **Dyck DJ, Peters SJ, Wendling PS, Chesley A, Hultman E, and Spriet LL.** Regulation of muscle glycogen phosphorylase activity during intense aerobic cycling with elevated FFA. *Am J Physiol* 270: E116-125, 1996.

53. **Dyck DJ, Peters SJ, Wendling PS, and Spriet LL.** Effect of high FFA on glycogenolysis in oxidative rat hindlimb muscles during twitch stimulation. *Am J Physiol* 270: R766-776, 1996.

54. **Dyck DJ, Putman CT, Heigenhauser GJ, Hultman E, and Spriet LL.** Regulation of fat-carbohydrate interaction in skeletal muscle during intense aerobic cycling. *Am J Physiol* 265: E852-859, 1993.

55. **Dyck DJ and Spriet LL.** Elevated muscle citrate does not reduce carbohydrate utilization during tetanic stimulation. *Can J Physiol Pharmacol* 72: 117-125, 1994.

56. **El-Mir MY, Nogueira V, Fontaine E, Averet N, Rigoulet M, and Leverve X.** Dimethylbiguanide inhibits cell respiration via an indirect effect targeted on the respiratory chain complex I. *J Biol Chem* 275: 223-228, 2000.

57. **Etgen GJ, Jr, Jensen J, Wilson CM, Hunt DG, Cushman SW, and Ivy JL.** Exercise training reverses insulin resistance in muscle by enhanced recruitment of GLUT-4 to the cell surface. *Am J Physiol Endocrinol Metab* 272: E864-869, 1997.

58. **Etgen GJ and Oldham BA.** Profiling of Zucker diabetic fatty rats in their progression to the overt diabetic state. *Metabolism* 49: 684-688, 2000.

59. **Folch J, Lees M, and Stanley GHS.** A simple method for the isolation and purification of total lipids from animal tissues. *J Biol Chem* 226: 497-509, 1957.

60. **Frosig C, Jorgensen SB, Hardie DG, Richter EA, and Wojtaszewski JF.** 5'-AMP-activated protein kinase activity and protein expression are regulated by endurance training in human skeletal muscle. *Am J Physiol Endocrinol Metab* 286: E411-417, 2004.

61. **Fryer LG, Parbu-Patel A, and Carling D.** The anti-diabetic drugs rosiglitazone and metformin stimulate AMP- activated protein kinase through distinct pathways. *J Biol Chem* 277: 25226-25232, 2002.

62. **Fulgencio JP, Kohl C, Girard J, and Pegorier JP.** Effect of metformin on fatty acid and glucose metabolism in freshly isolated hepatocytes and on specific gene expression in cultured hepatocytes. *Biochem Pharmacol* 62: 439-446, 2001.

63. **Galuska D, Zierath J, Thorne A, Sonnenfeld T, and Wallberg-Henriksson H.** Metformin increases insulin-stimulated glucose transport in insulin-resistant human skeletal muscle. *Diabete Metab* 17: 159-163, 1991.

64. **Garton AJ, Campbell DG, Carling D, Hardie DG, Colbran RJ, and Yeaman SJ.** Phosphorylation of bovine hormone-sensitive lipase by the AMP-activated protein kinase. *Eur J Biochem* 179: 249-254, 1989.

65. **Goodpaster BH, He J, Watkins S, and Kelley DE.** Skeletal muscle lipid content and insulin resistance: evidence for a paradox in endurance-trained athletes. *J Clin Endocrinol Metab* 86: 5755-5761, 2001.

66. **Goodpaster BH, Katsiaras A, and Kelley DE.** Enhanced Fat Oxidation Through Physical Activity Is Associated With Improvements in Insulin Sensitivity in Obesity. *Diabetes* 52: 2191-2197, 2003.

67. **Goodpaster BH, Kelley DE, Wing RR, Meier A, and Thaete FL.** Effects of weight loss on regional fat distribution and insulin sensitivity in obesity. *Diabetes* 48: 839-847, 1999.

68. **Goto M, Terada S, Kato M, Katoh M, Yokozeki T, Tabata I, and Shimokawa T.** cDNA Cloning and mRNA analysis of PGC-1 in epitrochlearis muscle in swimming-exercised rats. *Biochem Biophys Res Commun* 274: 350-354, 2000.

69. **Griffin ME, Marcucci MJ, Cline GW, Bell K, Barucci N, Lee D, Goodyear LJ, Kraegen EW, White MF, and Shulman GI.** Free fatty acid-induced insulin resistance is associated with activation of protein kinase C theta and alterations in the insulin signaling cascade. *Diabetes* 48: 1270-1274, 1999.

70. **Halseth AE, Ensor NJ, White TA, Ross SA, and Gulve EA.** Acute and chronic treatment of ob/ob and db/db mice with AICAR decreases blood glucose concentrations. *Biochem Biophys Res Commun* 294: 798-805, 2002.

71. **Hardie DG.** AMP-activated protein kinase: a key system mediating metabolic responses to exercise. *Med Sci Sports Exerc* 36: 28-34, 2004.

72. **Hardie DG.** *The Protein Kinase Factsbook*. San Diego: Academic Press, 1995.

73. **Hardie DG and Sakamoto K.** AMPK: a key sensor of fuel and energy status in skeletal muscle. *Physiology (Bethesda)* 21: 48-60, 2006.

74. **Hardie DG, Salt IP, Hawley SA, and Davies SP.** AMP-activated protein kinase: an ultrasensitive system for monitoring cellular energy charge. *Biochem J* 338: 717-722, 1999.

75. **Hawley SA, Davison M, Woods A, Davies SP, Beri RK, Carling D, and Hardie DG.** Characterization of the AMP-activated protein kinase kinase from rat liver and identification of threonine 172 as the major site at which it phosphorylates AMP-activated protein kinase. *J Biol Chem* 271: 27879-27887, 1996.

76. **Hawley SA, Gadalla AE, Olsen GS, and Hardie DG.** The antidiabetic drug metformin activates the AMP-activated protein kinase cascade via an adenine nucleotide-independent mechanism. *Diabetes* 51: 2420-2425., 2002.

77. **Hawley SA, Pan DA, Mustard KJ, Ross L, Bain J, Edelman AM, Frenguelli BG, and Hardie DG.** Calmodulin-dependent protein kinase kinase-beta is an alternative upstream kinase for AMP-activated protein kinase. *Cell Metab* 2: 9-19, 2005.

78. **Hayashi T, Hirshman MF, Kurth EJ, Winder WW, and Goodyear LJ.** Evidence for 5' AMP-activated protein kinase mediation of the effect of muscle contraction on glucose transport. *Diabetes* 47: 1369-1373., 1998.

79. **Health Canada.** Diabetes in Canada, Second Edition, edited by Health Canada Centre for Chronic Disease Prevention and Care, Population and Public Health Branch. Ottawa, 2002.

80. **Helge JW and Dela F.** Effect of Training on Muscle Triacylglycerol and Structural Lipids: A Relation to Insulin Sensitivity? *Diabetes* 52: 1881-1887, 2003.

81. **Hevener AL, He W, Barak Y, Le J, Bandyopadhyay G, Olson P, Wilkes J, Evans RM, and Olefsky J.** Muscle-specific Pparg deletion causes insulin resistance. *Nat Med* 9: 1491-1497, 2003.

82. **Heymsfield SB, Greenberg AS, Fujioka K, Dixon RM, Kushner R, Hunt T, Lubina JA, Patane J, Self B, Hunt P, and McCamish M.** Recombinant leptin for weight loss in obese and lean adults: a randomized, controlled, dose-escalation trial. *Jama* 282: 1568-1575, 1999.

83. **Hickey MS, Carey JO, Azevedo JL, Houmard JA, Pories WJ, Israel RG, and Dohm GL.** Skeletal muscle fiber composition is related to adiposity and in vitro glucose transport rate in humans. *Am J Physiol* 268: E453-457, 1995.

84. **Holmes BF, Kurth-Kraczek EJ, and Winder WW.** Chronic activation of 5'-AMP-activated protein kinase increases GLUT-4, hexokinase, and glycogen in muscle. *J Appl Physiol* 87: 1990-1995, 1999.

85. **Hong SP, Leiper FC, Woods A, Carling D, and Carlson M.** Activation of yeast Snf1 and mammalian AMP-activated protein kinase by upstream kinases. *Proc Natl Acad Sci U S A* 100: 8839-8843, 2003.

86. **Hoppeler H and Fluck M.** Plasticity of skeletal muscle mitochondria: structure and function. *Med Sci Sports Exerc* 35: 95-104, 2003.

87. **Hosoda K, Masuzaki H, Ogawa Y, Miyawaki T, Hiraoka J, Hanaoka I, Yasuno A, Nomura T, Fujisawa Y, Yoshimasa Y, Nishi S, Yamori Y, and Nakao K.** Development of radioimmunoassay for human leptin. *Biochem Biophys Res Commun* 221: 234-239, 1996.

88. **Hulver MW, Berggren JR, Carper MJ, Miyazaki M, Ntambi JM, Hoffman EP, Thyfault JP, Stevens R, Dohm GL, Houmard JA, and Muoio DM.** Elevated stearoyl-CoA desaturase-1 expression in skeletal muscle contributes to abnormal fatty acid partitioning in obese humans. *Cell Metab* 2: 251-261, 2005.

89. **Hulver MW, Berggren JR, Cortright RN, Dudek RW, Thompson RP, Pories WJ, MacDonald KG, Cline GW, Shulman GI, Dohm GL, and Houmard JA.** Skeletal muscle lipid metabolism with obesity. *Am J Physiol Endocrinol Metab* 284: E741-747, 2003.

90. **Hundal RS, Krssak M, Dufour S, Laurent D, Lebon V, Chandramouli V, Inzucchi SE, Schumann WC, Petersen KF, Landau BR, and Shulman GI.** Mechanism by which metformin reduces glucose production in type 2 diabetes. *Diabetes* 49: 2063-2069, 2000.

91. **Hurley RL, Anderson KA, Franzone JM, Kemp BE, Means AR, and Witters LA.** The Ca2+/calmodulin-dependent protein kinase kinases are AMP-activated protein kinase kinases. *J Biol Chem* 280: 29060-29066, 2005.

92. **Hutber CA, Hardie DG, and Winder WW.** Electrical stimulation inactivates muscle acetyl-CoA carboxylase and increases AMP-activated protein kinase. *Am J Physiol* 272: E262-E266, 1997.

93. **Ide T, Nakazawa T, Mochizuki T, and Murakami K.** Tissue-specific actions of antidiabetic thiazolidinediones on the reduced fatty acid oxidation in skeletal muscle and liver of Zucker diabetic fatty rats. *Metabolism* 49: 521-525, 2000.

94. **Ihlemann J, Ploug T, Hellsten Y, and Galbo H.** Effect of stimulation frequency on contraction-induced glucose transport in rat skeletal muscle. *Am J Physiol Endocrinol Metab* 279: E862-867, 2000.

95. **Itani SI, Ruderman NB, Schmieder F, and Boden G.** Lipid-induced insulin resistance in human muscle is associated with changes in diacylglycerol, protein kinase C, and IkappaB-alpha. *Diabetes* 51: 2005-2011, 2002.

96. **Ivy JL, Sherman WM, Cutler CL, and Katz AL.** Exercise and diet reduce muscle insulin resistance in obese Zucker rat. *Am J Physiol* 251: E299-305, 1986.

97. **Jessen N, Pold R, Buhl ES, Jensen LS, Schmitz O, and Lund S.** Effects of AICAR and exercise on insulin-stimulated glucose uptake, signaling, and GLUT-4 content in rat muscles. *J Appl Physiol* 94: 1373-1379, 2003.

98. **Kamohara S, Burcelin R, Halaas JL, Friedman JM, and Charron MJ.** Acute stimulation of glucose metabolism in mice by leptin treatment. *Nature* 389: 374-377, 1997.

99. **Karlsson HK, Hallsten K, Bjornholm M, Tsuchida H, Chibalin AV, Virtanen KA, Heinonen OJ, Lonnqvist F, Nuutila P, and Zierath JR.** Effects of metformin and rosiglitazone treatment on insulin signaling and glucose uptake in patients with newly diagnosed type 2 diabetes: a randomized controlled study. *Diabetes* 54: 1459-1467, 2005.

100. **Kaushik VK, Young ME, Dean DJ, Kurowski TG, Saha AK, and Ruderman NB.** Regulation of fatty acid oxidation and glucose metabolism in rat soleus muscle: effects of AICAR. *Am J Physiol Endocrinol Metab* 281: E335-340, 2001.

101. **Kelley DE, Goodpaster B, Wing RR, and Simoneau JA.** Skeletal muscle fatty acid metabolism in association with insulin resistance, obesity, and weight loss. *Am J Physiol* 277: E1130-1141, 1999.

102. **Kelley DE, Goodpaster B, Wing RR, and Simoneau JA.** Skeletal muscle fatty acid metabolism in association with insulin resistance, obesity, and weight loss. *Am J Physiol* 277: E1130-1141, 1999.

103. **Kelley DE, He J, Menshikova EV, and Ritov VB.** Dysfunction of mitochondria in human skeletal muscle in type 2 diabetes. *Diabetes* 51: 2944-2950, 2002.

104. **Kelley DE, Mokan M, Simoneau JA, and Mandarino LJ.** Interaction between glucose and free fatty acid metabolism in human skeletal muscle. *J Clin Invest* 92: 91-98, 1993.

105. **Kim JY, Hickner RC, Cortright RL, Dohm GL, and Houmard JA.** Lipid oxidation is reduced in obese human skeletal muscle. *Am J Physiol Endocrinol Metab* 279: E1039-1044, 2000.

106. **King H, Aubert RE, and Herman WH.** Global burden of diabetes, 1995-2025: prevalence, numerical estimates, and projections. *Diabetes Care* 21: 1414-1431, 1998.

107. **Knowler WC, Barrett-Connor E, Fowler SE, Hamman RF, Lachin JM, Walker EA, and Nathan DM.** Reduction in the incidence of type 2 diabetes with lifestyle intervention or metformin. *N Engl J Med* 346: 393-403, 2002.

108. **Kuhl JE, Ruderman NB, Musi N, Goodyear LJ, Patti ME, Crunkhorn S, Dronamraju D, Thorell A, Nygren J, Ljungkvist O, Degerblad M, Stahle A, Brismar TB, Andersen KL, Saha AK, Efendic S, and Bavenholm PN.** Exercise training decreases the concentration of malonyl-CoA and increases the expression and activity of

malonyl-CoA decarboxylase in human muscle. *Am J Physiol Endocrinol Metab* 290: E1296-1303, 2006.

109. **Langfort J, Ploug T, Ihlemann J, Baranczuk E, Donsmark M, Gorski J, and Galbo H.** Additivity of adrenaline and contractions on hormone-sensitive lipase, but not on glycogen phosphorylase, in rat muscle. *Acta Physiol Scand* 178: 51-60, 2003.

110. **Langfort J, Ploug T, Ihlemann J, Enevoldsen LH, Stallknecht B, Saldo M, Kjaer M, Holm C, and Galbo H.** Hormone-sensitive lipase (HSL) expression and regulation in skeletal muscle. *Adv Exp Med Biol* 441: 219-228, 1998.

111. **Langfort J, Ploug T, Ihlemann J, Holm C, and Galbo H.** Stimulation of hormone-sensitive lipase activity by contractions in rat skeletal muscle. *Biochem J* 351: 207-214, 2000.

112. **Lau R, Blinn WD, Bonen A, and Dyck DJ.** Stimulatory effects of leptin and muscle contraction on fatty acid metabolism are not additive. *Am J Physiol Endocrinol Metab* 281: E122-129, 2001.

113. **Lebrasseur NK, Kelly M, Tsao TS, Farmer SR, Saha AK, Ruderman NB, and Tomas E.** Thiazolidinediones can rapidly activate AMP-activated protein kinase in mammalian tissues. *Am J Physiol Endocrinol Metab* 291: E175-181, 2006.

114. **Lee JS, Pinnamaneni SK, Eo SJ, Cho IH, Pyo JH, Kim CK, Sinclair AJ, Febbraio MA, and Watt MJ.** Saturated, but not n-6 polyunsaturated, fatty acids induce insulin resistance: role of intramuscular accumulation of lipid metabolites. *J Appl Physiol* 100: 1467-1474, 2006.

115. **Lowry OH and Passoneau JV.** *A Flexible System of Enzymatic Analysis*. New York: Academic, 1972.

116. **Luiken JJ, Dyck DJ, Han XX, Tandon NN, Arumugam Y, Glatz JF, and Bonen A.** Insulin induces the translocation of the fatty acid transporter FAT/CD36 to the plasma membrane. *Am J Physiol Endocrinol Metab* 282: E491-495, 2002.

117. **Luiken JJFP, Arumugam Y, Dyck DJ, Bell RC, Pelsers MML, Turcotte LP, Tandon NN, Glatz JFC, and Bonen A.** Increased Rates of Fatty Acid Uptake and Plasmalemmal Fatty Acid Transporters in Obese Zucker Rats. *J Biol Chem* 276: 40567-40573, 2001.

118. **Luiken JJFP, Coort SLM, Willems J, Coumans WA, Bonen A, van der Vusse GJ, and Glatz JFC.** Contraction-Induced Fatty Acid Translocase/CD36 Translocation in Rat Cardiac Myocytes Is Mediated Through AMP-Activated Protein Kinase Signaling. *Diabetes* 52: 1627-1634, 2003.

119. **Ma Z, Gingerich RL, Santiago JV, Klein S, Smith CH, and Landt M.** Radioimmunoassay of leptin in human plasma. *Clin Chem* 42: 942-946, 1996.

120. **McGarry JD, Mannaerts GP, and Foster DW.** A possible role for malonyl-CoA in the regulation of hepatic fatty acid oxidation and ketogenesis. *J Clin Invest* 60: 265-270, 1977.

121. **McGarry JD, Mills SE, Long CS, and Foster DW.** Observations on the affinity for carnitine, and malonyl-CoA sensitivity, of carnitine palmitoyltransferase I in animal and human tissues. Demonstration of the presence of malonyl-CoA in non-hepatic tissues of the rat. *Biochem J* 214: 21-28, 1983.

122. **McGregor GP, Desaga JF, Ehlenz K, Fischer A, Heese F, Hegele A, Lammer C, Peiser C, and Lang RE.** Radiommunological measurement of leptin in plasma of obese and diabetic human subjects. *Endocrinology* 137: 1501-1504, 1996.

123. **Meltzer S, Leiter L, Daneman D, Gerstein HC, Lau D, Ludwig S, Yale JF, Zinman B, and Lillie D.** 1998 clinical practice guidelines for the management of diabetes in Canada. Canadian Diabetes Association. *CMAJ* 159 Suppl 8: S1-29, 1998.

124. **Menshikova EV, Ritov VB, Toledo FG, Ferrell RE, Goodpaster BH, and Kelley DE.** Effects of weight loss and physical activity on skeletal muscle mitochondrial function in obesity. *Am J Physiol Endocrinol Metab* 288: E818-825, 2005.

125. **Merrill GF, Kurth EJ, Hardie DG, and Winder WW.** AICA riboside increases AMP-activated protein kinase, fatty acid oxidation, and glucose uptake in rat muscle. *Am J Physiol* 273: E1107-1112, 1997.

126. **Merrill GF, Kurth EJ, Rasmussen BB, and Winder WW.** Influence of malonyl-CoA and palmitate concentration on rate of palmitate oxidation in rat muscle. *J Appl Physiol* 85: 1909-1914, 1998.

127. **Minokoshi Y, Kim YB, Peroni OD, Fryer LG, Muller C, Carling D, and Kahn BB.** Leptin stimulates fatty-acid oxidation by activating AMP-activated protein kinase. *Nature* 415: 339-343, 2002.

128. **Mu J, Brozinick JT, Valladares O, Bucan M, and Birnbaum MJ.** A role for AMP-activated protein kinase in contraction- and hypoxia-regulated glucose transport in skeletal muscle. *Mol Cell* 7: 1085-1094, 2001.

129. **Muoio DM, Dohm GL, Fiedorek FT, Jr., Tapscott EB, Coleman RA, and Dohn GL.** Leptin directly alters lipid partitioning in skeletal muscle. *Diabetes* 46: 1360-1363, 1997.

130. **Muoio DM, Seefeld K, Witters LA, and Coleman RA.** AMP-activated kinase reciprocally regulates triacylglycerol synthesis and fatty acid oxidation in liver and

muscle: evidence that sn-glycerol- 3-phosphate acyltransferase is a novel target. *Biochem J* 338: 783-791, 1999.

131. **Musi N, Hayashi T, Fujii N, Hirshman MF, Witters LA, and Goodyear LJ.** AMP-activated protein kinase activity and glucose uptake in rat skeletal muscle. *Am J Physiol Endocrinol Metab* 280: E677-684, 2001.

132. **Musi N, Hirshman MF, Nygren J, Svanfeldt M, Bavenholm P, Rooyackers O, Zhou G, Williamson JM, Ljunqvist O, Efendic S, Moller DE, Thorell A, and Goodyear LJ.** Metformin increases AMP-activated protein kinase activity in skeletal muscle of subjects with type 2 diabetes. *Diabetes* 51: 2074-2081, 2002.

133. **Nielsen JN, Mustard KJW, Graham DA, Yu H, MacDonald CS, Pilegaard H, Goodyear LJ, Hardie DG, Richter EA, and Wojtaszewski JFP.** 5'-AMP-activated protein kinase activity and subunit expression in exercise-trained human skeletal muscle. *J Appl Physiol* 94: 631-641, 2003.

134. **Odland LM, Heigenhauser GJ, Lopaschuk GD, and Spriet LL.** Human skeletal muscle malonyl-CoA at rest and during prolonged submaximal exercise. *Am J Physiol* 270: E541-544, 1996.

135. **Odland LM, Howlett RA, Heigenhauser GJ, Hultman E, and Spriet LL.** Skeletal muscle malonyl-CoA content at the onset of exercise at varying power outputs in humans. *Am J Physiol* 274: E1080-1085, 1998.

136. **Pan DA, Lillioja S, Kriketos AD, Milner MR, Baur LA, Bogardus C, Jenkins AB, and Storlien LH.** Skeletal muscle triglyceride levels are inversely related to insulin action. *Diabetes* 46: 983-988, 1997.

137. **Park H, Kaushik VK, Constant S, Prentki M, Przybytkowski E, Ruderman NB, and Saha AK.** Coordinate Regulation of Malonyl-CoA Decarboxylase, sn-Glycerol-3-phosphate Acyltransferase, and Acetyl-CoA Carboxylase by AMP-activated Protein Kinase in Rat Tissues in Response to Exercise. *J Biol Chem* 277: 32571-32577, 2002.

138. **Passoneau J and Lowry OH.** *Enzymatic analysis*. Totawa, NJ: Humana, 1993.

139. **Perdomo G, Commerford SR, Richard AM, Adams SH, Corkey BE, O'Doherty RM, and Brown NF.** Increased beta-Oxidation in Muscle Cells Enhances Insulin-stimulated Glucose Metabolism and Protects against Fatty Acid-induced Insulin Resistance Despite Intramyocellular Lipid Accumulation. *J Biol Chem* 279: 27177-27186, 2004.

140. **Peters SJ, Dyck DJ, Bonen A, and Spriet LL.** Effects of epinephrine on lipid metabolism in resting skeletal muscle. *Am J Physiol Endocrinol Metab* 275: E300-309, 1998.

141. **Peterson RG, Shaw WN, Neel M, Little LA, and Eichenberg J.** Zucker Diabetic Fatty Rat as a Model for Non-insulin-dependent Diabetes Mellitus. *ILAR News* 32: 16-19, 1990.

142. **Pold R, Jensen LS, Jessen N, Buhl ES, Schmitz O, Flyvbjerg A, Fujii N, Goodyear LJ, Gotfredsen CF, Brand CL, and Lund S.** Long-term AICAR administration and exercise prevents diabetes in ZDF rats. *Diabetes* 54: 928-934, 2005.

143. **Putman CT, Spriet LL, Hultman E, Lindinger MI, Lands LC, McKelvie RS, Cederblad G, Jones NL, and Heigenhauser GJ.** Pyruvate dehydrogenase activity and acetyl group accumulation during exercise after different diets. *Am J Physiol* 265: E752-760, 1993.

144. **Randle PJ, Hales CN, Garland PB, and Newsholme EA.** The Glucose Fatty-Acid Cycle: Its role in insulin sensitivity and the metabolic disturbances of diabetes mellitus. *The Lancet*: 785-789, 1963.

145. **Raney MA, Yee AJ, Todd MK, and Turcotte LP.** AMPK activation is not critical in the regulation of muscle FA uptake and oxidation during low intensity muscle contraction. *Am J Physiol Endocrinol Metab* 288: E592-598, 2005.

146. **Rasmussen BB and Winder WW.** Effect of exercise intensity on skeletal muscle malonyl-CoA and acetyl-CoA carboxylase. *J Appl Physiol* 83: 1104-1109, 1997.

147. **Rennie MJ and Holloszy JO.** Inhibition of glucose uptake and glycogenolysis by availability of oleate in well-oxygenated perfused skeletal muscle. *Biochem J* 168: 161-170, 1977.

148. **Ritov VB, Menshikova EV, He J, Ferrell RE, Goodpaster BH, and Kelley DE.** Deficiency of subsarcolemmal mitochondria in obesity and type 2 diabetes. *Diabetes* 54: 8-14, 2005.

149. **Roden M, Price TB, Perseghin G, Petersen KF, Rothman DL, Cline GW, and Shulman GI.** Mechanism of free fatty acid-induced insulin resistance in humans. *J Clin Invest* 97: 2859-2865, 1996.

150. **Roepstorff C, Thiele M, Hillig T, Pilegaard H, Richter EA, Wojtaszewski JF, and Kiens B.** Higher skeletal muscle {alpha}2AMPK activation and lower energy charge and fat oxidation in men than in women during submaximal exercise. In Press: *J Physiol*, 2006.

151. **Romijn JA, Coyle EF, Sidossis LS, Gastaldelli A, Horowitz JF, Endert E, and Wolfe RR.** Regulation of endogenous fat and carbohydrate metabolism in relation to exercise intensity and duration. *Am J Physiol* 265: E380-391, 1993.

152. **Russell RR, 3rd, Bergeron R, Shulman GI, and Young LH.** Translocation of myocardial GLUT-4 and increased glucose uptake through activation of AMPK by AICAR. *Am J Physiol* 277: H643-649, 1999.

153. **Sabina RL, Patterson D, and Holmes EW.** 5-Amino-4-imidazolecarboxamide riboside (Z-riboside) metabolism in eukaryotic cells. *J Biol Chem* 260: 6107-6114, 1985.

154. **Saha AK, Schwarsin AJ, Roduit R, Masse F, Kaushik V, Tornheim K, Prentki M, and Ruderman NB.** Activation of malonyl-CoA decarboxylase in rat skeletal muscle by contraction and the AMP-activated protein kinase activator 5-aminoimidazole-4-carboxamide-1-beta -D-ribofuranoside. *J Biol Chem* 275: 24279-24283, 2000.

155. **Sakamoto K, Goransson O, Hardie DG, and Alessi DR.** Activity of LKB1 and AMPK-related kinases in skeletal muscle: effects of contraction, phenformin, and AICAR. *Am J Physiol Endocrinol Metab* 287: E310-317, 2004.

156. **Sakoda H, Ogihara T, Anai M, Fujishiro M, Ono H, Onishi Y, Katagiri H, Abe M, Fukushima Y, Shojima N, Inukai K, Kikuchi M, Oka Y, and Asano T.** Activation of AMPK is essential for AICAR-induced glucose uptake by skeletal muscle but not adipocytes. *Am J Physiol Endocrinol Metab* 282: E1239-1244, 2002.

157. **Salt I, Celler JW, Hawley SA, Prescott A, Woods A, Carling D, and Hardie DG.** AMP-activated protein kinase: greater AMP dependence, and preferential nuclear

localization, of complexes containing the alpha2 isoform. *Biochem J* 334 (Pt 1): 177-187, 1998.

158. **Sambol NC, Brookes LG, Chiang J, Goodman AM, Lin ET, Liu CY, and Benet LZ.** Food intake and dosage level, but not tablet vs solution dosage form, affect the absorption of metformin HCl in man. *Br J Clin Pharmacol* 42: 510-512, 1996.

159. **Schenk S and Horowitz JF.** Co-immunoprecipitation of FAT/CD36 and CPT-I in skeletal muscle increases proportionally with fat oxidation after endurance exercise training. *Am J Physiol Endocrinol Metab*, 2006.

160. **Schmitz-Peiffer C, Browne CL, Oakes ND, Watkinson A, Chisholm DJ, Kraegen EW, and Biden TJ.** Alterations in the expression and cellular localization of protein kinase C isozymes epsilon and theta are associated with insulin resistance in skeletal muscle of the high-fat-fed rat. *Diabetes* 46: 169-178, 1997.

161. **Schmitz-Peiffer C, Craig DL, and Biden TJ.** Ceramide generation is sufficient to account for the inhibition of the insulin-stimulated PKB pathway in C2C12 skeletal muscle cells pretreated with palmitate. *J Biol Chem* 274: 24202-24210, 1999.

162. **Simoneau JA, Veerkamp JH, Turcotte LP, and Kelley DE.** Markers of capacity to utilize fatty acids in human skeletal muscle: relation to insulin resistance and obesity and effects of weight loss. *Faseb J* 13: 2051-2060, 1999.

163. **Sivitz WI, Fink BD, and Donohoue PA.** Fasting and leptin modulate adipose and muscle uncoupling protein: divergent effects between messenger ribonucleic acid and protein expression. *Endocrinology* 140: 1511-1519, 1999.

164. **Smith AC, Bruce CR, and Dyck DJ.** AMP kinase activation with AICAR further increases fatty acid oxidation and blunts triacylglycerol hydrolysis in contracting rat soleus muscle. *J Physiol* 565: 547-553, 2005.

165. **Smith AC, Bruce CR, and Dyck DJ.** AMP kinase activation with AICAR simultaneously increases fatty acid and glucose oxidation in resting rat soleus muscle. *J Physiol* 565: 537-546, 2005.

166. **Smith SA.** Central role of the adipocyte in the insulin-sensitising and cardiovascular risk modifying actions of the thiazolidinediones. *Biochimie* 85: 1219-1230, 2003.

167. **Spriet LL and Heigenhauser GJ.** Regulation of pyruvate dehydrogenase (PDH) activity in human skeletal muscle during exercise. *Exerc Sport Sci Rev* 30: 91-95, 2002.

168. **Sreenan S, Keck S, Fuller T, Cockburn B, and Burant CF.** Effects of troglitazone on substrate storage and utilization in insulin-resistant rats. *Am J Physiol Endocrinol Metab* 276: E1119-1129, 1999.

169. **Srere PA.** Citrate Synthase. In: *Methods in Enzymology*, 1969, p. 3-11.

170. **Sriwijitkamol A, Ivy JL, Christ-Roberts C, DeFronzo RA, Mandarino LJ, and Musi N.** LKB1-AMPK signaling in muscle from obese insulin-resistant Zucker rats and effects of training. *Am J Physiol Endocrinol Metab* 290: E925-932, 2006.

171. **Stapleton D, Gao G, Michell BJ, Widmer J, Mitchelhill K, Teh T, House CM, Witters LA, and Kemp BE.** Mammalian 5'-AMP-activated protein kinase non-catalytic subunits are homologs of proteins that interact with yeast Snf1 protein kinase. *J Biol Chem* 269: 29343-29346, 1994.

172. **Steinberg GR and Dyck DJ.** Development of leptin resistance in rat soleus muscle in response to high-fat diets. *Am J Physiol Endocrinol Metab* 279: E1374-1382, 2000.

173. **Steinberg GR, Dyck DJ, Calles-Escandon J, Tandon NN, Luiken JJ, Glatz JF, and Bonen A.** Chronic leptin administration decreases fatty acid uptake and fatty acid transporters in rat skeletal muscle. *J Biol Chem* 277: 8854-8860, 2002.

174. **Steinberg GR, Parolin ML, Heigenhauser GJ, and Dyck DJ.** Leptin increases FA oxidation in lean but not obese human skeletal muscle: evidence of peripheral leptin resistance. *Am J Physiol Endocrinol Metab* 283: E187-192, 2002.

175. **Steinberg GR, Smith AC, van Denderen BJW, Chen Z, Murthy S, Campbell DJ, Heigenhauser GJF, Dyck DJ, and Kemp BE.** AMP-Activated Protein Kinase Is Not Down-Regulated in Human Skeletal Muscle of Obese Females. *J Clin Endocrinol Metab* 89: 4575-4580, 2004.

176. **Steinberg GR, Smith AC, Wormald S, Malenfant P, Collier C, and Dyck DJ.** Endurance training partially reverses dietary-induced leptin resistance in rodent skeletal muscle. *Am J Physiol Endocrinol Metab* 286: E57-63, 2004.

177. **Stoppani J, Hildebrandt AL, Sakamoto K, Cameron-Smith D, Goodyear LJ, and Neufer PD.** AMP-activated protein kinase activates transcription of the UCP3 and HKII genes in rat skeletal muscle. *Am J Physiol Endocrinol Metab* 283: E1239-E1248, 2002.

178. **Storlien LH, Jenkins AB, Chisholm DJ, Pascoe WS, Khouri S, and Kraegen EW.** Influence of dietary fat composition on development of insulin resistance in rats.

Relationship to muscle triglyceride and omega-3 fatty acids in muscle phospholipid. *Diabetes* 40: 280-289, 1991.

179. **Straczkowski M, Kowalska I, Nikolajuk A, Dzienis-Straczkowska S, Kinalska I, Baranowski M, Zendzian-Piotrowska M, Brzezinska Z, and Gorski J.** Relationship between insulin sensitivity and sphingomyelin signaling pathway in human skeletal muscle. *Diabetes* 53: 1215-1221, 2004.

180. **Stumvoll M, Nurjhan N, Perriello G, Dailey G, and Gerich JE.** Metabolic effects of metformin in non-insulin-dependent diabetes mellitus. *N Engl J Med* 333: 550-554, 1995.

181. **Sullivan JE, Brocklehurst KJ, Marley AE, Carey F, Carling D, and Beri RK.** Inhibition of lipolysis and lipogenesis in isolated rat adipocytes with AICAR, a cell-permeable activator of AMP-activated protein kinase. *FEBS Lett* 353: 33-36, 1994.

182. **Summers SA, Garza LA, Zhou H, and Birnbaum MJ.** Regulation of insulin-stimulated glucose transporter GLUT4 translocation and Akt kinase activity by ceramide. *Mol Cell Biol* 18: 5457-5464, 1998.

183. **Sutherland CM, Hawley SA, McCartney RR, Leech A, Stark MJ, Schmidt MC, and Hardie DG.** Elm1p is one of three upstream kinases for the Saccharomyces cerevisiae SNF1 complex. *Curr Biol* 13: 1299-1305, 2003.

184. **Suwa M, Nakano H, and Kumagai S.** Effects of chronic AICAR treatment on fiber composition, enzyme activity, UCP3, and PGC-1 in rat muscles. *J Appl Physiol* 95: 960-968, 2003.

185. **Tan GD, Fielding BA, Currie JM, Humphreys SM, Desage M, Frayn KN, Laville M, Vidal H, and Karpe F.** The effects of rosiglitazone on fatty acid and triglyceride metabolism in type 2 diabetes. *Diabetologia* 48: 83-95, 2005.

186. **Tomas E, Tsao TS, Saha AK, Murrey HE, Zhang Cc C, Itani SI, Lodish HF, and Ruderman NB.** Enhanced muscle fat oxidation and glucose transport by ACRP30 globular domain: acetyl-CoA carboxylase inhibition and AMP-activated protein kinase activation. *Proc Natl Acad Sci U S A* 99: 16309-16313, 2002.

187. **Tremblay F, Lavigne C, Jacques H, and Marette A.** Dietary cod protein restores insulin-induced activation of phosphatidylinositol 3-kinase/Akt and GLUT4 translocation to the T-tubules in skeletal muscle of high-fat-fed obese rats. *Diabetes* 52: 29-37, 2003.

188. **Trumble GE, Smith MA, and Winder WW.** Evidence of a biotin dependent acetyl-coenzyme A carboxylase in rat muscle. *Life Sci* 49: 39-43, 1991.

189. **Trumble GE, Smith MA, and Winder WW.** Purification and characterization of rat skeletal muscle acetyl-CoA carboxylase. *Eur J Biochem* 231: 192-198, 1995.

190. **Turinsky J, Bayly BP, and O'Sullivan DM.** 1,2-Diacylglycerol and ceramide levels in rat liver and skeletal muscle in vivo. *Am J Physiol* 261: E620-627, 1991.

191. **Verhoeven AJ, Woods A, Brennan CH, Hawley SA, Hardie DG, Scott J, Beri RK, and Carling D.** The AMP-activated protein kinase gene is highly expressed in rat skeletal muscle. Alternative splicing and tissue distribution of the mRNA. *Eur J Biochem* 228: 236-243, 1995.

192. **Voss MD, Beha A, Tennagels N, Tschank G, Herling AW, Quint M, Gerl M, Metz-Weidmann C, Haun G, and Korn M.** Gene expression profiling in skeletal

muscle of Zucker diabetic fatty rats: implications for a role of stearoyl-CoA desaturase 1 in insulin resistance. *Diabetologia* 48: 2622-2630, 2005.

193. **WATT MJ, STEINBERG GR, CHAN S, GARNHAM A, KEMP BE, and FEBBRAIO MA.** {beta}-adrenergic stimulation of skeletal muscle HSL can be overridden by AMPK signaling. *FASEB J* 18: 1445-1446, 2004.

194. **Weekes J, Hawley SA, Corton J, Shugar D, and Hardie DG.** Activation of rat liver AMP-activated protein kinase by kinase kinase in a purified, reconstituted system: Effects of AMP and AMP analogues. *Eur J Biochem* 219: 751-757, 1994.

195. **Weyer C, Funahashi T, Tanaka S, Hotta K, Matsuzawa Y, Pratley RE, and Tataranni PA.** Hypoadiponectinemia in obesity and type 2 diabetes: close association with insulin resistance and hyperinsulinemia. *J Clin Endocrinol Metab* 86: 1930-1935, 2001.

196. **Wilkes JJ, Nelson E, Osborne M, Demarest KT, and Olefsky JM.** Topiramate is an insulin-sensitizing compound in vivo with direct effects on adipocytes in female ZDF rats. *Am J Physiol Endocrinol Metab* 288: E617-624, 2005.

197. **Wilmsen HM, Ciaraldi TP, Carter L, Reehman N, Mudaliar SR, and Henry RR.** Thiazolidinediones upregulate impaired fatty acid uptake in skeletal muscle of type 2 diabetic subjects. *Am J Physiol Endocrinol Metab* 285: E354-362, 2003.

198. **Winder WW, Arogyasami J, Barton RJ, Elayan IM, and Vehrs PR.** Muscle malonyl-CoA decreases during exercise. *J Appl Physiol* 67: 2230-2233, 1989.

199. **Winder WW, Arogyasami J, Elayan IM, and Cartmill D.** Time course of exercise-induced decline in malonyl-CoA in different muscle types. *Am J Physiol* 259: E266-271, 1990.

200. **Winder WW and Hardie DG.** Inactivation of acetyl-CoA carboxylase and activation of AMP-activated protein kinase in muscle during exercise. *Am J Physiol* 270: E299-304, 1996.

201. **Winder WW, Holmes BF, Rubink DS, Jensen EB, Chen M, and Holloszy JO.** Activation of AMP-activated protein kinase increases mitochondrial enzymes in skeletal muscle. *J Appl Physiol* 88: 2219-2226, 2000.

202. **Winder WW, Wilson HA, Hardie DG, Rasmussen BB, Hutber CA, Call GB, Clayton RD, Conley LM, Yoon S, and Zhou B.** Phosphorylation of rat muscle acetyl-CoA carboxylase by AMP-activated protein kinase and protein kinase A. *J Appl Physiol* 82: 219-225, 1997.

203. **Witters LA, Kemp BE, and Means AR.** Chutes and Ladders: the search for protein kinases that act on AMPK. *Trends Biochem Sci* 31: 13-16, 2006.

204. **Wojtaszewski JF, Jorgensen SB, Hellsten Y, Hardie DG, and Richter EA.** Glycogen-dependent effects of 5-aminoimidazole-4-carboxamide (AICA)- riboside on AMP-activated protein kinase and glycogen synthase activities in rat skeletal muscle. *Diabetes* 51: 284-292, 2002.

205. **Wojtaszewski JFP, MacDonald C, Nielsen JN, Hellsten Y, Hardie DG, Kemp BE, Kiens B, and Richter EA.** Regulation of 5'AMP-activated protein kinase activity and substrate utilization in exercising human skeletal muscle. *Am J Physiol Endocrinol Metab* 284: E813-822, 2003.

206. **Wojtaszewski JFP, Nielsen P, Hansen BF, Richter EA, and Kiens B.** Isoform-specific and exercise intensity-dependent activation of 5'-AMP-activated protein kinase in human skeletal muscle. *J Physiol (Lond)* 528: 221-226, 2000.

207. **Wolfe BM, Klein S, Peters EJ, Schmidt BF, and Wolfe RR.** Effect of elevated free fatty acids on glucose oxidation in normal humans. *Metabolism* 37: 323-329, 1988.

208. **Woods A, Dickerson K, Heath R, Hong SP, Momcilovic M, Johnstone SR, Carlson M, and Carling D.** Ca2+/calmodulin-dependent protein kinase kinase-beta acts upstream of AMP-activated protein kinase in mammalian cells. *Cell Metab* 2: 21-33, 2005.

209. **Woods A, Johnstone SR, Dickerson K, Leiper FC, Fryer LG, Neumann D, Schlattner U, Wallimann T, Carlson M, and Carling D.** LKB1 is the upstream kinase in the AMP-activated protein kinase cascade. *Curr Biol* 13: 2004-2008, 2003.

210. **Yamauchi T, Kamon J, Minokoshi Y, Ito Y, Waki H, Uchida S, Yamashita S, Noda M, Kita S, Ueki K, Eto K, Akanuma Y, Froguel P, Foufelle F, Ferre P, Carling D, Kimura S, Nagai R, Kahn BB, and Kadowaki T.** Adiponectin stimulates glucose utilization and fatty-acid oxidation by activating AMP-activated protein kinase. *Nat Med* 8: 1288-1295, 2002.

211. **Ye JM, Dzamko N, Cleasby ME, Hegarty BD, Furler SM, Cooney GJ, and Kraegen EW.** Direct demonstration of lipid sequestration as a mechanism by which rosiglitazone prevents fatty-acid-induced insulin resistance in the rat: comparison with metformin. *Diabetologia* 47: 1306-1313, 2004.

212. **Yu JG, Javorschi S, Hevener AL, Kruszynska YT, Norman RA, Sinha M, and Olefsky JM.** The effect of thiazolidinediones on plasma adiponectin levels in normal, obese, and type 2 diabetic subjects. *Diabetes* 51: 2968-2974, 2002.

213. **Yu X, McCorkle S, Wang M, Lee Y, Li J, Saha AK, Unger RH, and Ruderman NB.** Leptinomimetic effects of the AMP kinase activator AICAR in leptin-

resistant rats: prevention of diabetes and ectopic lipid deposition. *Diabetologia* 47: 2012-2021, 2004.

214. **Zang M, Zuccollo A, Hou X, Nagata D, Walsh K, Herscovitz H, Brecher P, Ruderman NB, and Cohen RA.** AMP-activated protein kinase is required for the lipid-lowering effect of metformin in insulin-resistant human HepG2 cells. *J Biol Chem* 279: 47898-47905, 2004.

215. **Zheng D, MacLean PS, Pohnert SC, Knight JB, Olson AL, Winder WW, and Dohm GL.** Regulation of muscle GLUT-4 transcription by AMP-activated protein kinase. *J Appl Physiol* 91: 1073-1083, 2001.

216. **Zhou G, Myers R, Li Y, Chen Y, Shen X, Fenyk-Melody J, Wu M, Ventre J, Doebber T, Fujii N, Musi N, Hirshman MF, Goodyear LJ, and Moller DE.** Role of AMP-activated protein kinase in mechanism of metformin action. *J Clin Invest* 108: 1167-1174, 2001.

217. **Zhou M, Lin B-Z, Coughlin S, Vallega G, and Pilch PF.** UCP-3 expression in skeletal muscle: effects of exercise, hypoxia, and AMP-activated protein kinase. *Am J Physiol Endocrinol Metab* 279: E622-629, 2000.

218. **Zhou Q, Dolan PL, and Dohm GL.** Dephosphorylation increases insulin-stimulated receptor kinase activity in skeletal muscle of obese Zucker rats. *Mol Cell Biochem* 194: 209-216, 1999.

APPENDIX 1: MUSCLE VIABILITY

In order to verify the viability of muscle in the *in vitro* preparation used in the experiments that are part of this thesis, muscle strips were incubated in base KHB (1 mM) and were rapidly frozen in liquid N_2 after 30, 60, 90 or 120 min and compared to control strips frozen after excision. Muscle metabolites were isolated in neutralized PCA extracts and concentrations of ATP and PCr were measured spectrophotometrically. The results of these experiments are summarized in *Table 1* (**CHAPTER 3**). Additionally, to determine whether the incorporation of palmitate label was linear during the incubation protocol, the incorporation of [1-^{14}C] palmitate into DAG, TAG and the oxidative production of $^{14}CO_2$ (*Table 9*) after 30, 60 and 90 min was measured. We observed linear incorporation of radiolabeled DAG and TAG, as well as production of $^{14}CO_2$ and from FA oxidation over 90 minutes, which further validated this technique to monitor changes in FA metabolism acutely.

Table 9: Incorporation of [1-^{14}C] palmitate into the diacylglycerol, triacylglycerol pools and production of [1-$^{14}CO_2$] in rat soleus muscle
Values are means ± SEM, *n* = 3-4 per group, nmol/g wet wt.

	^{14}C-Palmitate		
	30'	**60'**	**90'**
DAG	10.7 ± 0.9	18.7 ± 0.3	28.8 ± 1.1
TAG	105.5 ± 13.3	218.2 ± 8.7	303.7 ± 2.2
Oxidation	39.3 ± 3.4	78.6 ± 8.1	149.1 ± 8.4

APPENDIX 2: METFORMIN AND EXERCISE PILOT DATA

Pilot studies were performed with Sprague-Dawley rats to determine 1) the solubility and palatability of metformin in drinking water 2) whether exercise or metformin had effects on glucose transport, FA metabolism at rest and during contraction and isoform-specific AMPK activity in soleus muscle. The studies were also conducted to gain familiarity with operation of the rodent treadmill. Previous studies examining metformin's effects on food intake in rodent models are equivocal, so control rats were pair-fed (PF-C). However, food intake in the metformin rats was not significantly different from food intake typically expected in rats (5g/100g body weight). Therefore, female ZDF rats were fed *ad libitum*. Appropriate increases in insulin-stimulated glucose transport were observed in soleus muscle (~2-3-fold) and there were no differences in insulin-stimulated glucose uptake between the groups (*Tables 10-12*). There were no significant differences in DAG esterification (*Table 13*). TAG esterification was increased in soleus muscle from trained rats (*Table 14*), as has been previously demonstrated (50), while surprisingly, there were no differences in FA oxidation (*Table 15*). The lack of increase in FA oxidation was possibly due to the training protocol lasting only 4 weeks, where increases have been observed after 8 weeks of endurance training (50). Importantly, we observed a trend toward an increase in AMPKα1 activity (*Table 16*) after 4 weeks of metformin treatment in healthy rats ($P = 0.10$), suggesting that metformin does have direct effects on skeletal muscle AMPK.

Table 10: Basal and insulin-stimulated glucose transport in soleus muscle from pair-fed (control, PF-C) Sprague-Dawley rats for four weeks

	PF-C	
	Basal Glucose Transport	Insulin-stimulated Glucose Transport
	144	208
	81	256
	99	225
	77	310
Mean Glucose Transport, nmol/g/5 min	100 ± 15	250 ± 22

Table 11: Basal and insulin-stimulated glucose transport in soleus muscle from Sprague-Dawley rats treated with metformin for four weeks

	Metformin	
	Basal Glucose Transport	Insulin-stimulated Glucose Transport
	116	209
	90	216
	149	221
	117	274
Mean Glucose Transport, nmol/g/5 min	118 ± 12	230 ± 15

Table 12: Basal and insulin-stimulated glucose transport in soleus muscle from Sprague-Dawley rats treadmill trained for four weeks

	Trained	
	Basal Glucose Transport	Insulin-stimulated Glucose Transport
	70	172
	119	249
	102	231
	82	173
Mean Glucose Transport, nmol/g/5 min	93 ± 11	206 ± 20

Table 13: DAG esterification (nmol/g wet wt) in soleus muscle from Sprague-Dawley rats pair-fed to metformin rats for four weeks

	Rest			Contraction		
	PF-C	Metformin	Trained	PF-C	Metformin	Trained
	17	14	15	22	22	25
	28	21	11	32	19	17
	17	33	18	21	22	21
	15	17	17	14	16	23
Mean	19 ± 3	21 ± 4	15 ± 3	22 ± 4	20 ± 1	21 ± 2

Table 14: TAG esterification (nmol/g wet wt) in soleus muscle from Sprague-Dawley rats pair-fed to metformin rats for four weeks

	Rest			Contraction		
	PF-C	Metformin	Trained	PF-C	Metformin	Trained
	94	76	101	120	122	211
	89	104	77	85	110	129
	71	120	99	82	106	145
	81	77	121	72	58	143
Mean	84 ± 5	94 ± 11	100 ± 18	90 ± 10	99 ± 14	157 ± 37*

Table 15: FA oxidation (nmol/g wet wt) in soleus muscle from Sprague-Dawley rats pair-fed to metformin rats for four weeks

	Rest			Contraction		
	PF-C	Metformin	Trained	PF-C	Metformin	Trained
	42	45	106	73	49	62
	54	65		82	45	62
	58	81	63	75	106	80
	127	44	40	77	133	103
Mean	59 ± 9	70 ± 19	70 ± 46	77 ± 2	83 ± 22	77 ± 19

Table 16: AMPKα1 and AMPKα2 in soleus muscle from Sprague-Dawley rats pair-fed to metformin rats for four weeks

	AMPKα1			AMPKα2		
	PF-C	Metformin	Trained	PF-C	Metformin	Trained
	1.5	6.1	2.4	0.452	0.63	0.26
	7.3	8.5	3.9	0.478	0.30	0.33
	7.0	7.2	8.1	0.170	0.37	0.57
	3.0	7.8	5.4	0.265	0.13	0.37
Mean	4.7 ± 3.0	7.4 ± 0.5*	4.9 ± 1.2	0.3 ± 0.1	0.4 ± 0.1	0.4 ± 0.1

APPENDIX 3: RESEARCH DIETS C13004 HIGH FAT DIET INFORMATION

C13004 diet is composed of Purina rodent chow #5015, supplemented with **30% Ho-Milc 7-60**, GMI Fat Supplement (*Table 17 & 18*). Ho-Milc is a homogeneous product containing micro-encapsulated fat from animal sources with BHA (as a preservative), whey, casein and lecithin.

Table 17: Calories (kcal%) provided by Purina C5008, C5015 and Research Diets C13004

	Purina 5008	Purina 5015	RD C13004
kcal%			
Protein	26.8	18.3	11.5
Carbohydrate	56.4	55.9	40.6
Fat	16.7	25.8	47.9
Total	100%	100%	100%

Table 18: Fatty Acid Profile provided by the makers of Merrick's Ho-Milc 7-60

Fatty Acid	Chain Length	% FA
Palmitic	C16:0	13.2
Stearic	C18:0	9.9
Oleic	C18:1	25.8
Linoleic	C18:2	4.8
Linolenic	C18:3	0.6
	Total	**55%**

Appendix 4: Quality Control for Plasma Glucose Determination

Weekly (0, 4 and 8 weeks) and endpoint plasma glucose values were determined with the Ascensia Elite® Glucometer (Bayer, Inc.), as this method measured plasma glucose levels from very small volumes of blood. To verify that this glucometer was accurate for plasma glucose with such small blood volumes, three readings were taken from healthy Sprague-Dawley rats and plasma was analyzed fluorometrically (*Table 20*). The glucometer analysis yielded a low coefficient of variation (3.7 ± 1.0 %) and glucometer values were not significantly different from plasma glucose analyzed fluorometrically from the same rats.

Table 19: Glucometer quality control analyses for plasma glucose determination

	Glucometer Analysis		
Sample	Average of 3 Readings (mM)	Coefficient of Variation (%)	Fluorometric Glucose Value (mM)
1	7.3	5.8	5.5
2	7.1	1.4	7.1
3	7.6	1.9	7.0
4	7.3	6.5	7.4
5	6.8	3.1	6.7
Mean ± SEM	7.2 ± 0.1	3.7 ± 1.0	6.8 ± 0.3

APPENDIX 5: WESTERN BLOT PROTOCOLS FOR PROTEINS EXAMINED IN CHAPTER 5

Table 20: Western Blot Protocols for Proteins Examined in Chapter 5

Protein	Source	MW	Gel	Transfer	Block*	Wash	1° Ab (Overnight)[5]	Wash	2° Ab (1 hr)	Wash	Detect**
pAMPK[1]	Cell Signaling 2535	63	10%	1-1.5 hr	5% NFM TBS-T	3 x 5 min TBS-T	1:1,000 5% BSA TBS-T	3 x 5 min TBS-T	1:2,000 5% NFM PBS-T	3 X 5 min PBS-T	2 x 2 min or 2 x 5 min
tAMPKα	Cell Signaling 2532	63	10%	1-1.5 hr	5% NFM TBS-T	3 x 5 min TBS-T	1:1,000 5% BSA TBS-T	3 x 5 min TBS-T	1:2,000 5% NFM TBS-T	3 x 5 min TBS-T	2 x 2 min
AMPKα2	Upstate 07-363	63	10%	1-1.5 hr	5% NFM PBS-T	3 x 5 min PBS-T	1:1000 5% NFM PBS-T	3 x 5 min PBS-T	1:2,000 5% NFM PBS-T	3 x 5 min PBS-T	2 x 2 min
AMPKα1	Upstate 07-350	63	10%	1-1.5 hr	5% NFM PBS-T	3 x 5 min PBS-T	1:1,000 5% NFM PBS-T	3 x 5 min PBS-T	1:2,000 5% NFM PBS-T	3 x 5 min PBS-T	2 x 2 min or 1 X 5 min
pACC[1]	Cell Signaling 3661	250	6.5%	Overnight[4]	2.5% BSA TBS-T	3 x 5 min TBS-T	1:1,000 2.5% BSA TBS-T	3 x 5 min TBS-T	1:2,000 PBS	(3-5) x 5 min PBS-T	2 x 5 min
Mo25 (FAT/CD36)	Gift: Dr. Calles-Escandon[2]	88	10%	1-1.5 hr	7.5% BSA TBS-T	3 x 5 min TBS-T	1:20,000 7.5% BSA TBS-T	3 x 5 min TBS-T	1:20,000 TBS-T	3 x 5 min TBS-T	2 x 2 min
FABPpm	Gift: Dr Tandon[3]	40	10%	1-1.5 hr	10% NFM TBST	3 x 5 min TBS-T	1:30,000 10% NFM TBS-T	3 x 5 min TBS-T	1:3,000 TBS-T	3 x 5 min TBS-T	2 x 1 min or 2 x 2 min
GLUT4	Chemicon AB1346	48	10%	1-1.5 hr	10% NFM TBST	3 x 5 min TBS-T	1:4,000 10% NFM TBS-T	3 x 5 min TBS-T	1:4,000 TBS-T	3 x 5 min TBS-T	2 x 2 min
PGC-1α	Calbiochem 29421	90	10%	1-1.5 hr	2.5% BSA TBS-T	3 x 5 min TBS-T	1:1,000 2.5% BSA TBS-T	3 x 5 min TBS-T	1:1,000 TBS-T	3 x 5 min TBS-T	2 x 1 min

Notes on Western Protocols

[1]It is recommended that phospho-proteins be incubated with PBS-based solutions, especially if also using non-fat milk as a blocking agent, as casein itself is a phospho-protein and will non-specifically bind to the PVSF membrane and increase background; the 2°Ab and final wash were in PBS-T solutions

[2]Wake Forest University School of Medicine

[3]Otsuka Maryland Medicinal Laboratories

[4]Overnight transfer is a minimum of 8 hr (max15 hr, due to heat production), 4°C, transfer unit packed on ice, 25-40 V (low voltage for less heat production)
[5]Overnight incubation with all 1°Ab except pACC (1-2 hr)

*Total incubation time of proteins bound to PVSF membrane (block to final wash) was kept to a maximum of 15 hours so as not to have over-exposure to Tween-20

** PVSF membranes can be dried at room temperature, wrapped in plastic wrap, frozen at -80°C. Proteins will be stable to re-incubate or blot for another protein after stripping procedure.